Green Chemistry

RSC Publishing

PAPER

View Article Online
View Journal | View Issue

Published on 03 June 2013. Downloaded by Université Laval on 15/05/2014 21:48:14.

Cite this: *Green Chem.*, 2013, **15**, 2121

Mineral neogenesis as an inspiration for mild, solvent-free synthesis of bulk microporous metal–organic frameworks from metal (Zn, Co) oxides†

Cristina Mottillo,[a] Yuneng Lu,[a] Minh-Hao Pham,[b] Matthew J. Cliffe,‡[c] Trong-On Do[b] and Tomislav Friščić*[a]

"Accelerated aging" is a simple and conceptually novel methodology for the synthesis of functional metal–organic materials, which seeks to provide a scalable, mild and environmentally-friendly alternative to solution-based or mechanochemical syntheses. Accelerated aging draws inspiration from slow processes of geological biomineralization and mineral neogenesis, and adapts them for the low-energy and solvent-free synthesis of modern metal–organic materials. This systematic study outlines the development of an accelerated aging synthesis of microporous frameworks from metal oxides CoO and ZnO. Whereas metal oxides often require high temperatures or aggressive reagents, accelerated aging allows their spontaneous transformation into porous materials under surprisingly mild conditions, akin to those of molecular self-assembly (humid air, up to 45 °C). Here, we describe how accelerated aging can be optimized for the one-step synthesis of multi-gram amounts of microporous solids. As targets, we selected popular zeolitic imidazolate frameworks (ZIFs): the sodalite-topology ZIF-8, its cobalt analogue ZIF-67, and a related zeolite RHO framework. Unlike conventional solution or mechanochemical syntheses, accelerated aging is diffusion-controlled and does not require continuous agitation, bulk solvent or high temperature. The syntheses of ZIF-8 and ZIF-67 contrast the conventional paradigm of metal–organic framework synthesis, by demonstrating that microporous materials can be spontaneously and efficiently assembled from a close-packed metal oxide without using solvents, high temperature or other activation (*e.g.* microwave, sonochemical, mechanochemical).

Received 19th March 2013,
Accepted 3rd June 2013

DOI: 10.1039/c3gc40520f

www.rsc.org/greenchem

Introduction

The increasingly limited energy and materials resources, coupled with growing concerns of industrial contamination have made the development of cleaner and more efficient synthetic methodologies an imperative of modern research.[1] Metal–organic frameworks (MOFs)[2] continue to attract attention due to their tunable porosity suitable for catalysis and sensing,[3] gas storage and separation,[4] and optical properties, including light-harvesting applications.[5] Particular attention has been drawn to metal azolates, such as zeolitic imidazolate frameworks (ZIFs)[6] of which the sodalite (*sod*) topology zinc 2-methylimidazolate (ZIF-8,[7] MAF-4[8]) is now commercially produced (Basolite Z1200®). Various methods have been employed for MOF synthesis in solution, including solvothermal, electrochemical, sonochemical and ionothermal approaches.[9] Further development of metal–organic materials and their applications, however, requires clean, efficient and scalable methods of their synthesis.[10] In the context of environmentally-friendly routes for making ZIFs, syntheses of ZIF-8[11,12] and its Co(II)-analogue ZIF-67[12] in water or high-pressure steam[13] were recently reported. Solution-based methodologies, however, suffer from the need to use soluble reagents, in the form of toxic and/or corrosive metal salts, which generate acids as a byproduct of MOF synthesis and are often susceptible to solvolysis. In contrast, using inexpensive metal oxides as synthetic precursors would offer an opportunity to avoid toxic and corrosive metal salts[14] and external bases.[15] Indeed, the desirability of metal oxides as

[a]*Department of Chemistry and FRQNT Centre for Green Chemistry and Catalysis, McGill University, Montreal, Canada. E-mail: tomislav.friscic@mcgill.ca; Fax: +1-514-398-3757; Tel: +1-514-398-3959*

[b]*Department of Chemical Engineering, Laval University, G1V 0A6, Quebec City and FRQNT Centre for Green Chemistry and Catalysis, Canada. E-mail: trong-on.do@gch.ulaval.ca*

[c]*Department of Chemistry, University of Cambridge, Cambridge, UK*

†Electronic supplementary information (ESI) available: Experimental and analytical details, synthesis of salt additives, results of PXRD, SSNMR, FTIR-ATR, TGA and gas sorption measurements. CCDC 922334 for (**Hcaf**)(HSO_4) (a summary of data collection is given in ESI Table S1). For ESI and crystallographic data in CIF or other electronic format see DOI: 10.1039/c3gc40520f

‡Currently at Oxford University.

Published on 03 June 2013. Downloaded by Université Laval on 15/05/2014 21:48:14.

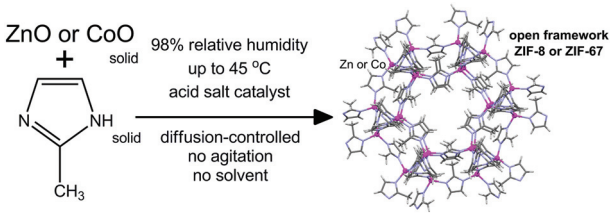

Scheme 1

starting materials for industrial MOF synthesis has been recently recognised.[16] However, the low solubility and relatively inert nature caused by high lattice enthalpies (*e.g.* >4 MJ mol^{-1} for ZnO)[17] make metal oxides incompatible with solution chemistry, unless aggressive conditions (*e.g.* mineral acids, conventional or microwave heating) are used.[18,19] Development of mild methodologies for MOF synthesis from metal oxides, therefore, calls for the development of novel and non-conventional solvent-free or solid-state methodologies.

While solvent-free metal- and oxide-based ZIF syntheses in the melt have been reported,[20] our aim, in contrast, is to develop general solvent-free approaches that would be simple, not energy-intensive, and operate at or near room temperature. Although mechanochemistry[21] represents a potential route to achieve this goal, it has not yet demonstrated a sufficiently broad scope. To develop a simple and scalable ZIF synthesis without sacrificing the arguments of solvent-free and low-energy chemistry, we proposed[22] "accelerated aging": a synthetic concept inspired by processes of geological biomineralization known as mineral weathering (or mineral neogenesis). Mineral weathering generates metal–organic minerals by long-term exposure of oxide or sulfide minerals to small molecules of biological origin.[23] We discovered[22] that reactions resembling mineral weathering can be used to synthesise close-packed ZIFs with quartz (*qtz*),[21] diamondoid (*dia*)[13] and zinc imidazolate (*zni*)[24] topologies, by aging of ZnO with a suitable imidazole in a solvent-free, low-energy manner. The normally slow aging reactions were accelerated by a combination of mild temperature (45 °C), high relative humidity (RH) and catalytic amounts (*ca.* 5 mol% or less) of ammonium (NH_4^+) salt. While such accelerated aging was readily scalable to 10 grams, we were not able to prepare microporous structures central to modern materials chemistry.

We now demonstrate how accelerated aging can be adapted and optimised for the quantitative synthesis of microporous materials in multi-gram amounts. In particular, we have developed a multi-gram synthesis of microporous ZIF-8 directly from ZnO and 2-methylimidazole (**HMeIm**) (Scheme 1). We also show this methodology is applicable to other metals by synthesizing microporous ZIF-67 directly from CoO, and to other ligands by synthesizing the microporous RHO-topology ZIF based on zinc and 2-ethylimidazole (**HEtIm**, Fig. 1a). We have also observed previously unreported Co(II) analogues of Zn(**EtIm**)$_2$ frameworks with quartz (*qtz*) and RHO topologies.

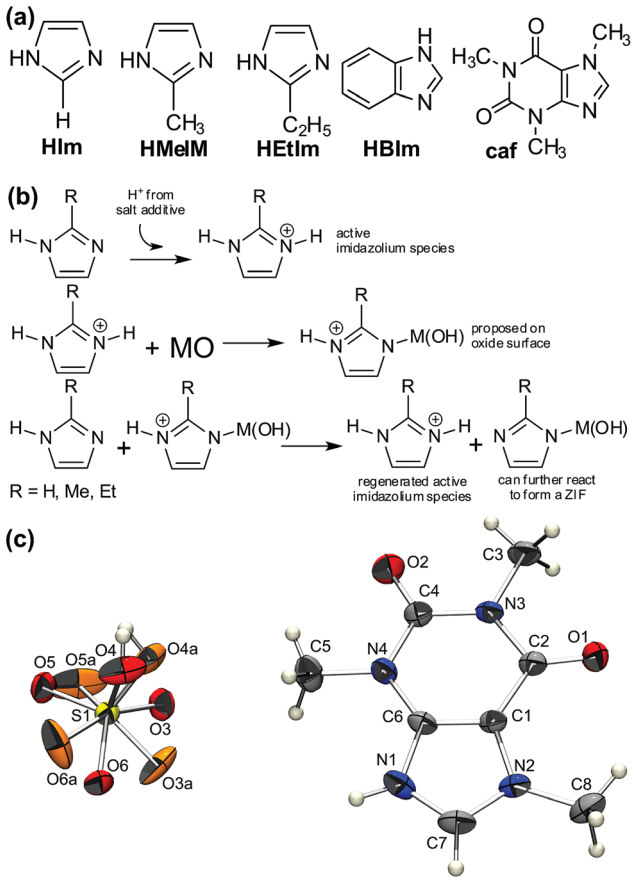

Fig. 1 (a) Imidazoles used for the synthesis of salt additives; (b) proposed mechanism of accelerated aging[20] and (c) ORTEP view of the asymmetric unit of (**Hcaf**)(HSO_4) at 30% ellipsoid probability. Oxygen atoms of the disordered hydrogensulfate are shown in red and orange for occupancies 0.76 and 0.24, respectively. M represents a divalent metal, such as zinc or cobalt.

Experimental section

Preparation of reaction mixtures

Our first experiments into accelerated aging[22] utilised reaction mixtures prepared by manual mixing of reactants and the salt additive using a ceramic or agate mortar and pestle. This procedure minimised unwanted mechanical activation, but is also tedious and likely to be insufficiently reproducible for a systematic study of reaction conditions. For current work we instead prepared reaction mixtures by brief (5 minutes) automated milling, which rapidly and reproducibly mixed the sample without noticeable mechanochemical activation. For several selected reactions, aging of mixtures prepared by mechanical or manual mixing yielded almost identical results (ESI Fig. S7–S11†), indicating that mechanical activation is not critical for accelerated aging and showing that manual mixing is a viable, inexpensive alternative to sophisticated electrical equipment. The method of mixing did not affect the tendency (ESI Fig. S31†) of ZIF-8 to collapse into *dia*-Zn(**MeIm**)$_2$ in the presence of $(NH_4)_2SO_4$.

 This journal is © The Royal Society of Chemistry 2013

Published on 03 June 2013. Downloaded by Université Laval on 15/05/2014 21:48:14.

For reactions conducted at the 0.5 gram scale, the reaction mixtures were normally prepared by brief (5 minutes) milling of 2 mmol of metal oxide (ZnO, CoO), 4 mmol of the imidazole ligand (**HMeIm** or **HEtIm**), and 4 mol% (unless otherwise specified) of the salt additive [$(NH_4)_2SO_4$), $KHSO_4$, $(\mathbf{H_2Im})_2SO_4{\cdot}H_2O$, (**Hcaf**)($HSO_4$), (**Hcaf**)($HSO_4$)·$H_2O$, or $(\mathbf{H_2BIm})_2(SO_4)$, percentage calculated with respect to ZnO]. Mixing was conducted in a 10 mL stainless steel milling jar using one stainless steel ball of 7 mm diameter. Unless specified otherwise, the mixtures were mixed in a Retsch MM400 ball mill at 29.5 Hz. Reactions at the 5 grams scale were premixed in either 10 mL or 25 mL jars.

Accelerated aging experiments

Samples containing no salt additive, or salt additives other than $(NH_4)_2SO_4$, were left to age in commercial (Secador®) chambers of 22 dm^3 volume in which humidity was controlled by equilibration with a saturated K_2SO_4 solution (for 98% RH) or pure water (for nominal 100% RH). These controlled humidity chambers were situated in a walk-in incubator set at 45 °C. Samples containing $(NH_4)_2SO_4$ salt additive were placed in glass chambers under the same conditions, to avoid possible absorption of NH_3 within the container walls and contamination of subsequent samples. Humidity was monitored with Traceable® Humidity-on-a-Card indicators. Upon complete disappearance of X-ray reflections of the metal oxide in powder X-ray diffraction (PXRD) patterns, samples for thermogravimetric analysis (TGA) were washed overnight with water, methanol (MeOH), or acetonitrile to remove catalyst or any remaining ligand.

Results and discussion

Selection of salt additives

The ESI† contains extensive experimental and analytical (X-ray diffraction, spectroscopy, thermal analysis and gas sorption) data, of which only the most important and conclusive are highlighted in text.

For generalizing accelerated aging reactivity we considered the acid-catalysis mechanism proposed for earlier experiments involving $(NH_4)_2SO_4$ (Fig. 1b).[21] We realised that the mechanism allows the reactions to be induced by a number of protic salts, thus providing an opportunity to control and optimise accelerated aging reactions. We focused on salts of imidazole (**HIm**), **HMeIm**, **HEtIm** and benzimidazole (**HBIm**) (Fig. 1) which, due to the chemical similarity to ZIF ligands might become incorporated into the final product and minimise the need for subsequent washing. We also explored salts of caffeine (**caf**), which might provide a highly acidic species suitable to initiate the acid-catalysis mechanism but unable to permanently interfere with metal–ligand bond formation due to methylation of N–H groups. To ensure reproducibility, we sought salts that are readily prepared, characterized, handled and stored. Screening indicated benzimidazolium sulfate $(\mathbf{H_2BIm})_2(SO_4)$, caffeinium hydrogensulfate (**Hcaf**)(HSO_4) (Fig. 1c), hydrated imidazolium sulfate[22,25a] $(\mathbf{H_2Im})_2SO_4{\cdot}2H_2O$ and caffeinium hydrogensulfate hydrate[25b] (**Hcaf**)(HSO_4)·H_2O as the most suitable candidates. Salts were characterized by thermogravimetric analysis (TGA), calorimetry (DSC), Fourier-transform infrared attenuated total reflection (FTIR-ATR) spectroscopy, powder X-ray diffraction (PXRD) and, where needed, by elemental analysis, single crystal X-ray diffraction and solid-state NMR (SSNMR). Salts provided a range of pK_a values potentially relevant in reaction design (calculated pK_a values for $\mathbf{Hcaf}^+$, $\mathbf{H_2Im}^+$, $\mathbf{H_2BIm}^+$ and HSO_4^- are −0.92, 6.97, 5.79 and 1.90).[26]

Synthesis of microporous ZIF-8

Screening for accelerated aging synthesis of ZIF-8 was conducted by aging of mechanically prepared mixtures of 2 mmol of ZnO (160 mg), 4 mmol of **HMeIm** (328 mg) and 4 mol% (with respect to zinc) of a salt additive. As evidenced by PXRD, just mixing did not induce any notable reaction for (**Hcaf**)(HSO_4), (**Hcaf**)(HSO_4)·H_2O and $(\mathbf{H_2BIm})_2(SO_4)$ additives (ESI,† Section 2). With $(\mathbf{H_2Im})_2SO_4{\cdot}2H_2O$, however, weak X-ray reflections of ZIF-8 were noticeable immediately after mixing.

After four days at 98% RH and 45 °C all reaction mixtures remained solid and, as revealed by PXRD, underwent partial conversion to ZIF-8. PXRD features of ZnO were least apparent for reactions containing $(\mathbf{Hcaf})_2(SO_4)$ and $(\mathbf{H_2Im})_2SO_4{\cdot}2H_2O$, indicating higher conversion (Fig. 2). After 11 days aging with (**Hcaf**)(HSO_4), reflections of ZnO were no longer distinguishable from those of ZIF-8. Calcination of the washed and evacuated sample in air gave 36.3% residue (calculated for ZnO: 35.8%), indicating quantitative formation of ZIF-8 (ESI† Sections 2 and 5). Interestingly, PXRD revealed that (**Hcaf**)(HSO_4)·H_2O was less efficient in accelerated aging than its anhydrous form (**Hcaf**)(HSO_4) (ESI Fig. S1†).

For $(\mathbf{H_2BIm})_2(SO_4)$ additive, PXRD analysis revealed unreacted ZnO even after 61 days. With $(\mathbf{H_2Im})_2SO_4{\cdot}2H_2O$, weak X-ray reflections of ZnO were still discernible in the PXRD pattern of the reaction mixture after 40 days (*e.g.* ESI Fig. S4, S5†). TGA of the washed and evacuated sample yielded 39.0% residue, corresponding to *ca.* 87% conversion (Table 1). However, for this salt additive the PXRD pattern after washing also displayed weak reflections of an unknown material.

Thus, our systematic screen revealed that all investigated salt additives have enabled the formation of ZIF-8 by accelerated aging. Moreover, the use of (**Hcaf**)(HSO_4) as the salt additive enabled the quantitative transformation of ZnO into ZIF-8 at 98%RH and 45 °C. This represents a significant advance with respect to our preliminary report of accelerated aging, which employed $(NH_4)_2SO_4$ as the catalytic salt additive, and in which the direct conversion of ZnO into ZIF-8 was not possible. Accelerated aging reactivity was also evident by FTIR-ATR spectroscopy (ESI,† Section 4) which evidenced the disappearance of the ligand N–H band centered at 2600 cm^{-1}. As (**Hcaf**)(HSO_4) was particularly efficient for the accelerated aging synthesis of ZIF-8, and even induced formation of ZIF-8 at ambient temperature and humidity (ESI Fig. S2, S3†), we decided to verify its structure by SSNMR. Cross-polarization

Published on 03 June 2013. Downloaded by Université Laval on 15/05/2014 21:48:14.

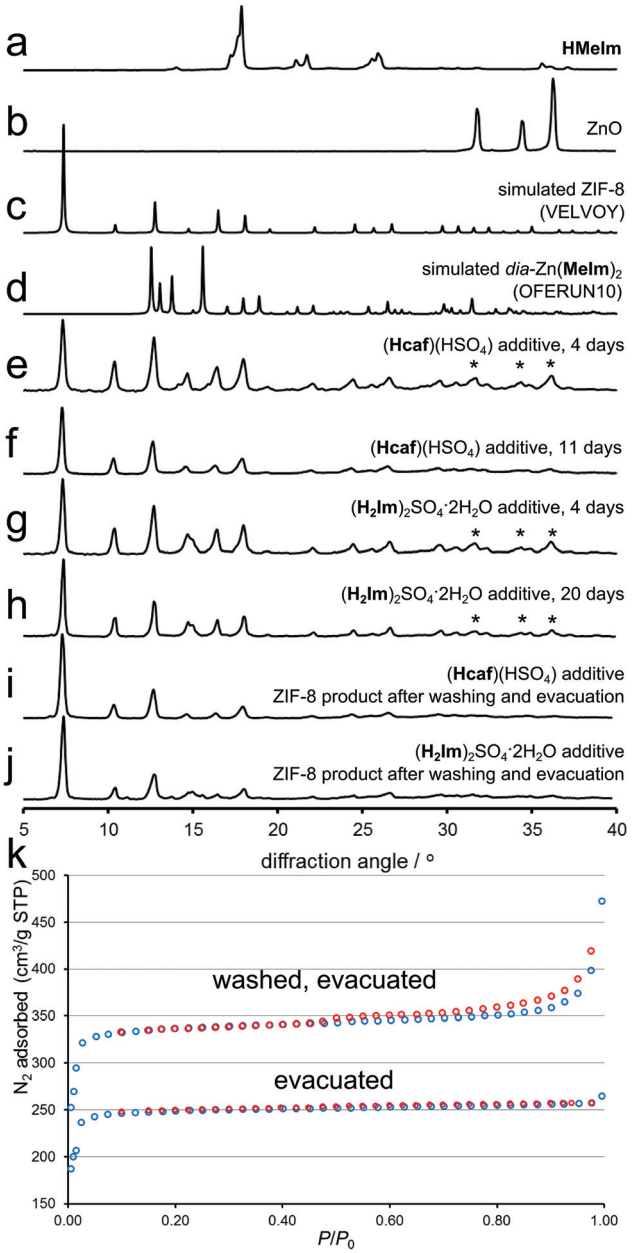

Fig. 2 PXRD patterns for: (a) **HMeIm**; (b) ZnO; (c) ZIF-8 (MECWEX); (d) *dia*-Zn(**MeIm**)$_2$ (OFERUN10) and accelerated aging reactions after: (e) 4 days and (f) 11 days with (**Hcaf**)(HSO$_4$); (g) 4 days and (h) 20 days with (**H$_2$Im**)$_2$SO$_4$·2H$_2$O; (i) ZIF-8 made using (**Hcaf**)(HSO$_4$) after washing and evacuation and (j) ZIF-8 made using (**H$_2$Im**)$_2$SO$_4$·2H$_2$O after washing with acetonitrile and evacuation. Characteristic ZnO reflections, where resolvable from those of ZIF-8, are labeled with '*'. (k) N_2 sorption of ZIF-8 made by aging with (**Hcaf**)·(HSO$_4$): pristine (below) and after washing (above).

magic-angle spinning (CP-MAS) ^{15}N spectrum of (**Hcaf**)·(HSO$_4$) was consistent with **caf** protonation (ESI Fig. S34†).[27]

Selected TGA and nitrogen sorption measurements on samples prepared by accelerated aging are summarised in Table 1. Importantly, pristine ZIF-8 obtained by aging with (**Hcaf**)·(HSO$_4$) or (**H$_2$Im**)$_2$SO$_4$·2H$_2$O additives exhibited Brunauer–Emmett–Teller (BET) areas of 822 m^2 g^{-1} and 930 m^2 g^{-1}, respectively, confirming a microporous structure.

Table 1 Metal oxide conversion (%) and porous properties for selected ZIF-8 and ZIF-67 prepared by accelerated aging at 45 °C and 98% RH[a,b]

Product	Additive	Conversion (%)	BET area (m^2 g^{-1})	Pore volume (cm^3 g^{-1})
ZIF-8	(**Hcaf**)(HSO$_4$)	99	822[c], 1137[d]	0.40[c], 0.58[d]
ZIF-8	(**H$_2$Im**)$_2$(SO$_4$)·2H$_2$O	87	930[c]	0.44[c]
ZIF-8	KHSO$_4$[e]	96	1413[d]	0.69[d]
ZIF-67	(**Hcaf**)(HSO$_4$)	72	943[c], 1115[d]	0.45[c], 0.56[d]
ZIF-67	KHSO$_4$	61	1058[d]	0.53[d]
ZIF-67	(NH$_4$)$_2$SO$_4$	71	1227[d]	0.60[d]

[a] Conversion based on TGA of samples washed and evacuated to remove catalytic additives and excess ligand. [b] Table gives only selected results, faster and higher conversions into ZIF-8 (99%) and ZIF-67 (77%) were observed at 45 °C, 100% RH. [c] Before washing. [d] After washing. [e] Using 20% excess **HMeIm**.

These values are consistent with those observed for ZIF-8 (typically between 800 m^2 g^{-1} and 1600 m^2 g^{-1}).[28–30]

We find it remarkable that ZIF-8 obtained by a heterogeneous, oxide-based process, without excess reagents or prior activation, exhibits microporosity comparable to solution-made samples. The BET area of ZIF-8 prepared with (**Hcaf**)·(HSO$_4$) could be further increased to 1137 m^2 g^{-1} by washing with acetonitrile, which was explained by the removal of the salt additive included in the porous product. We note that this value exceeds most of those reported for ZIF-8 obtained at room temperature or in water.[29,31] To explore whether large organic cations are necessary for the solid-state assembly of ZIF-8, we also explored KHSO$_4$ as a small-molecule inorganic additive (4 mol%). After 2 weeks PXRD indicated the transformation of the reaction mixture into ZIF-8 (ESI Fig. S6†). Although complete disappearance of ZnO was not observed, this experiment demonstrates the formation ZIF-8 without any organic additives or solvents.

Structural instability of ZIF-8

The formation of stable microporous ZIF-8 when using protonated imidazolium and xanthine salt additives is an important step in developing accelerated aging reactivity, as our initial results[22] involving ammonium (NH$_4^+$) salt additives yielded ZIF-8 only as a short-lived intermediate before forming close-packed *dia*-Zn(**MeIm**)$_2$. Sensitivity of ZIF-8 to collapse in the presence of ammonium salts is surprising in the light of the known stability of this framework to water, milling, temperature and pressures up to *ca.* 10^3 atmospheres.[28,32,33] To confirm that the collapse of ZIF-8 into the *dia*-framework in the presence of NH$_4^+$ is not an artefact of accelerated aging, a solution-made sample[17] of ZIF-8 was manually ground with 4 mol% of (NH$_4$)$_2$SO$_4$ (based on zinc). As indicated by PXRD, aging of the sample at 45 °C at high humidity led to the degradation into the *dia*-framework (Fig. 3). Such collapse of ZIF-8 was also observed for a sample of commercial Basolite Z1200 (ESI Fig. S30†) upon mixing with 4 mol% (NH$_4$)$_2$SO$_4$ and exposing to high humidity.

 This journal is © The Royal Society of Chemistry 2013

Published on 03 June 2013. Downloaded by Université Laval on 15/05/2014 21:48:14.

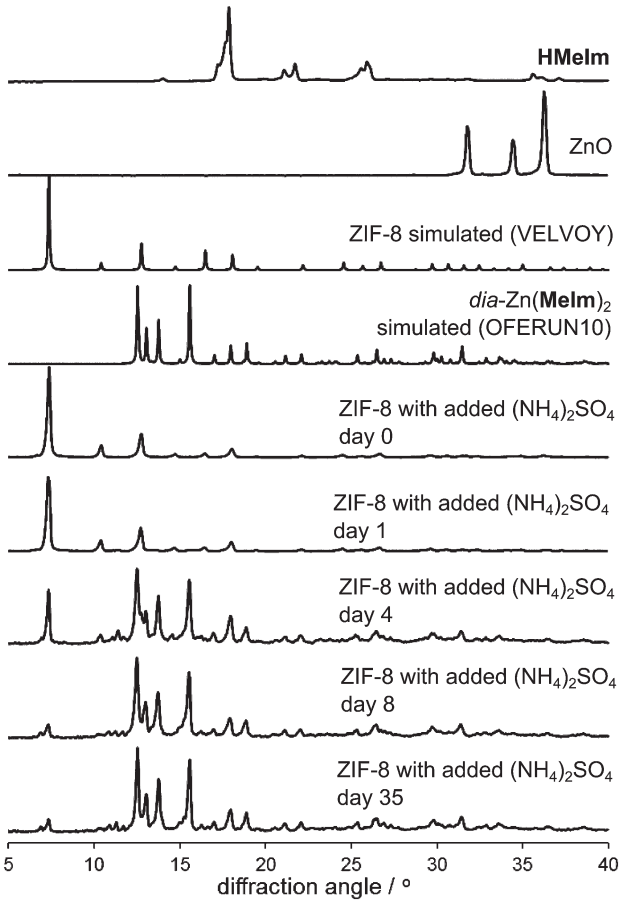

Fig. 3 PXRD patterns for the degradation of ZIF-8 upon mixing with 4 mol% $(NH_4)_2SO4$ and aging at 45 °C and 100% RH.

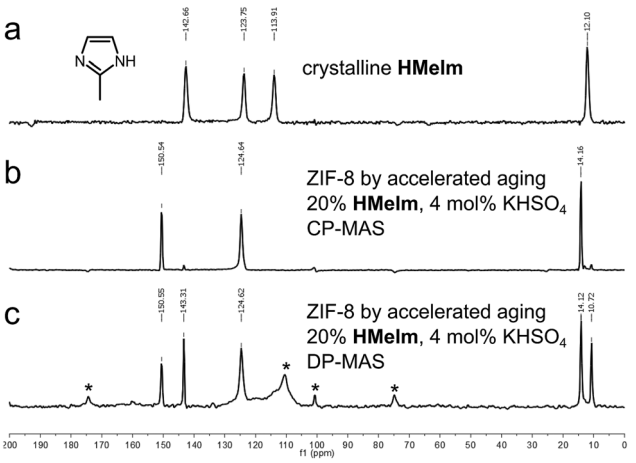

Fig. 4 Solid-state MAS ^{13}C SSNMR spectra for experiments involving 20 mol% excess **HMeIm** and 4 mol% $KHSO_4$: (a) **HMeIm**; (b) CP spectrum of ZIF-8 prepared at 98% RH and (c) DP spectrum of the same sample. Spinning sidebands and the signal of the teflon insert (110 ppm) are labelled by '*'. The spectra show that the small excess of **HMeIm** deliberately added to the reaction is invisible in CP-mode, but appears under DP, consistent with inclusion as a guest in the ZIF product.

Ligand deactivation by inclusion in the nascent framework

We speculated that incomplete reactions observed for all salts except (**Hcaf**)(HSO_4) might be associated either with evaporative loss of ligand during aging, or the entrapment of ligand in the nascent porous product. The TGA study of **HMeIm** in nitrogen flow indicated that up to 3% of material is lost after 14 hours at 45 °C (ESI Fig. S45†). While the loss of **HMeIm** is probably over-exaggerated by the gas flow, we were urged to address this possibility. Consequently, we again explored the synthesis of ZIF-8 using $KHSO_4$, a salt less active than (**Hcaf**)(HSO_4), but now with a 20% excess of **HMeIm**. After two weeks aging at 45 °C and 98% RH, the sample was analysed by TGA and BET analysis (Table 1, also ESI† Section 5). Visual comparison of PXRD patterns of samples with and without excess **HMeIm** did not reveal significant differences, indicating that ligand evaporation is not a factor limiting accelerated aging of ZIF-8. Despite residual ZnO, however, PXRD indicated complete disappearance of **HMeIm**. To reconcile these observations, we next turned to magic angle spinning (MAS) SSNMR (Fig. 4). Comparison of cross-polarization (CP) and direct polarization (DP) spectra revealed two types of methylimidazole species in the aged samples. Whereas both ^{13}C CP-MAS and DP-MAS NMR revealed imidazolate anions of the ZIF-8 framework, DP-MAS also detected an additional species whose chemical shifts resembled those of pure **HMeIm**. This was attributed to excess ligand that is either amorphous or included in the pores of ZIF-8 (Fig. 4), which would explain its absence from the PXRD pattern. Consequently, we concluded that the formation of ZIF-8 could sometimes be hindered by the *in situ* entrapment of the ligand within the porous framework.

Synthesis of cobalt-based ZIF-67

After Zn^{2+}, the second most frequently used ion in ZIF design is Co^{2+}.[7,8,34] In mechanochemical reactions, CoO is noticeably less active than ZnO: we unsuccessfully attempted the mechanosynthesis of ZIF-67 using the ILAG procedure previously used[21] to make ZIF-8. After 90 minutes milling, PXRD did not indicate any trace of reaction (ESI Fig. S24†). Poor reactivity of CoO was also noted in a recent exploration of thermochemical ZIF syntheses from the melt.[20b]

We investigated the accelerated aging synthesis of ZIF-67 from CoO using (**Hcaf**)(HSO_4) and $KHSO_4$ as additives. After 8 days, PXRD indicated the formation of the *sod*-topology ZIF-67 and disappearance of CoO with (**Hcaf**)(HSO_4) additive (Fig. 5). ZIF-67 formation was also observed without salt additives, but the reaction was clearly slower (ESI Fig. S14†). With $KHSO_4$, the disappearance of CoO was observed after 11 days at 45 °C, 98% RH. The PXRD pattern of the reaction mixture also indicated a not yet identified by-product (noted by an X-ray reflection below $2\theta = 15°$, Fig. 5d) that disappeared after washing with water. For both reactions, ZIF-67 formation was accompanied by the black reaction mixture turning purple. FTIR-ATR spectra of ZIF-67 were almost identical to those of isostructural ZIF-8 (ESI,† Section 4). Due to X-ray fluorescence, CoO disappearance could not be ascertained by PXRD and we

Published on 03 June 2013. Downloaded by Université Laval on 15/05/2014 21:48:14.

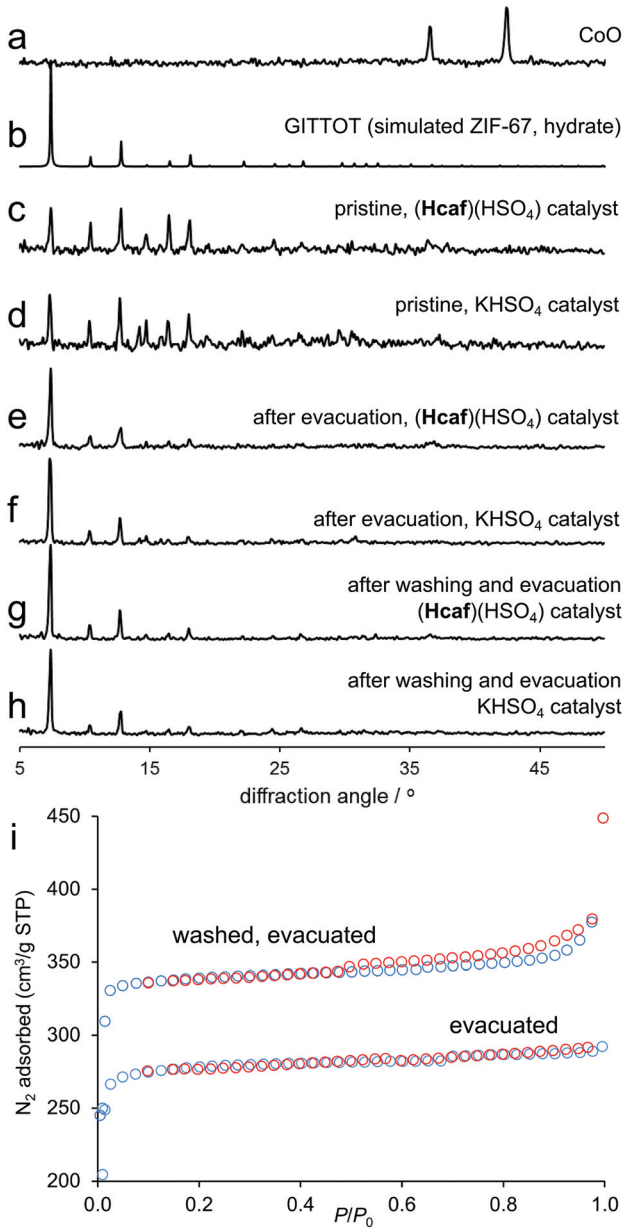

Fig. 5 Selected PXRD patterns for accelerated aging of CoO and **HMeIm**: (a) commercial CoO (97%); (b) simulated for ZIF-67 (GITTOT); (c) sample obtained by aging with (**Hcaf**)(HSO_4) for 8 days; (d) sample obtained by aging with $KHSO_4$ for 11 days; (e) evacuated sample obtained by aging with (**Hcaf**)(HSO_4); (f) evacuated sample obtained by aging with $KHSO_4$; (g) sample obtained by aging with (**Hcaf**)(HSO_4) after washing with MeOH and evacuation; (h) sample obtained by aging with $KHSO_4$ after washing with water and evacuation and (i) N_2 sorption isotherms for ZIF-67 obtained by aging with (**Hcaf**)(HSO_4) before (top) and after (bottom) washing with MeOH.

analyzed the materials by TGA. The results indicated 72% conversion with (**Hcaf**)(HSO_4) additive, and 61% conversion with $KHSO_4$. Although not quantitative, these reactions demonstrate a simple new entry into making porous MOFs directly from CoO without solvothermal conditions, melting or milling. Like in ZIF-8 synthesis, samples immediately exhibited high porosity: BET area of the pristine sample prepared using (**Hcaf**)(HSO_4) was 943 $m^2\ g^{-1}$ (Fig. 5i, Table 1). After washing, the area increased to 1115 $m^2\ g^{-1}$. It is remarkable that, despite lower conversion of CoO, ZIF-67 samples displayed higher microporosity than their ZIF-8 counterparts (Table 1). In further contrast to ZnO, accelerating aging of CoO and **HMeIm** with 4 mol% $(NH_4)_2SO_4$ did not lead to the formation of close-packed *dia*-structure. Instead, the product was always the porous ZIF-67 (71% conversion for a 5 gram synthesis, Table 1).

Synthesis of ZIFs based on 2-ethylimidazole

We next explored the synthesis of open ZIFs from **HEtIm**, known to form two porous ZIFs with zeolite ρ (RHO, Fig. 6a) and analcime topologies, as well as a non-porous phase with quartz topology (*qtz*).[21,35] Accelerated aging with NH_4^+ salts

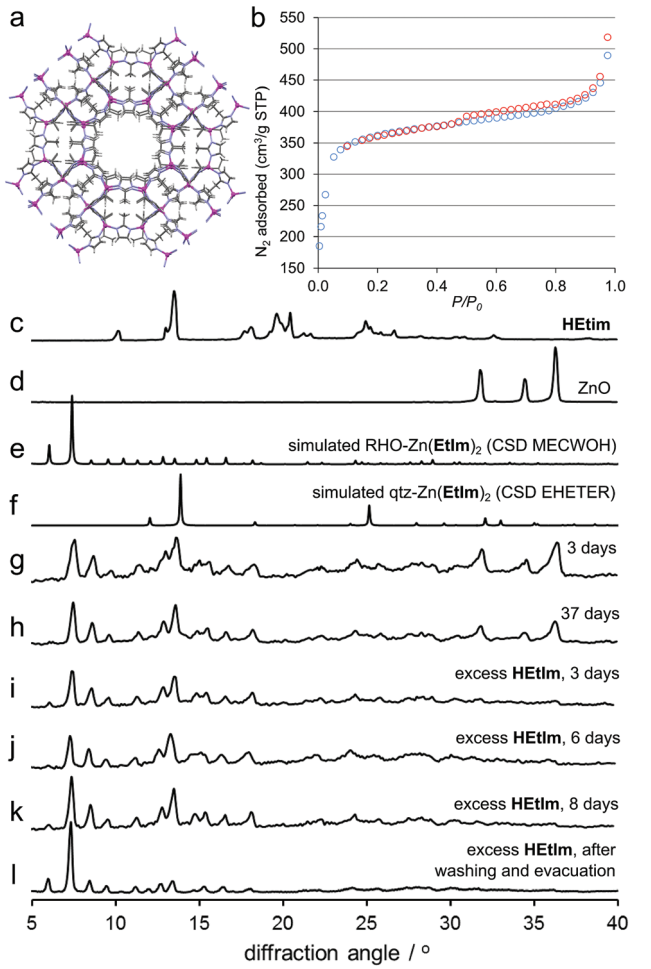

Fig. 6 (a) Fragment of the crystal structure of RHO-Zn(**EtIm**)$_2$ (CCDC code MECWOH);[30] (b) nitrogen sorption of RHO-Zn(**EtIm**)$_2$ prepared by accelerated aging with excess **HEtIm** and 4 mol% (**Hcaf**)(HSO_4). PXRD patterns: (c) **HEtIm**; (d) ZnO; (e) simulated for RHO-Zn(**EtIm**)$_2$; (f) simulated for *qtz*-Zn(**EtIm**)$_2$; (g) accelerated aging of 1 : 2 mixture of ZnO and **HEtIm**, 3 days; (h) accelerated aging of 1 : 2 mixture of ZnO and **HEtIm**, 37 days; (i) accelerated aging of mixture of ZnO and **HEtIm** (150% excess), 3 days; (j) accelerated aging of mixture of ZnO and **HEtIm** (150% excess), 6 days; (k) accelerated aging of mixture of ZnO and **HEtIm** (150% excess), 8 days and (l) sample represented by pattern (k) after washing with methanol and evacuation.

This journal is © The Royal Society of Chemistry 2013

Published on 03 June 2013. Downloaded by Université Laval on 15/05/2014 21:48:14.

previously yielded exclusively the *qtz*-framework, *via* the short-lived RHO intermediate. Consequently, we speculated that a different salt could enable the synthesis of a porous ZIF as described for ZIF-8 in previous section. Indeed, aging of ZnO and two equivalents of **HEtIm** with either (**Hcaf**)(HSO_4), (**Hcaf**)-(HSO_4)·H_2O or $KHSO_4$ yielded the RHO framework that was identified by comparison of the PXRD pattern to that simulated for the reported structure (CSD code MECWOH). The additives were present in 4–7 mol% amounts, based on ZnO. In contrast to aging with NH_4^+ salts, the RHO structure did not collapse even after a month (Fig. 6). However, the reactions never proceeded to the complete disappearance of ZnO and appeared to halt after 4 days. As the PXRD patterns of reaction mixtures indicated residual ZnO, but not **HEtIm**, we speculated that reactivity could again be limited by the absorption of the unreacted ligand in the porous product, as observed for ZIF-8 synthesis using $KHSO_4$ catalyst. In such a scenario, excess **HEtIm** would play the role of a space-filling or templating agent that becomes trapped in the porous materials and is no longer capable of reaction. To verify this possibility, we conducted the reaction in the presence of 150 mol% excess **HEtIm**. Under such conditions, complete disappearance of ZnO X-ray reflections was observed within a week (Fig. 6i–k). The RHO-Zn(**EtIm**)$_2$ obtained by accelerated aging with excess ligand was also investigated by SSNMR. CP-MAS measurements provided ^{13}C signals consistent with 2-ethylimidazolate building blocks of the published zeolite RHO structure. However, DP-MAS also revealed ^{13}C signals resembling those of crystalline **HEtIm** (ESI Fig. S33†). These signals were interpreted as residual ligand included in the ZIF, consistent with the **HEtIm** reactant becoming inactivated by entrapment in the porous product during its formation.

After washing the sample with methanol, the RHO topology ZIF demonstrated a high porosity of 1241 $m^2\ g^{-1}$ (Fig. 6b). Calculations in the P/P_0 range 0.05–0.20 of the nitrogen adsorption isotherm gave a pore volume of 0.66 $cm^3\ g^{-1}$. To the best of our knowledge, this is the first selective synthesis, and the first measurement of bulk porosity for this ZIF. Namely, this framework was previously obtained only in the form of single crystals in a mixture with other products of solvothermal synthesis.[35] The RHO-framework made by accelerated aging did not collapse after several months following washing and evacuation (ESI Fig. S20–S23†).

Attempts to synthesize the cobalt analogue of RHO-Zn(**EtIm**)$_2$ were conducted using 200% excess of **HEtIm**. The synthesis was only partially successful, as the RHO-structure was observed in a mixture with a phase that is, according to PXRD, isostructural to non-porous *qtz*-Zn(**EtIm**)$_2$ (ESI Fig. S23†).

Improving reaction speed and yield: quantitative reactions at 100% RH

All described experiments clearly demonstrate the ability to convert metal oxides into porous metal–organic materials using reactivity reminiscent of natural mineral weathering. We also investigated improvements in our experiment design that would make such reactivity attractive from a synthetic standpoint. We established that reactions can be further accelerated (Fig. 7) at 100% RH, established by using pure water

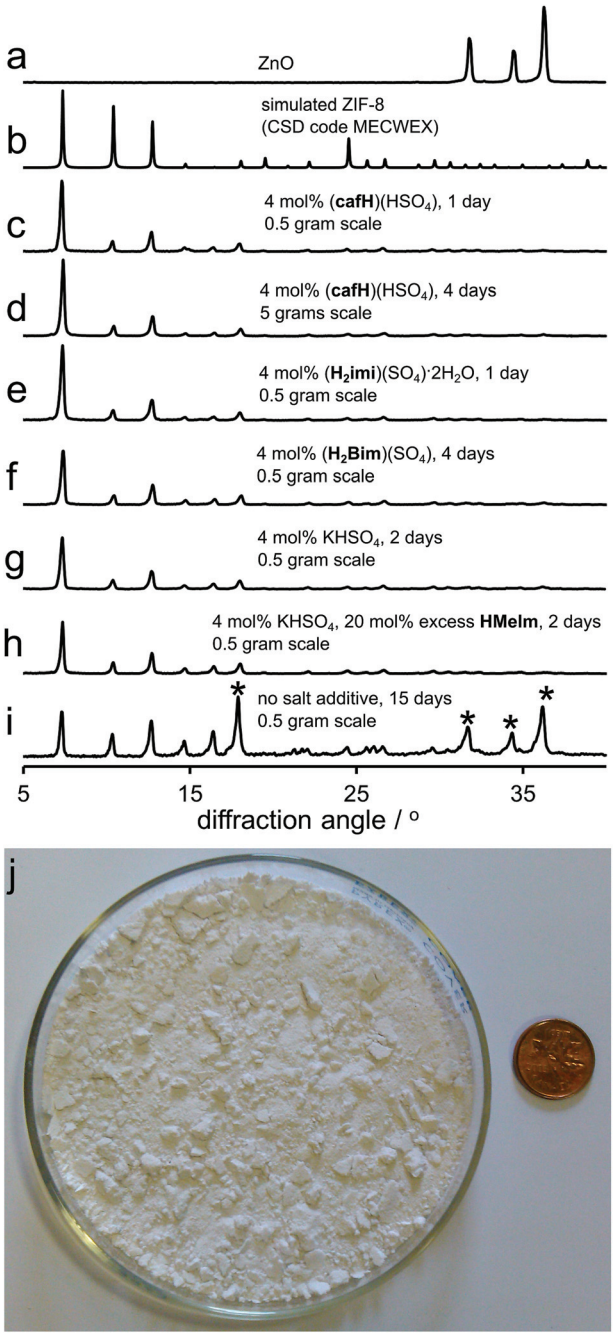

Fig. 7 PXRD patterns for ZIF-8 synthesis by accelerated aging of ZnO and **HMeIm** at 100% RH and 45 °C: (a) ZnO; (b) calculated for ZIF-8; (c) reaction with 4 mol% (**Hcaf**)(HSO_4) after 1 day; (d) reaction with 4 mol% (**Hcaf**)(HSO_4) after 4 days, scaled to 5 grams; (e) reaction with 4 mol% (**H_2Im**)$_2$(SO_4)·2H_2O after 1 day; (f) reaction with 4 mol% (**H_2BIm**)$_2$(SO_4) after 4 days; (g) reaction with 4 mol% $KHSO_4$ after 2 days; (h) reaction with 4 mol% $KHSO_4$ and 20 mol% excess **HMeIm** after 2 days and (i) mixture of ZnO and **HMeIm** without a salt additive after 15 days, highly deliquescent. Characteristic reflections of ZnO and **HMeIm** are labeled with '*'. (j) 5 grams of ZIF-8 made by quantitative reaction of ZnO and **HMeim**, with 4 mol% (**Hcaf**)(HSO_4) after 4 days at 45 °C and 100% RH. Sample size is illustrated by comparison to Canadian one penny coin.

Published on 03 June 2013. Downloaded by Université Laval on 15/05/2014 21:48:14.

rather than saturated K_2SO_4 solution as the vapour source. At 0.5 gram scale, such conditions led the complete transformation of ZnO to ZIF-8 in 2 days for (**Hcaf**)(HSO_4) and for (**H_2Im**)(SO_4)·2H_2O. Conversion of ZnO into ZIF-8 with (**HBIm**)$_2$(SO_4) reached 93% after 4 days (Fig. 7c–f). Reactions involving $KHSO_4$, with or without 20% excess **HMeIm**, demonstrated complete disappearance of ZnO in two days (Fig. 7g). Interestingly, even after such reactivity enhancement the ability of (**Hcaf**)(HSO_4)·H_2O to accelerate ZIF-8 synthesis lagged behind that of (**Hcaf**)(HSO_4) (ESI Fig. S27†).

Two identical experiments at 100% RH and 45 °C confirmed that a 5-gram scale-up of ZIF-8 synthesis with (**Hcaf**)(HSO_4) was completed in 4 days (Fig. 7d and j; ESI Fig. S29†). These reaction conditions also enabled the 77% conversion of a 1 : 2 stoichiometric mixture of CoO and **HMeIm** into ZIF-67 within 3 days (ESI Fig. S50†). Efficiency of ZIF-67 synthesis by accelerated aging is highlighted by comparison to a recent thermochemical synthesis which achieved 67% oxide conversion after 2.5 days thermal treatment (100 °C–160 °C) and using 100% ligand excess.[20b]

To verify the importance of increased relative humidity for improving accelerated aging reactions, we conducted numerous comparative experiments at a smaller (0.5 gram) scale. The reactions were all conducted for the same period of time, at 45 °C and without disturbing the samples, at either 98% or 100% RH. All reactions conducted at 98% RH consistently yielded lower conversion than those at 100% RH, demonstrating that the small increase in relative humidity is indeed responsible for the dramatic improvement in reaction yield and speed.

Samples made by accelerated aging remain free-flowing powders throughout the process. If the reaction of ZnO and **HMeIm** at 100% RH is attempted without a salt additive, the mixture partially deliquesces into a liquid. Synthesis under such conditions is slow and incomplete even after 15 days (Fig. 4i).

It is worth highlighting that accelerated aging enabled a quantitative conversion (*i.e.* >99%) of a 1 : 2 stoichiometric mixture of ZnO and **HMeIm** into ZIF-8 on a multi-gram scale. Whereas ZIF-8 can be synthesized rapidly (in 4 hours) at room temperature from zinc nitrate and **HMeIm** in methanol, reported yields are *ca.* 50% even with 4-fold excess of ligand.[30a,31] A rapid solvothermal synthesis gave ZIF-8 in 63% yield.[30b] We believe that the high atom-efficiency of accelerated aging might be explained by the high local concentration of **HMeIm** in our solvent-free system. This is corroborated by a recent systematic study of ZIF-8 synthesis from zinc nitrate in aqueous solution conducted by Kida *et al.*, who found that very high yields can be obtained using a large (20- to 50-fold) excess of ligand.[30c]

Conclusions

It was demonstrated that ZnO and CoO, despite their high melting points and high lattice stabilisation energies (*ca.* 4 MJ mol^{-1}),[17] can spontaneously assemble into stable microporous materials under mild, diffusion-controlled conditions. Five gram (in principle, at least ten gram[22]) reactions achieved quantitative conversion without agitation, yielding products that are microporous even without activation. Although such efficiency is surprising for diffusion-controlled reactions, we note that cocrystal formation was recently found achievable by simple mixing of reactants, if molecular diffusion was enhanced by organic vapours,[36] deliquescence[37] or diminution of particle size.[38] Similar principles are likely to be valid for accelerated aging. Accelerated aging is not simply explained by deliquescence but is regulated by the salt additive. Without such additives, reactions partially deliquesced and liquefied but provided only small amounts of products; with a salt additive, reactions remained solid and gave high product yield.

In terms of emergent synthetic opportunities, accelerated aging provided easy access to bulk microporous ZIF-8 (quantitative conversion), cobalt-based ZIF-67 (conversion 77%), as well as RHO-Zn(**EtIm**)$_2$ which was previously characterized and prepared only in single crystal quantities. The materials were obtained without using soluble, potentially explosive (nitrate) or corrosive (chloride) metal salts, ligand excess, external templates, bases, solvothermal treatment or mechanochemical agitation. Accelerated aging also highlighted differences between ZIFs: unlike zinc-based ZIF-8, its cobalt analogue ZIF-67 showed no tendency to collapse into a non-porous *dia*-framework. The inclusion of ligand within the porous product was revealed to be an important factor controlling the efficiency of ZIF synthesis. The observation that RHO-Zn(**EtIm**)$_2$ was accessible in quantitative yield only when using a large excess of ligand was explained by a combination of solid-state NMR and PXRD, which revealed that the ligand became included, and therefore deactivated, within the nascent framework. A similar effect was also observed for ZIF-8 synthesis, but could be overcome by a suitable selection of the acid salt catalyst, which enabled the quantitative synthesis of ZIF-8 without excess reagents.

As the mild conditions of accelerated aging resemble those associated with self-assembly of small molecules, we believe its further exploration will provide new insights into the neogenesis of minerals and inspire the development of "greener" biomimetic alternatives[39] for the bulk synthesis of metal–organic materials. We envisage such synthetic alternatives would operate under mild conditions which resemble those encountered in the synthesis of molecular materials (*e.g.* cocrystals), rather than harsh conditions of solvothermal synthesis, melt reactions, sonochemistry or milling associated with metal oxides and mineral processing.[40,41] Procedures demonstrated in this and earlier contributions[22] have focused on reaction batches of up to 10 grams, significantly exceeding the scale of conventional solution syntheses. Moreover, the simplicity of experimental procedure facilitates parallel reaction batches and, in our laboratory, this readily yielded 50 gram amounts of ZIF-8. In further support of scalability and synthetic potential of accelerated aging, we note that a historically important "Dutch process" for manufacturing lead white pigment, first mentioned as long as 300 B.C.,[42] is based on a batch procedure resembling accelerated aging. A number of recently reported gas- and vapour-induced

 This journal is © The Royal Society of Chemistry 2013

transformations[43,44] suggests that synthetic procedures resembling accelerated aging (*e.g.* "vapour digestion" introduced by the Braga group[36]) might be applicable to a variety of organic, organometallic and pharmaceutical products.

Acknowledgements

We acknowledge funding from McGill University, Canada Foundation for Innovation (CFI) Leaders' Opportunity Fund, FRQNT Noveaux Chercheurs Grant and NSERC Discovery Grant. YL acknowledges the NSERC SURA program and the FRQNT Centre for Self-Assembled Chemical Structures. Initial experiments were done at the University of Cambridge (UK) with the aid of the Herchel Smith fund.

Published on 03 June 2013. Downloaded by Université Laval on 15/05/2014 21:48:14.

Notes and references

1 (*a*) J. C. Crittenden and H. S. White, *J. Am. Chem. Soc.*, 2010, **132**, 4503; (*b*) D. J. C. Constable, P. J. Dunn, J. D. Hayler, G. R. Humphret, J. L. Leazer Jr., R. J. Linderman, K. Lorenz, J. Manley, B. A. Pearlman, A. Wells, A. Zaks and T. Y. Zhang, *Green Chem.*, 2007, **9**, 411; (*c*) W. J. W. Watson, *Green Chem.*, 2012, **14**, 251; (*d*) P. Anastas and N. Eghbali, *Chem. Soc. Rev.*, 2010, **39**, 301.

2 (*a*) S. R. Batten, N. R. Champness, X.-M. Chen, J. Garcia-Martinez, S. Kitagawa, L. Öhrström, M. O'Keeffe, M. P. Suh and J. Reedijk, *CrystEngComm*, 2012, **14**, 3001; (*b*) O. M. Yaghi, M. O'Keeffe, N. W. Ockwig, H. K. Chae, M. Eddaoudi and J. Kim, *Nature*, 2003, **423**, 705; (*c*) S. A. K. Robinson, M.-V. L. Mempin, A. J. Cairns and K. T. Holman, *J. Am. Chem. Soc.*, 2011, **133**, 1634; (*d*) K. T. Holman, *Angew. Chem., Int. Ed.*, 2011, **50**, 1228.

3 (*a*) J. M. Roberts, B. M. Fini, A. A. Sarjeant, O. K. Farha, J. T. Hupp and K. A. Scheidt, *J. Am. Chem. Soc.*, 2012, **134**, 3334; (*b*) L. E. Kreno, K. Leong, O. K. Farha, M. Allendorf, R. P. Van Duyne and J. T. Hupp, *Chem. Rev.*, 2012, **112**, 1105.

4 (*a*) K. Sumida, D. L. Rogow, J. A. Mason, T. M. McDonald, E. D. Bloch, Z. R. Herm, T.-H. Bae and J. R. Long, *Chem. Rev.*, 2012, **112**, 724; (*b*) E. D. Bloch, W. L. Queen, R. Krishna, J. M. Zadrozny, C. M. Brown and J. R. Long, *Science*, 2012, **335**, 1606; (*c*) J. J. Gassensmith, H. Furukawa, R. A. Smaldone, R. S. Forgan, Y. Y. Botros, O. M. Yaghi and J. F. Stoddart, *J. Am. Chem. Soc.*, 2011, **133**, 15312; (*d*) R. Vaidhyanathan, S. S. Iremonger, G. K. H. Shimizu, P. G. Boyd, S. Alavi and T. K. Woo, *Science*, 2010, **330**, 650.

5 (*a*) C. Y. Lee, O. K. Farha, B. J. Hong, A. A. Sarjeant, S. T. Nguyen and J. T. Hupp, *J. Am. Chem. Soc.*, 2011, **133**, 15858; (*b*) C. Wang, T. Zhang and W. Lin, *Chem. Rev.*, 2012, **112**, 1084.

6 (*a*) A. Phan, C. J. Doonan, F. J. Uribe-Romo, C. B. Knobler, M. O'Keeffe and O. M. Yaghi, *Acc. Chem. Res.*, 2010, **43**, 58; (*b*) R. Banerjee, H. Furukawa, D. Britt, C. Knobler, M. O'Keeffe and O. M. Yaghi, *J. Am. Chem. Soc.*, 2009, **131**, 3875.

7 R. Banerjee, A. Phan, B. Wang, C. Knobler, H. Furukawa, M. O'Keeffe and O. M. Yaghi, *Science*, 2008, **319**, 939.

8 J.-P. Zhang, Y.-B. Zhang, J.-B. Lin and X.-M. Chen, *Chem. Rev.*, 2012, **112**, 1001.

9 (*a*) M. Klimakow, P. Klobes, A. F. Thünemann, K. Rademann and F. Emmerling, *Chem. Mater.*, 2010, **22**, 5216; (*b*) W. Yuan, J. O'Connor and S. L. James, *CrystEngComm*, 2010, **12**, 3515; (*c*) K. Fujii, A. Lazuen Garay, J. Hill, E. Sbircea, Z. Pan, M. Xu, D. C. Apperley, S. L. James and K. D. M. Harris, *Chem. Commun.*, 2010, **46**, 7572; (*d*) G. A. V. Martins, P. J. Byrne, P. Allan, S. J. Teat, A. M. Z. Slawin, Y. Li and R. E. Morris, *Dalton Trans.*, 2010, **39**, 1758; (*e*) H. Sakamoto, R. Matsuda and S. Kitagawa, *Dalton Trans.*, 2012, **41**, 3956; (*f*) C. J. Adams, M. F. Haddow, M. Lusi and A. G. Orpen, *Proc. Natl. Acad. Sci. U. S. A.*, 2010, **107**, 16033.

10 (*a*) I. A. Ibarra, P. A. Bayliss, E. Pérez, S. Yang, A. J. Blake, H. Nowell, D. R. Allan, M. Polyakoff and M. Schröder, *Green Chem.*, 2012, **14**, 117; (*b*) N. Stock and S. Biswas, *Chem. Rev.*, 2012, **112**, 933; (*c*) R. A. Smaldone, R. S. Forgan, H. Furukawa, J. J. Gassensmith, A. M. Z. Slawin, O. M. Yaghi and J. F. Stoddart, *Angew. Chem., Int. Ed.*, 2010, **49**, 8630.

11 Y. Pan, Y. Liu, G. Zeng, L. Zhao and Z. Lai, *Chem. Commun.*, 2011, **47**, 2071.

12 A. F. Gross, E. Sherman and J. J. Vajo, *Dalton Trans.*, 2012, **41**, 5458.

13 Q. Shi, Z. Chen, Z. Song, J. Li and J. Dong, *Angew. Chem., Int. Ed.*, 2011, **50**, 672.

14 T. Friščić and L. Fábián, *CrystEngComm*, 2009, **11**, 743.

15 C. J. Adams, M. A. Kurawa, M. Lusi and A. G. Orpen, *CrystEngComm*, 2008, **10**, 1790.

16 (*a*) A. Czaja, E. Leung, N. Trukhan and U. Müller, Industrial MOF synthesis in *Metal–Organic Frameworks: Applications from Catalysis to Gas Storage*, ed. D. Farrusseng, John Wiley & Sons, 1st edn, 2011; (*b*) B. Yilmaz, N. Trukhan and U. Müller, *Chin. J. Catal.*, 2012, **33**, 3–10.

17 *CRC Handbook of Chemistry and Physics*, Editor-in-Chief W. M. Haynes, 92nd edn, 2011–2012.

18 J. Reboul, S. Furukawa, N. Horike, M. Tsotsalas, K. Hirai, H. Uehara, M. Kondo, N. Louvain, O. Sakata and S. Kitagawa, *Nat. Mater.*, 2012, **11**, 717–723.

19 Recent ZIF-8 synthesis from zinc carbonate in methanol gave low surface area, contaminated with ZnO: M. Zhu, S. R. Venna, J. B. Jasinski and M. A. Carreon, *Chem. Mater.*, 2011, **23**, 3590.

20 (*a*) J.-B. Lin, R.-B. Lin, X.-N. Cheng, J.-P. Zhang and X.-M. Chen, *Chem. Commun.*, 2011, **47**, 9185; (*b*) M. Lanchas, D. Vallejo-Sánchez, G. Beobide, O. Castillo, A. T. Aguayo, A. Luque and P. Román, *Chem. Commun.*, 2012, **48**, 9930; (*c*) K. Müler-Buschbaum and F. Schönfeld, *Zeit. Anorg. Allg. Chem.*, 2012, **637**, 955.

Published on 03 June 2013. Downloaded by Université Laval on 15/05/2014 21:48:14.

21 (*a*) T. Friščić, I. Halasz, P. J. Beldon, A. M. Belenguer, F. Adams, S. A. J. Kimber, V. Honkimäki and R. E. Dinnebier, *Nat. Chem.*, 2013, **5**, 66; (*b*) P. J. Beldon, L. Fábián, R. S. Stein, A. Thirumurugan, A. K. Cheetham and T. Friščić, *Angew. Chem., Int. Ed.*, 2010, **49**, 9640; (*c*) V. André, A. Hardeman, I. Halasz, R. S. Stein, G. J. Jackson, D. G. Reid, M. J. Duer, C. Curfs, M. T. Duarte and T. Friščić, *Angew. Chem., Int. Ed.*, 2011, **50**, 7858; (*d*) X. Ma, G. K. Lim, K. D. M. Harris, D. C. Apperley, P. N. Horton, M. B. Hursthouse and S. L. James, *Cryst. Growth Des.*, 2012, **12**, 5869.

22 M. J. Cliffe, C. Mottillo, R. S. Stein, D.-K. Bučar and T. Friščić, *Chem. Sci.*, 2012, **3**, 2495.

23 (*a*) T. Echigo and M. Kimata, *Can. Mineral.*, 2010, **48**, 1329; (*b*) G. M. Gadd, *Microbiology*, 2010, **156**, 609; (*c*) J. A. Sayer and G. M. Gadd, *Mycol. Res.*, 1997, **101**, 653; (*d*) J. Chen, H.-P. Blume and L. Beyer, *Catena*, 2000, **39**, 121; (*e*) P. Piantone, F. Bodénan and L. Chatelet-Snidaro, *Appl. Geochem.*, 2004, **19**, 1891; (*f*) M. Fomina, S. Hillier, J. M. Charnock, K. Melville, I. J. Alexander and G. M. Gadd, *Appl. Environ. Microbiol.*, 2005, **71**, 371.

24 E. C. Spencer, R. J. Angel, N. L. Ross, B. E. Hanson and J. A. K. Howard, *J. Am. Chem. Soc.*, 2009, **131**, 4022.

25 (*a*) H. C. Freeman, F. Huq, J. M. Rosalky and I. F. Taylor Jr., *Acta Crystallogr., Sect. B: Struct. Crystallogr. Cryst. Chem.*, 1975, **31**, 2833; (*b*) C. V. Jerin and S. Athimoolam, *Acta Crystallogr., Sect. E: Struct. Rep. Online*, 2011, **67**, o2290.

26 pK_a calculations were done using Marvin, ChemAxon online calculator (http://www.chemaxon.com/marvin/sketch/index.jsp).

27 T. Friščić, D. G. Reid, G. M. Day, M. J. Duer and W. Jones, *Cryst. Growth Des.*, 2011, **11**, 972.

28 (*a*) G. Lu, S. Li, Z. Guo, O. K. Farha, B. G. Hauser, X. Qi, Y. Wang, X. Wang, S. Han, X. Liu, J. S. DuChene, H. Zhang, Q. Zhang, X. Chen, J. Ma, S. C. J. Loo, W. D. Wei, Y. Yang, J. T. Hupp and F. Huo, *Nat. Chem.*, 2012, **4**, 310; (*b*) K. S. Park, Z. Ni, A. P. Côté, J. Y. Choi, R. Huang, F. J. Uribe-Romo, H. K. Chae, M. O'Keeffe and O. M. Yaghi, *Proc. Natl. Acad. Sci. U. S. A.*, 2006, **103**, 10186.

29 (*a*) S. K. Nune, P. K. Thallapally, A. Dohnalkova, C. Wang, J. Liu and G. J. Exarhos, *Chem. Commun.*, 2010, **46**, 4878; (*b*) S. R. Venna and M. A. Carreon, *J. Am. Chem. Soc.*, 2010, **132**, 76; (*c*) D. Fairen-Jimenez, S. A. Moggach, M. T. Wharmby, P. A. Wright, S. Parsons and T. Düren, *J. Am. Chem. Soc.*, 2011, **133**, 8900.

30 (*a*) J. Cravillon, S. Münzer, S.-J. Lohmeier, A. Feldhoff, K. Huber and M. Wiebcke, *Chem. Mater.*, 2009, **21**, 1410–1412; (*b*) J. Cravillon, C. A. Schröder, H. Bux, A. Rothkirch, J. Caro and M. Wiebcke, *CrystEngComm*, 2012, **14**, 492–498; (*c*) K. Kida, M. Okita, K. Fujita, S. Tanaka and Y. Miyake, *CrystEngComm*, 2013, **15**, 1794.

31 In our hands, the reported method for the rapid room-temperature synthesis of ZIF-8[30*a*] in methanol yielded 16% of the material, based on zinc nitrate reactant.

32 (*a*) W. Morris, C. J. Stevens, R. E. Taylor, C. Dybowski, O. M. Yaghi and M. A. Garcia-Garibay, *J. Phys. Chem. C*, 2012, **116**, 13307; (*b*) J. C. Tan and A. K. Cheetham, *Chem. Soc. Rev.*, 2011, **40**, 1059; (*c*) S. A. Moggach, T. D. Bennett and A. K. Cheetham, *Angew. Chem., Int. Ed.*, 2009, **48**, 7087; (*d*) K. W. Chapman, G. J. Halder and P. J. Chupas, *J. Am. Chem. Soc.*, 2009, **131**, 17546; (*e*) T. D. Bennett, S. Cao, J. C. Tan, D. A. Keen, E. G. Bithell, P. J. Beldon, T. Friščić and A. K. Cheetham, *J. Am. Chem. Soc.*, 2011, **133**, 14546.

33 The exchange of imidazole ligands on ZIF-8 under sonochemical conditions was recently reported, see: O. Karagiaridi, M. B. Lalonde, W. Bury, A. A. Sarjeant, O. K. Farha and J. T. Hupp, *J. Am. Chem. Soc.*, 2012, **134**, 18790.

34 (*a*) Y.-Q. Tian, Z.-X. Chen, L.-H. Weng, H.-B. Guo, S. Gao and D. Y. Zhao, *Inorg. Chem.*, 2004, **43**, 4631; (*b*) Y.-Q. Tian, C.-X. Cai, X.-M. Ren, C.-Y. Duan, Y. Xu, Y. S. Gao and S. X.-Z. You, *Chem.–Eur. J.*, 2003, **9**, 5673; (*c*) Y.-Q. Tian, C.-X. Cai, Y. Ji, X.-Z. You, S.-M. Peng and G.-S. Lee, *Angew. Chem., Int. Ed.*, 2002, **41**, 1384.

35 X.-C. Huang, Y.-Y. Lin, J.-P. Zhang and X.-M. Chen, *Angew. Chem., Int. Ed.*, 2006, **45**, 1557.

36 (*a*) D. Braga, S. L. Giaffreda, F. Grepioni, M. R. Chierotti, R. Gobetto, G. Palladino and M. Polito, *CrystEngComm*, 2007, **9**, 879–881; (*b*) L. Maini, D. Braga, P. P. Mazzeo and B. Ventura, *Dalton Trans.*, 2012, **41**, 531–539.

37 (*a*) A. Jayasankar, D. J. Good and N. Rodríguez-Hornedo, *Mol. Pharm.*, 2007, **4**, 360–372; (*b*) C. Maheshwari, A. Jayasankar, N. A. Khan, G. E. Amidon and N. Rodríguez-Hornedo, *CrystEngComm*, 2009, **11**, 493–500.

38 A. Y. Ibrahim, R. T. Forbes and N. Blagden, *CrystEngComm*, 2011, **13**, 1141–1152.

39 F. Nudelman and N. A. J. M. Sommerdijk, *Angew. Chem., Int. Ed.*, 2012, **51**, 6582.

40 Mechanosynthesis of metal–organic materials could also be relevant in understanding biologically-induced mineral transformations, as the latter can involve mechanical force exerted by the growing organism, *e.g.* extruding fungal hypha: M. M. Smits, A. M. Herrmann, M. Duane, O. W. Duckworth, S. Bonneville, L. G. Benning and U. Lundström, *Fungal Biol. Rev.*, 2009, **23**, 122.

41 Tentative connection between mechanochemistry and geology has been made early in the development of this field: P. A. Thiessen, G. Heinicke and H.-P. Hennig, *Z. Chem.*, 1971, **11**, 193.

42 Described by Theophrastus of Eresos in *Peri tōn lithōn biblion* (*History of Stones*), translated by J. Hill (1774), pp. 223–225.

43 (*a*) D. Cinčić, I. Brekalo and B. Kaitner, *Chem. Commun.*, 2012, **48**, 11683; (*b*) D. Cinčić, I. Brekalo and B. Kaitner, *Cryst. Growth Des.*, 2012, **12**, 44; (*c*) M. A. Ziganshin, I. G. Efimova, V. V. Gorbatchuk, S. A. Ziganshina, A. P. Chuklanov, A. A. Bukharaev and D. V. Soldatov, *J. Pept. Sci.*, 2012, **18**, 209; (*d*) R. Anneda, D. V. Soldatov, I. L. Moudrakovski, M. Casu and J. A. Ripmeester, *Chem. Mater.*, 2008, **20**, 2908; (*e*) G. M. Espallargas, M. Hippler, A. J. Florence, P. Fernandes, J. van de Streek, M. Brunelli, W. I. F. David, K. Shankland and L. Brammer, *J. Am. Chem. Soc.*, 2007, **129**, 15606.

 This journal is © The Royal Society of Chemistry 2013

44 (*a*) J. Tian, S. J. Dalgarno and J. L. Atwood, *J. Am. Chem. Soc.*, 2011, **133**, 1399; (*b*) J. Tian, P. Thallapally, J. Liu, G. J. Exarhos and J. L. Atwood, *Chem. Commun.*, 2011, **47**, 701; (*c*) B. D. Chandler, G. D. Enright, K. A. Udachin, S. Pawsey, J. A. Ripmeester, D. T. Cramb and G. K. H. Shimizu, *Nat. Mater.*, 2008, 229; (*d*) P. K. Thallapally, B. P. McGrail, S. J. Dalgarno, H. T. Schaef, J. Tian and J. L. Atwood, *Nat. Mater.*, 2008, **7**, 146.

Published on 03 June 2013. Downloaded by Université Laval on 15/05/2014 21:48:14.

Electronic Supplementary Material (ESI) for Green Chemistry
This journal is © The Royal Society of Chemistry 2013

Supplementary Material

Mineral neogenesis as an inspiration for mild, solvent-free synthesis of bulk microporous metal-organic frameworks from metal (Zn, Co) oxides

Cristina Mottillo, Yuneng Lu, Hao-Min Phan, Matthew J. Cliffe, Trong-On Do and Tomislav Friščić

Table of contents

This journal is © The Royal Society of Chemistry 2013

1. EXPERIMENTAL SECTION

1.1 General details

Zinc oxide was calcinated in a Thermolyne furnace at 400 °C overnight prior to use in all reactions. Zinc oxide (≥99.0%), cobalt oxide (-325 mesh, 97%), imidazole (98%), 2-ethylimidazole (98%), benzimidazole (98%), and caffeine (ReagentPlus grade) were purchased from Sigma Aldrich. 2-methylimidazole (97%) was purchased from Alfa Aesar. Potassium hydrogen sulfate (Analytical reagent grade) was purchased from Mallinckrodt and potassium sulfate (ACS Reagent grade) was obtained from Anachemia. Sulfuric acid (95-98% assay) was purchased from ACP and all solvents with the exception of ethanol were obtained from Fisher. Anhydrous ethanol was purchased from Commercial Alcohols.

1.2 Instrumental analysis

Powder X-ray diffraction (PXRD) patterns were collected using a Bruker D2 Phaser powder diffractometer equipped with a Cu-K_α (λ=1.54060 Å) source and Lynxeye detector. The patterns were collected in the range of 4° to 40° in the case of samples containing ZnO and 4° to 50° in the case of CoO. The lower discriminal of the detector was increased from 0.110 V to 0.200 V to minimize noise resulting from x-ray fluorescence in Co-based samples. Analysis of PXRD patterns was conducted using Panalytical X'Pert Highscore Plus software.

Fourier-transform infrared attenuated total reflectance (FTIR-ATR) spectra were collected using a Perkin Elmer FTIR Spectrum BX spectrometer in the range 550 cm^{-1} to 4000 cm^{-1}.

Thermogravimetric analysis (TGA) was conducted on a TA Instruments Q1000 Thermogravimetric System with a Pt pan under dynamic atmosphere of air. Samples were heated to an upper temperature limit ranging from 800°C to 900°C at a rate of 20°C/min. The balance and purge flow were 40 ml/min and 60 ml/min respectively. TGA data were used to determine the yields of the accelerated aging reactions by calcinating the well-washed and evacuated samples of synthesized frameworks up to 600 ^oC in air. Washing and evacuation were performed in order to remove the salt additive as well as unreacted imidazole ligand. Consequently, after washing and evacuation the samples consisted of the product framework and unreacted metal oxide ZnO or CoO. Calcination of such mixture in air leads to the oxidation of the organic framework constituents and complete conversion to either ZnO or Co_3O_4. The conversion of the metal oxide (x) is calculated from the weight fraction of ZnO (w_{ZnO}) using the equation $x = \frac{M_{ZnO}}{w_{ZnO}(M_{ZIF}-M_{ZnO})} - \frac{M_{ZnO}}{M_{ZIF}-M_{ZnO}}$ and from the weight fraction (w) of Co_3O_4 using the analogous expression $x = \frac{\frac{1}{3}M_{Co_3O_4}}{w_{Co_3O_4}(M_{ZIF}-M_{CoO})} - \frac{M_{CoO}}{M_{ZIF}-M_{CoO}}$, where M_{ZIF} is the molecular weight of the product framework (normally ZIF-8 or ZIF-67).

Solid-state C^{13} and N^{15} CP-MAS NMR spectra were collected on a 400 MHz Varian VNMR equipped with a 7.5 mm CPMAS probe at a spin rate of 5 KHz. All N^{15} spectra were referenced to nitromethane. All spectra were collected with a contact time of 2 ms and recycle delay of 2 s, except for that of caffeine, where the contact time was increased to 5 ms. Solution C^{13} NMR spectra were collected in D_2O on a 300 MHz Varian Mercury spectrometer equipped with a 5 mm AutoSW PFG $^1H/X[^{15}N$-$^{31}P]$ probe.

This journal is © The Royal Society of Chemistry 2013

Single crystal X-ray diffraction data was collected on a Bruker APEX II diffractometer with MoK_α (λ=0.71073 Å) source and CCD detector. The structures were determined by least squares refinement against F^2 using SHELX-97 software.

1.3 Synthesis of salt additives

Caffeinium hydrogensulfate: For the synthesis of **(Hcaf)(HSO$_4$)** caffeine (3 mmol, 0.58 g) was dissolved in acetonitrile. Concentrated sulfuric acid (3 mmol, 160 µL) was added and upon stirring, a white precipitate formed. The solid was filtered and dried over vacuum. The product isolated in 90% yield was analyzed by PXRD, ^{13}C CP-MAS NMR, FTIR-ATR, and determined to be (**HCaf**)·(HSO$_4$) by elemental analysis. Storage in dry atmosphere was necessary to prevent conversion to (**Hcaf**)·(HSO$_4$)·H$_2$O, observable by PXRD. Single crystals for single crystal X-ray diffraction structure determination (Table S1) were obtained by dissolving (**Hcaf**)($^-$HSO$_4$) in a 1:4 v/v solution of nitromethane and anhydrous EtOH and allowing the solvent to evaporate slowly overnight. X-ray single crystal structure determination confirmed the composition (**Hcaf**)(HSO$_4$), and crystallographic data has been deposited with the Crystal Structure Database. The bulk composition of the product was confirmed by comparison of powder X-ray diffraction patterns to the one simulated for the determined crystal structure. Elemental analysis for (**Hcaf**)(HSO$_4$): C (calculated: 32.88%, measured: 32.87%), H (calculated: 4.14%, measured: 4.14%), N (calculated: 19.17%, measured: 19.02%).

Table S1. General and crystallographic data for (**Hcaf**)(HSO$_4$)

Formula	$C_8H_{12}N_4O_6S$
M_r	292.28
Crystal system	Orthorhombic
a/Å	6.406(1)
b/Å	8.167(1)
c/Å	23.311(4)
V/Å^3	1219.6(3)
T/K	293(2)
Space group	$P2_12_12_1$
Z	4
Radiation type	MoK_α
μ/mm^{-1}	0.297
No. of reflections measured	13570
No. of independent reflections	2616
R_{int}	0.0772
R_1 (for $I > 2\sigma(I)$)	0.0430
$wR(F^2)$ (for $I > 2\sigma(I)$)	0.0897
R_1 (all data)	0.0712
$wR(F^2)$ (all data)	0.1006
S	0.955

Caffeinium hydrogensulfate hydrate: (**Hcaf**)(HSO$_4$) was allowed to sit in 98% RH atmosphere overnight to obtain (**Hcaf**)(HSO$_4$)·H$_2$O. The product was analyzed by FTIR-ATR spectroscopy, PXRD and TGA. Powder X-ray diffraction pattern matched to that simulated from the known crystal structure (see Jerin, Athimoolam, *Acta Crystallogr.* **2011**, *E67*, o2290); **Benzimidazolium sulfate:** Benzimidazole (8 mmol, 0.55 g) was dissolved in acetonitrile. Concentrated sulfuric acid (8 mmol, 520 µL) was added to form a beige precipitate. The product was collected, dried over vacuum to obtain 97% isolated yield, and characterized by PXRD and FTIR-ATR spectroscopy. **Imidazolium Sulfate Dihydrate:** Imidazole (4 mmol, 0.272 g) was dissolved in a 1:9 water:ethanol (v/v) mixture. Concentrated sulfuric acid (2.1 mmol, 111 µL) was added and a white precipitate formed. The

This journal is © The Royal Society of Chemistry 2013

product was collected over vacuum and dried over air (96% isolated yield). Elemental analysis for (**H_2Im**)$_2$(SO_4)·2H_2O: C (calculated: 26.67%, measured: 26.41%), H (calculated: 5.22%; measured: 5.54%), N (calculated: 20.73%, measured: 20.38%).

1.4 Accelerated aging

In a typical experiment, 2 mmol of metal oxide (ZnO or CoO), 4 mmol of the imidazole ligand (**HMeIm** or **HEtIm**), and 4 mol% (unless otherwise specified) of the salt additive [(NH_4)$_2SO_4$), $KHSO_4$, (**H_2Im**)$_2SO_4$·H_2O, (**Hcaf**)(HSO_4), (**Hcaf**)(HSO_4)·H_2O, or (**H_2BIm**)$_2$(SO_4), percentage calculated with respect to ZnO] were added to a 10 mL stainless steel milling jar along with one stainless steel ball of 7 mm diameter. Unless specified otherwise, the mixtures were briefly milled using a Retsch MM400 ball mill for 5 minutes at 29.5 Hz. The samples not containing ammonium salt were left to age in a Secador controlled humidity chamber at 98% RH or nominal 100% RH, which was situated in an incubator set at 45°C. Samples containing ammonium sulfate as the additive were placed in a separate controlled humidity glass chambers under the same conditions, so as to avoid possible absorption of NH_3 within the container walls and contamination of subsequent samples. Saturated K_2SO_4 solution (for 98% RH) or just water (for nominal 100% RH) were used to maintain humid atmosphere. Upon complete disappearance of X-reflections representing the metal oxides in PXRD patterns, samples were washed overnight and filtered over vacuum in H_2O, MeOH, or acetonitrile to remove trace amounts of catalyst or organic ligand. Samples for gas adsorption analysis were evacuated in a vacuum oven at 80 °C overnight.

2. SELECTED POWDER X-RAY DIFFRACTION (PXRD) PATTERNS

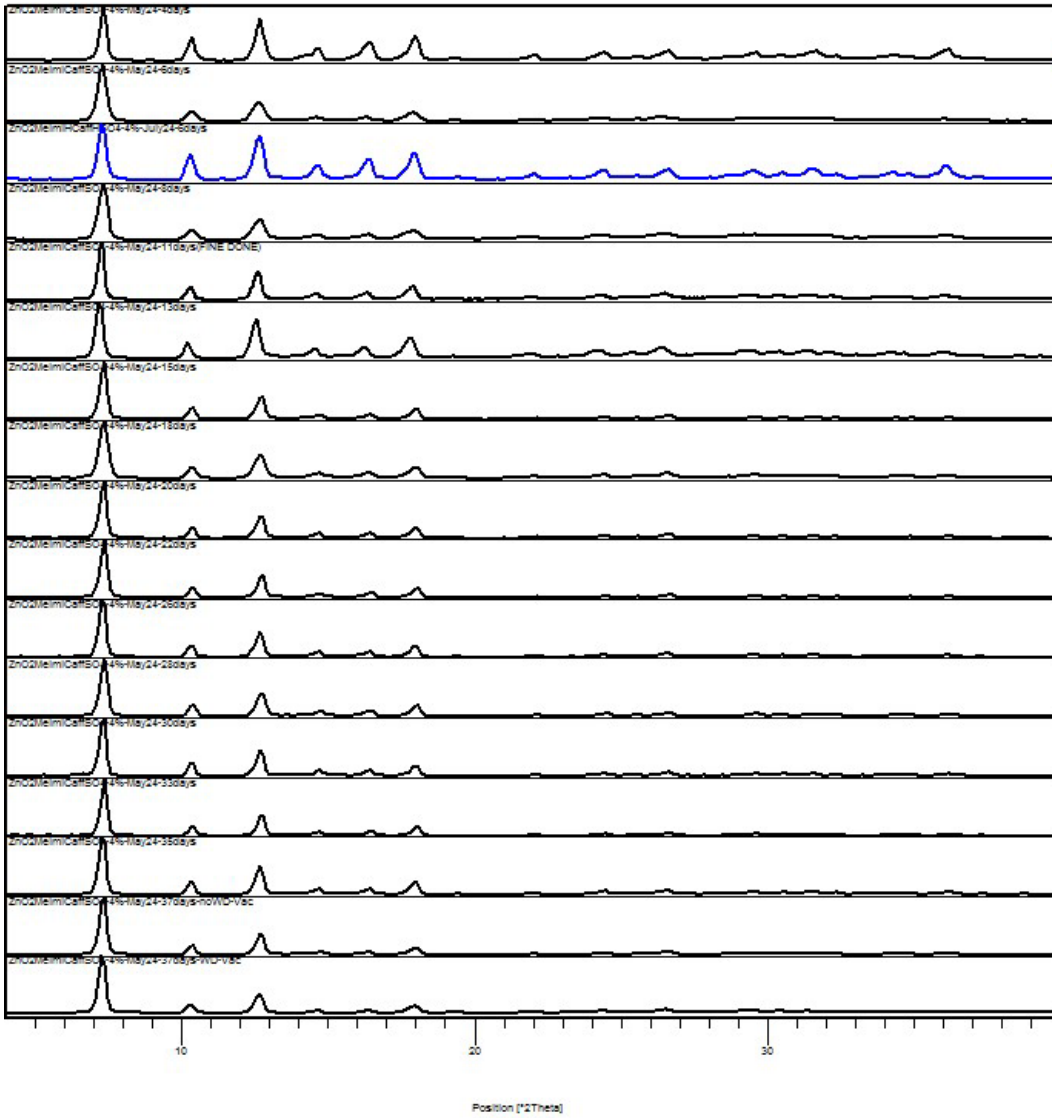

Figure S1. Powder X-ray diffraction patterns for the accelerated aging reaction of **HMeIm** and ZnO, with (**Hcaf**)(HSO_4) as the ionic additive (from top to bottom), at 45 ^oC and 98% RH: 4 days aging; 6 days aging; the sample obtained after 6 days aging with (**Hcaf**)(HSO_4)·H_2O (blue) shown for comparison with the previous sample; 8 days aging; 11 days aging; 13 days aging; 15 days aging; 18 days aging; 20 days aging; 22 days aging; 26 days aging; 28 days aging; 30 days aging; 33 days aging; 35 days aging; evacuated sample after 37 days aging and washed (acetonitrile?) and evacuated sample after 37 days aging.

The comparison of the PXRD pattern for the sample obtained after 6 days aging with 4 mol% (**Hcaf**)(HSO_4)·H_2O (shown in blue) with the sample obtained after 6 days aging with 4mol% (**Hcaf**)(HSO_4) clearly demonstrates a larger amount of ZnO present with the hydrated salt as the additive.

This journal is © The Royal Society of Chemistry 2013

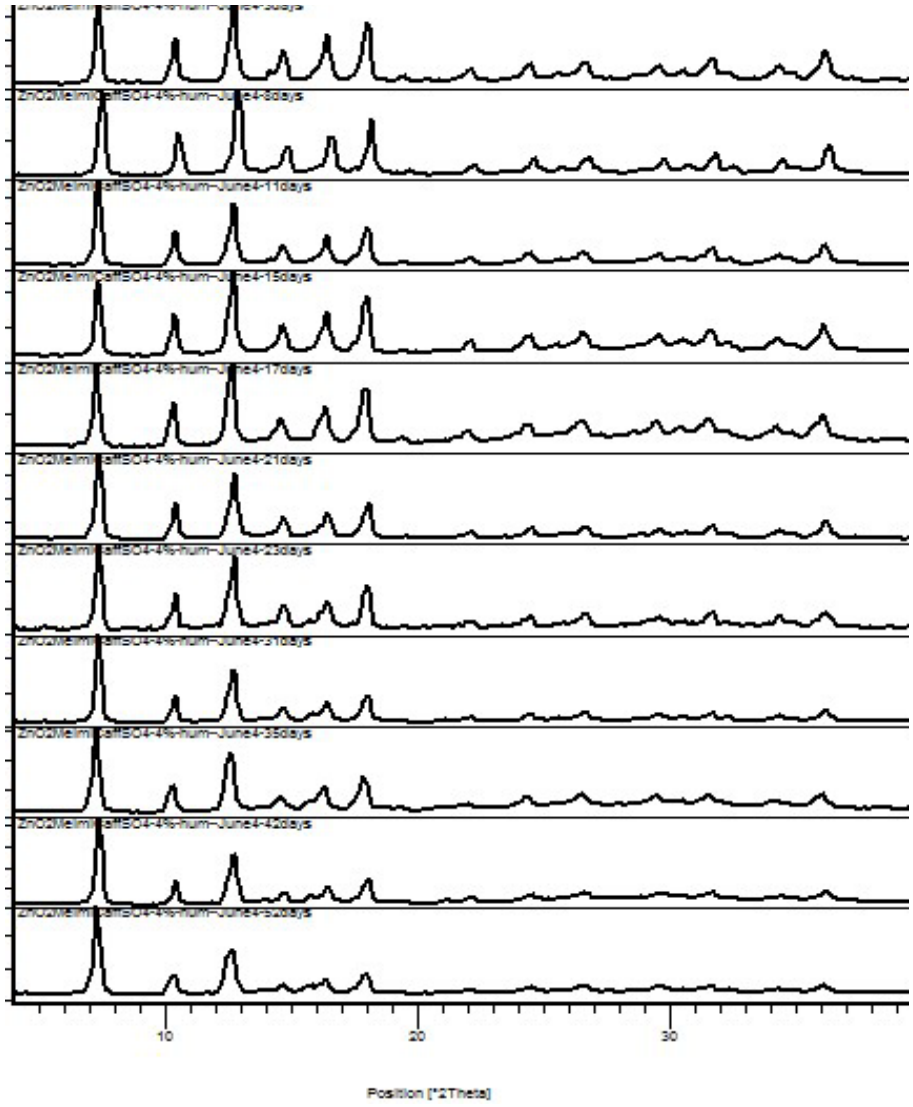

Figure S2. Powder X-ray diffraction patterns for the accelerated aging reaction of **HMeIm** and ZnO, with (**Hcaf**)(HSO_4) as the ionic additive (from top to bottom), at 98% RH and room temperature: 3 days aging; 8 days aging; 11 days aging; 15 days aging; 17 days aging; 21 days aging; 23 days aging; 31 days aging; 35 days aging; 42 days aging; 52 days aging.

This journal is © The Royal Society of Chemistry 2013

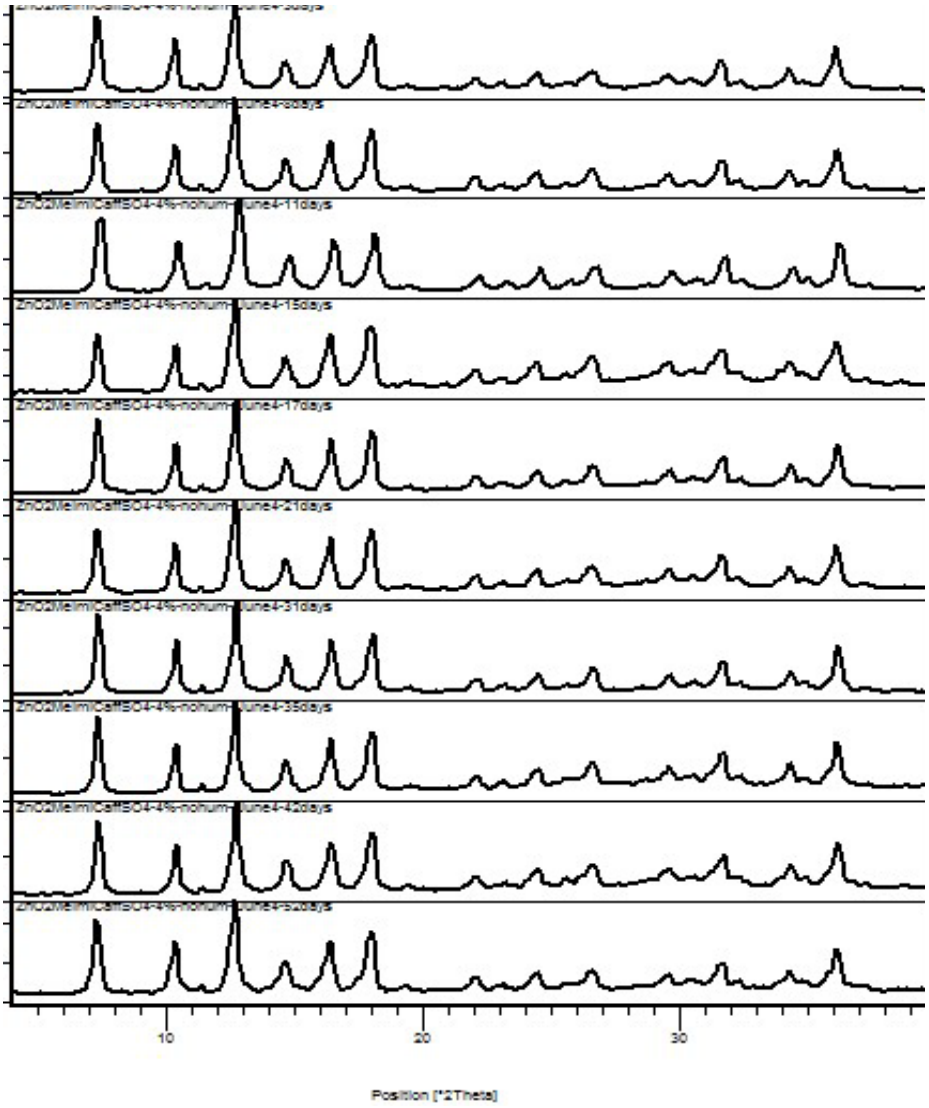

Figure S3. Powder X-ray diffraction patterns for the accelerated aging reaction of **HMeIm** and ZnO, with (**Hcaf**)(HSO_4) as the ionic additive (from top to bottom), at room temperature and humidity: 3 days aging; 8 days aging; 11 days aging; 15 days aging; 17 days aging; 21 days aging; 31 days aging; 35 days aging; 42 days aging; 52 days aging.

This journal is © The Royal Society of Chemistry 2013

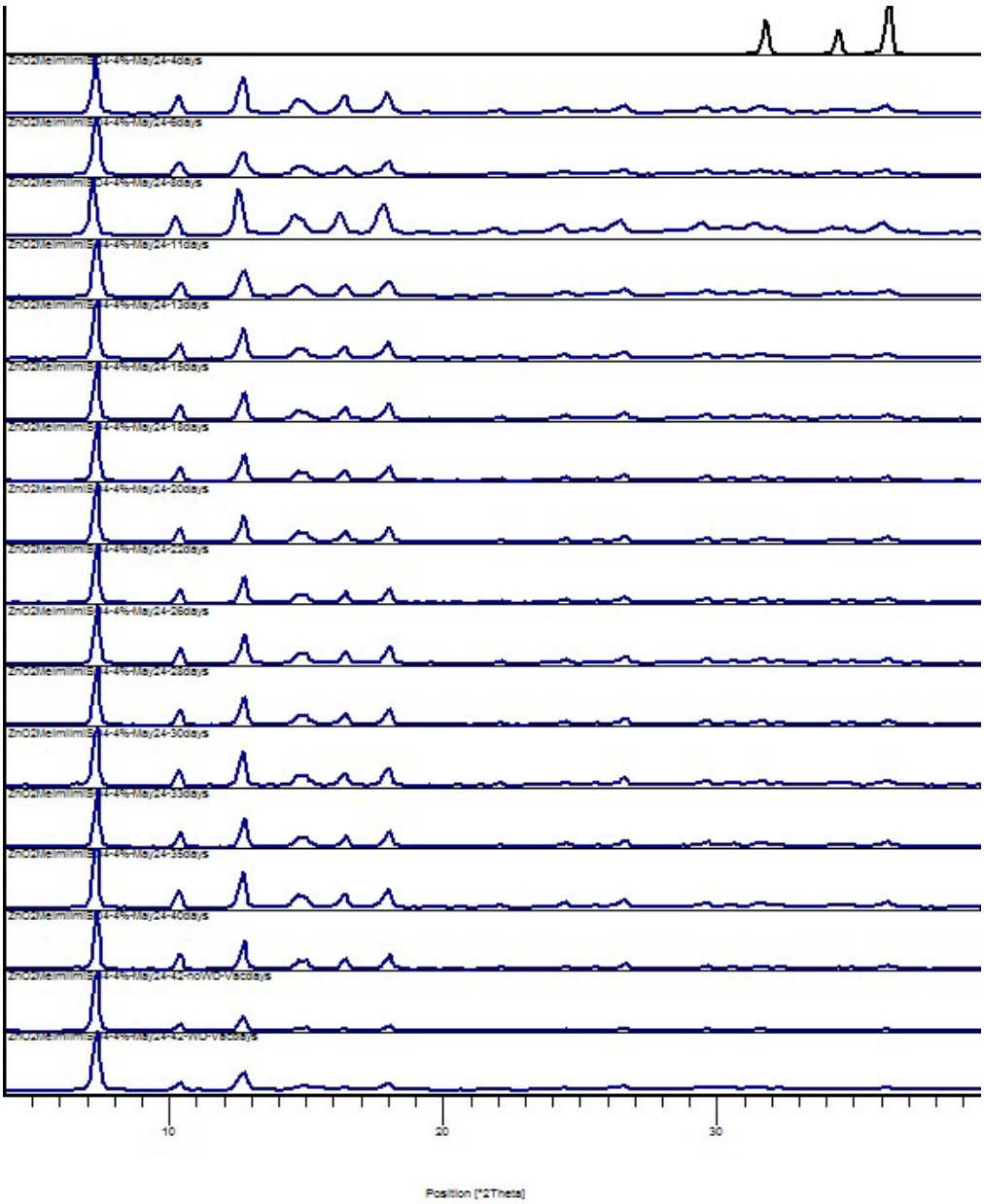

Figure S4. Powder X-ray diffraction patterns for the accelerated aging reaction of **HMeIm** and ZnO, with (**H_2Im**)$_2$(SO_4)·2H_2O as the ionic additive (from top to bottom), at 45 ^oC and 98% RH: ZnO reactant; sample after 4 days aging; 6 days aging; 8 days aging; 11 days aging; 13 days aging; 15 days aging; 18 days aging; 20 days aging 22 days aging; 26 days aging; 28 days aging; 30 days aging; 33 days aging; 35 days aging; 40 days aging; sample after 40 days aging and evacuation; sample after 40 days aging, washing with methanol and evacuation.

This journal is © The Royal Society of Chemistry 2013

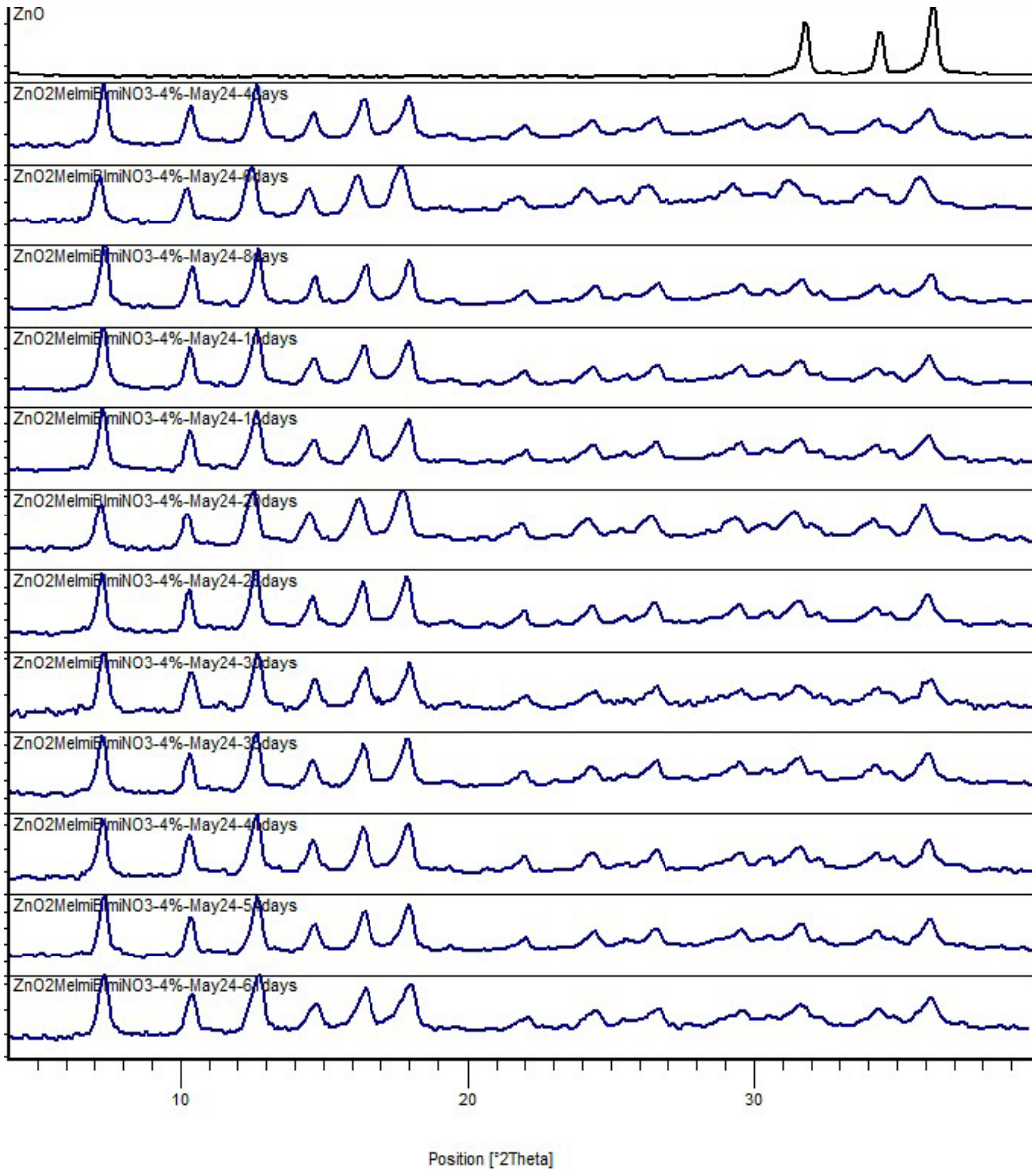

Figure S5. Powder X-ray diffraction patterns for the accelerated aging reaction of **HMeIm** and ZnO, with (**H_2BIm**)$_2SO_4$ as the ionic additive (from top to bottom), at 45 ^oC and 98% RH: ZnO reactant; sample after 4 days aging; 6 days aging; 8 days aging; 11 days aging; 13 days aging; 20 days aging; 26 days aging; 30 days aging; 35 days aging; 41 days aging; 54 days aging and after 61 day aging.

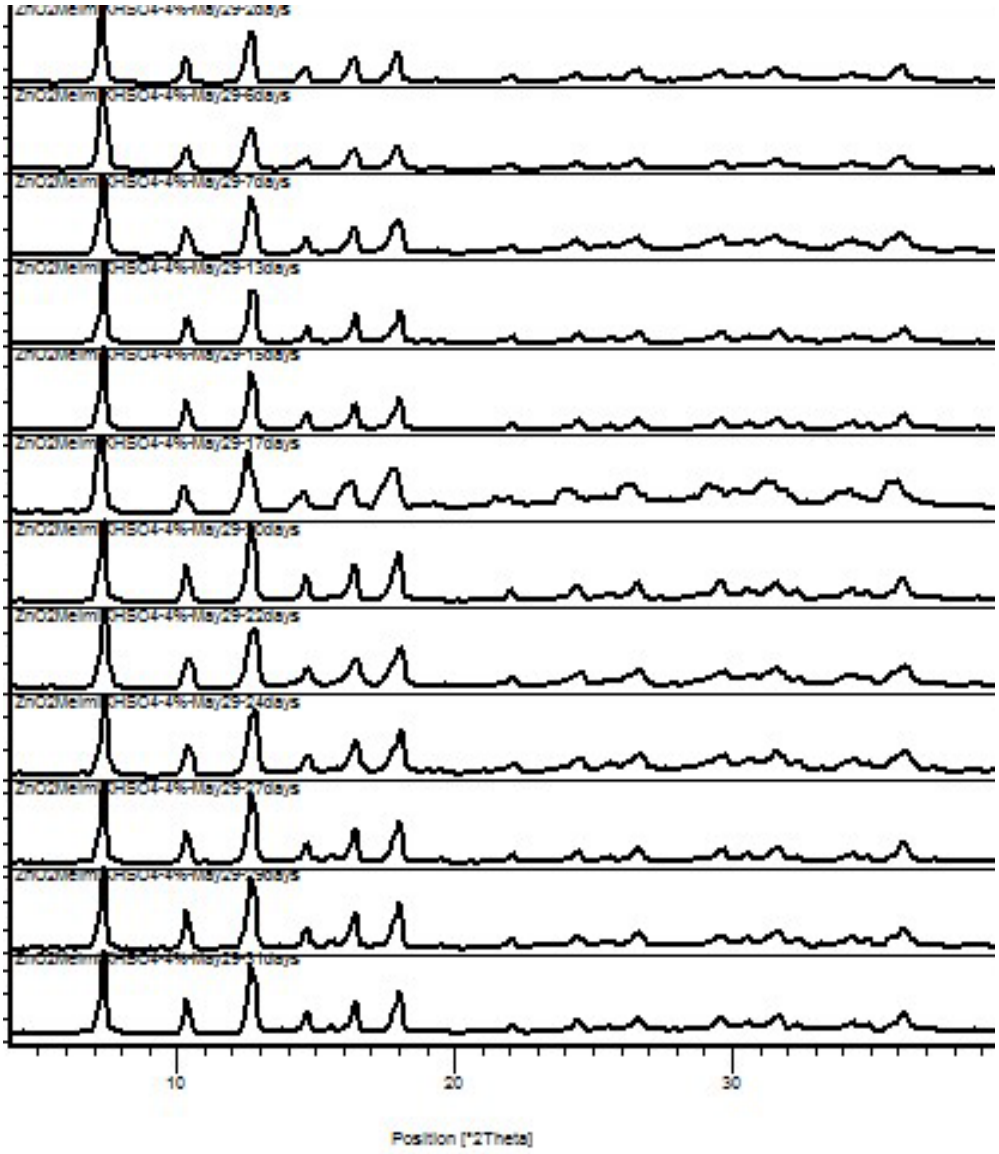

Figure S6. Powder X-ray diffraction patterns for the accelerated aging reaction of **HMeIm** and ZnO, with $KHSO_4$ as the ionic additive (from top to bottom), at 45 ^{o}C and 98% RH: 2 days aging; 6 days aging; 7 days aging; 13 days aging; 15 days aging; 17 days aging; 20 days aging; 22 days aging; 24 days aging; 27 days aging; 29 days aging; 31 days aging.

This journal is © The Royal Society of Chemistry 2013

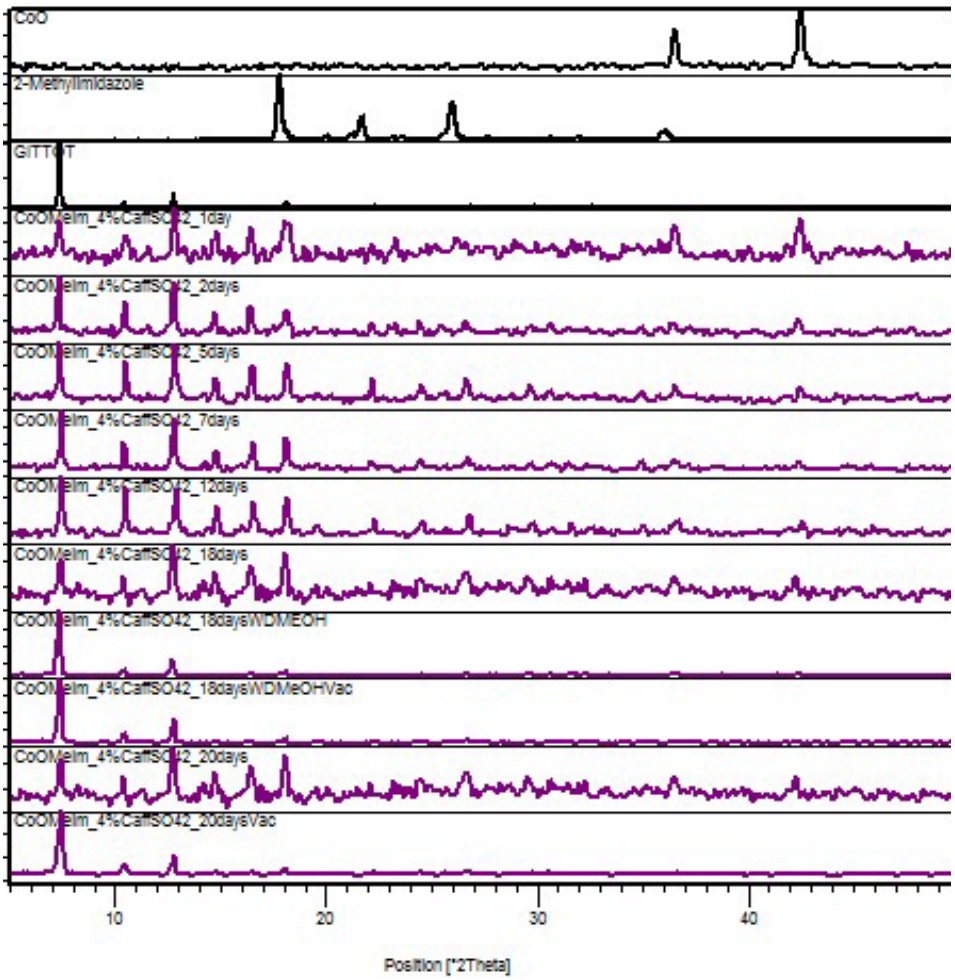

Figure S7. Powder X-ray diffraction patterns for the accelerated aging reaction of **HMeIm** and CoO, with (**Hcaf**)(HSO_4) (4 mol% with respect to CoO) as the ionic additive at 45 ^{o}C and 98% RH (from top to bottom): CoO reactant, **HMeIm** reactant; calculated pattern for ZIF-67 (CCDC code GITTOT); 1 day aging; 2 days aging; 5 days aging; 7 days aging; 12 days aging; 18 days aging; sample after 18 days aging after washing with methanol; sample after 18 days aging after washing with methanol and evacuation; sample after 20 days aging; sample after 20 days aging after evacuation.

This journal is © The Royal Society of Chemistry 2013

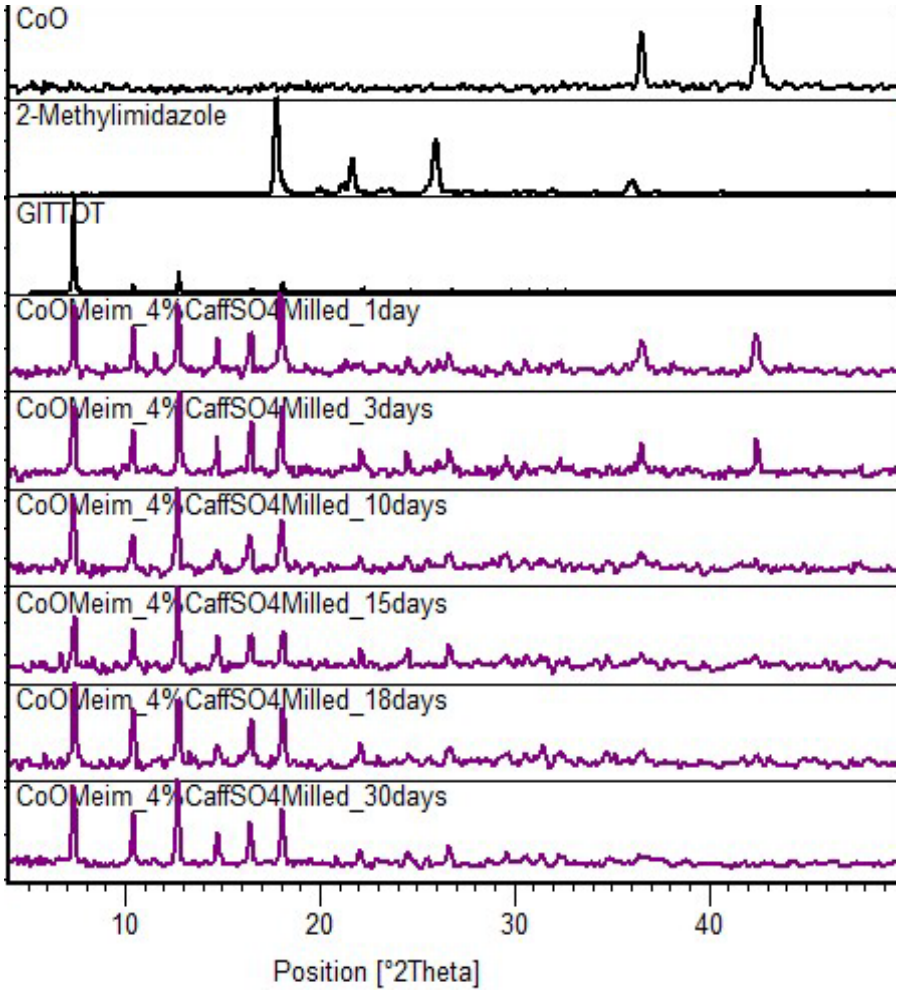

Figure S8. Powder X-ray diffraction patterns for the repeated accelerated aging reaction of **HMeIm** and CoO, with (**Hcaf**)(HSO_4) (4 mol% with respect to CoO) as the ionic additive at 45 ^{o}C and 98% RH (from top to bottom): CoO reactant, **HMeIm** reactant; calculated pattern for ZIF-67 (CSD code GITTOT); 1 day aging; 3 days aging; 10 days aging; 15 days aging; 18 days aging and 30 days aging.

This journal is © The Royal Society of Chemistry 2013

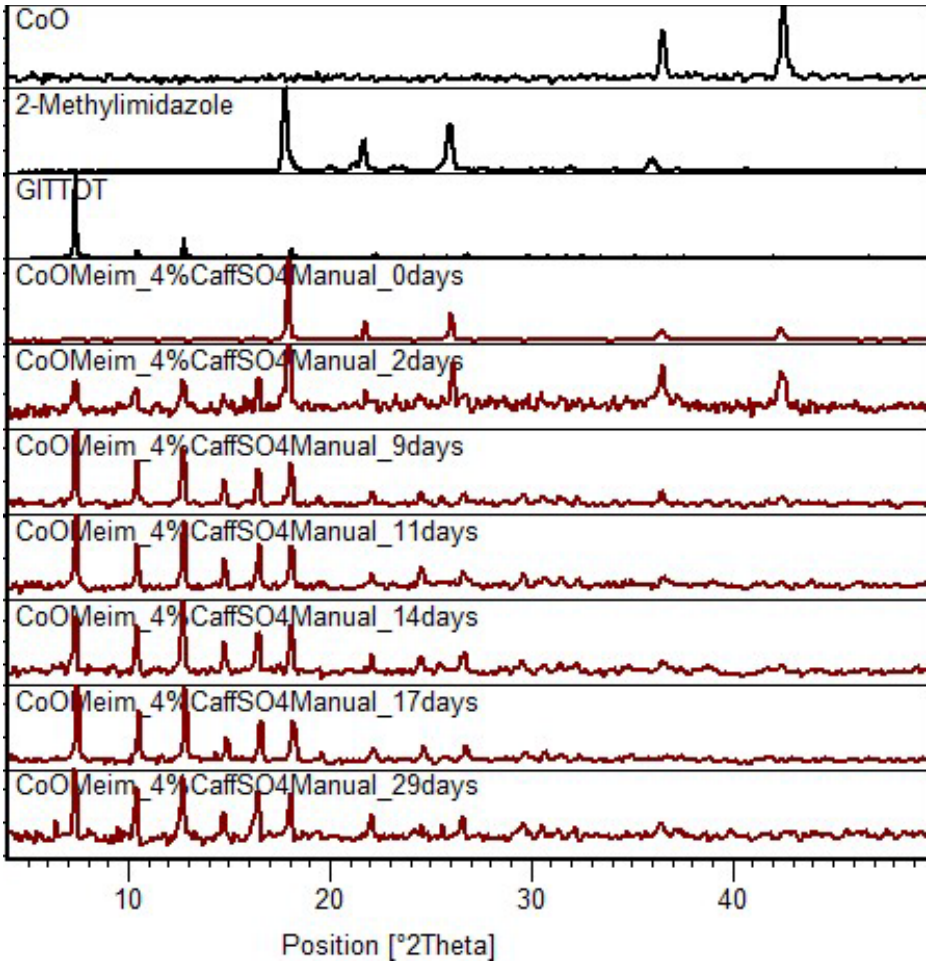

Figure S9. Powder X-ray diffraction patterns for the repeated accelerated aging reaction of **HMeIm** and CoO, with (**Hcaf**)(HSO_4) (4 mol% with respect to CoO) as the ionic additive. The reaction mixture was prepared by manual mixing in a mortar and pestle, in order to investigate the potential role of mechanical activation in other samples prepared by milling. The accelerated aging was conducted at 45 ^{o}C and 98% RH (from top to bottom): CoO reactant, **HMeIm** reactant; calculated pattern for ZIF-67 (CSD code GITTOT); reaction mixture immediately after mixing; 2 days aging; 9 days aging; 11 days aging; 14 days aging; 17 days aging and 29 days aging.

This journal is © The Royal Society of Chemistry 2013

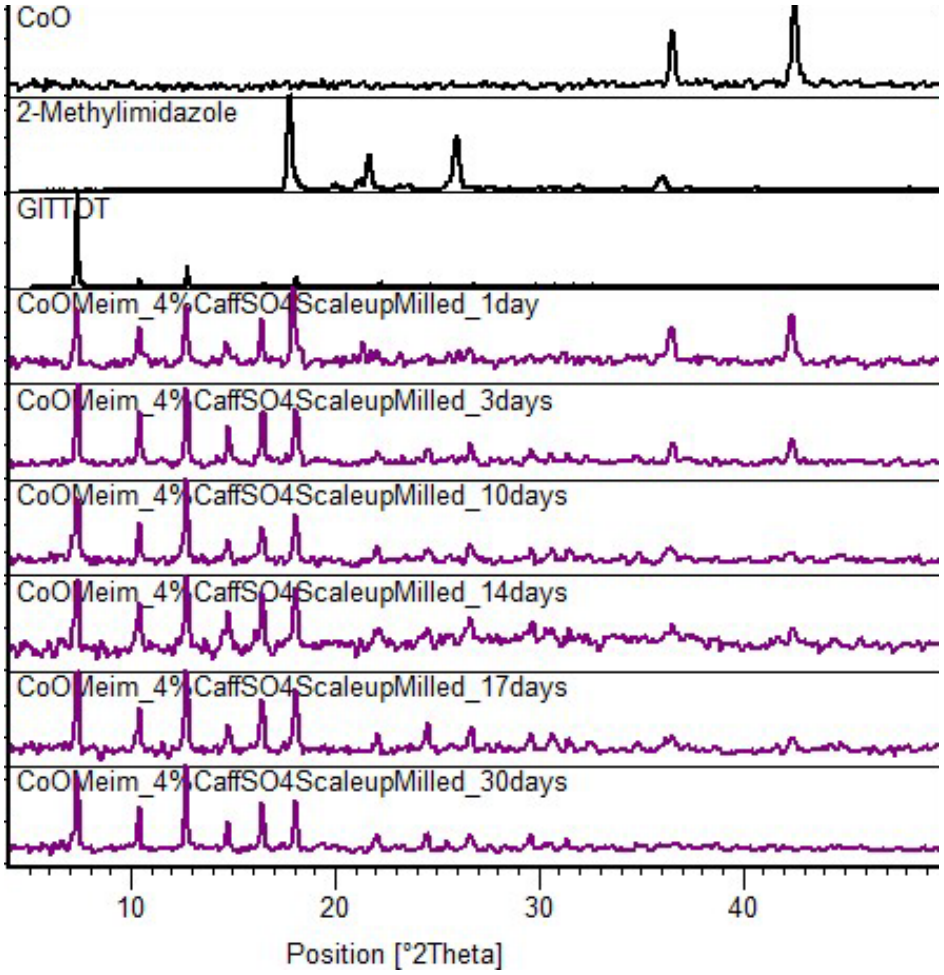

Figure S10. Powder X-ray diffraction patterns for the 5-gram scale accelerated aging reaction of **HMeIm** and CoO, with (**Hcaf**)(HSO_4) (4 mol% with respect to CoO) as the ionic additive. The reaction mixture was prepared by manual mixing of reactants and the catalytic salt in a mortar and pestle. The accelerated aging was conducted at 45 ^{o}C and 98% RH (from top to bottom): CoO reactant, **HMeIm** reactant; calculated pattern for ZIF-67 (CSD code GITTOT); reaction mixture after 1 day aging; 3 days aging; 10 days aging; 14 days aging; 17 days aging and 30 days aging.

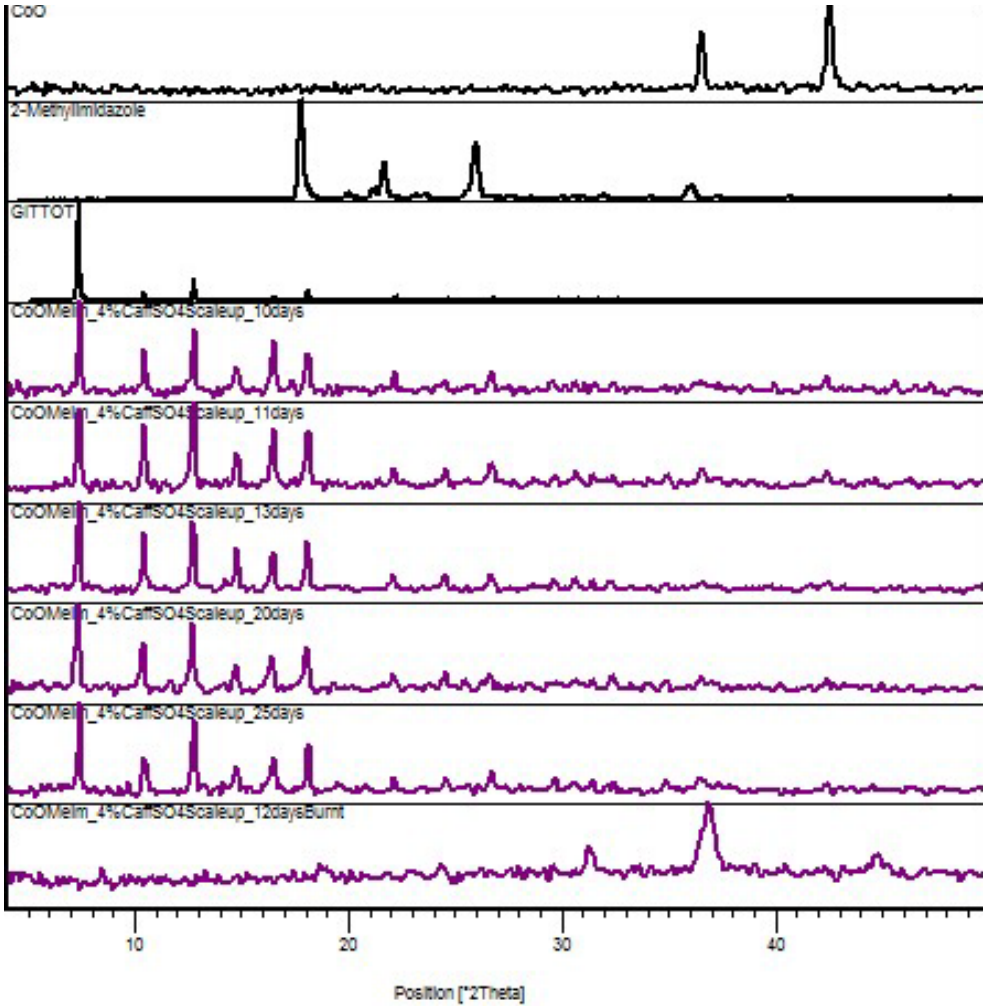

Figure S11. Powder X-ray diffraction patterns for the 5-gram scale accelerated aging reaction of **HMeIm** and CoO, with (**Hcaf**)(HSO_4) (4 mol% with respect to CoO) as the ionic additive. The reaction mixture was prepared by 5 minute milling of reactants and the catalytic salt in a 25 mL stainless steel milling jar. The accelerated aging was conducted at 45 ^{o}C and 98% RH (from top to bottom): CoO reactant, **HMeIm** reactant; calculated pattern for ZIF-67 (CSD code GITTOT); reaction mixture after 10 days aging; 11 days aging; 13 days aging; 20 days aging; 25 days aging and the reaction product after calcination in air. The PXRD pattern of the calcined product corresponds to Co_3O_4.

This journal is © The Royal Society of Chemistry 2013

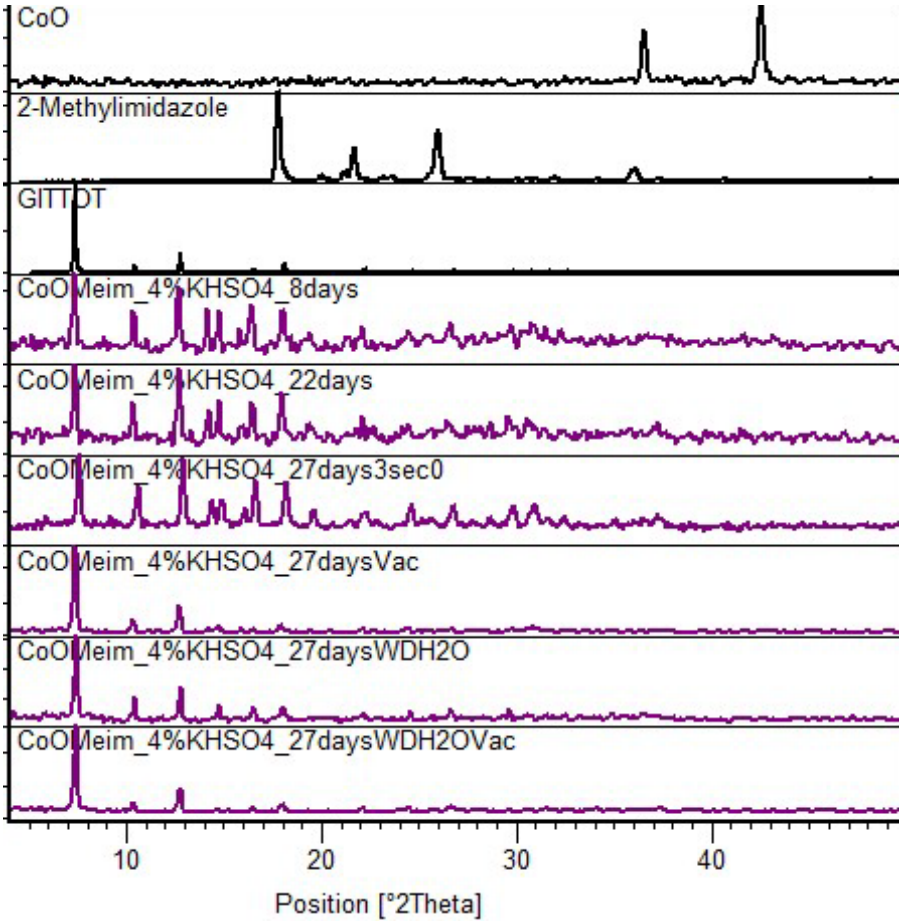

Figure S12. Powder X-ray diffraction patterns for the accelerated aging reaction of **HMeIm** and CoO, with $KHSO_4$ (4 mol% with respect to CoO) as the ionic additive. The reaction mixture was prepared by 5 minute milling of reactants and the catalytic salt in a 10 mL stainless steel milling jar. The accelerated aging was conducted at 45 ^{o}C and 98% RH (from top to bottom): CoO reactant, **HMeIm** reactant; calculated pattern for ZIF-67 (CSD code GITTOT); reaction mixture after 8 days; after 22 days; after 27 days; reaction mixture after 27 days accelerated aging, and evacuation; reaction mixture after 27 days accelerated aging, washed with water and reaction mixture after 27 days accelerated aging, washed with water and evacuated.

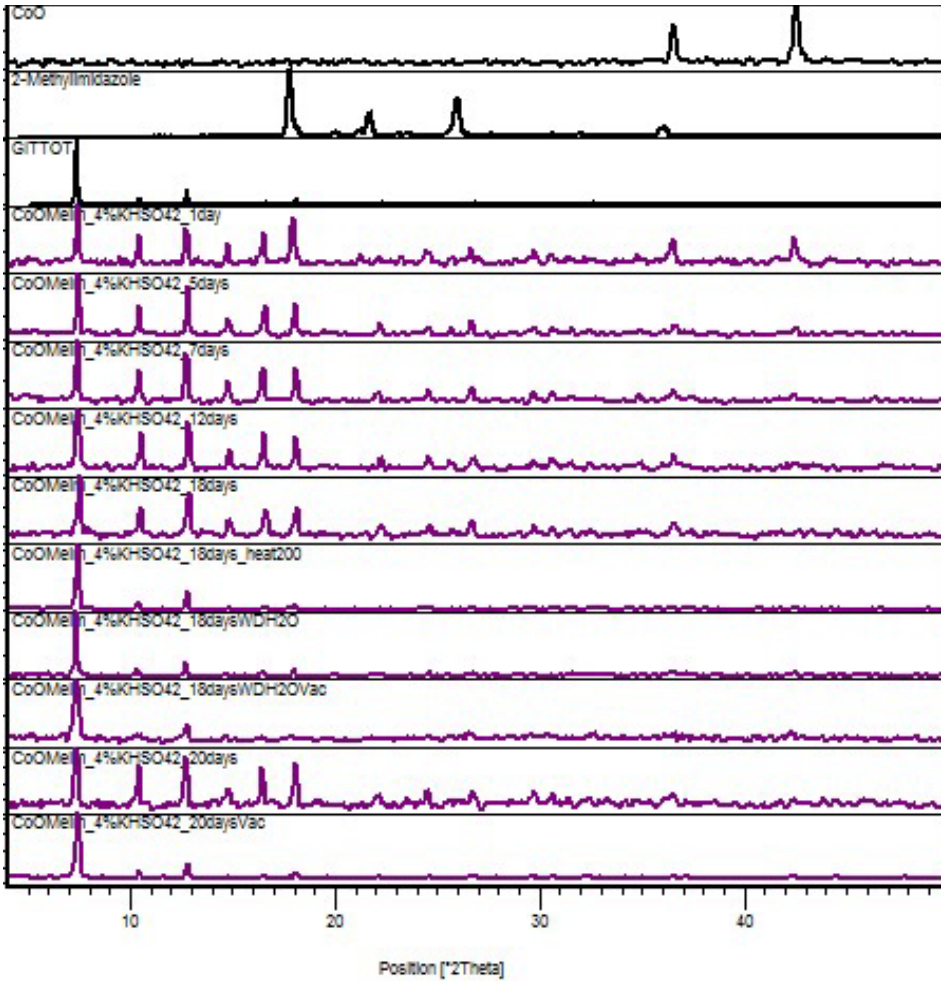

Figure S13. Powder X-ray diffraction patterns for the repeated accelerated aging reaction of **HMeIm** and CoO with $KHSO_4$ (4 mol% with respect to CoO) as the ionic additive. The reaction mixture was prepared by 5 minute milling of reactants and the catalytic salt in a 10 mL stainless steel milling jar. The accelerated aging was conducted at 45 ^{o}C and 98% RH (from top to bottom): CoO reactant, **HMeIm** reactant; calculated pattern for ZIF-67 (CSD code GITTOT); reaction mixture after 1 day; after 5 days; after 7 days; after 12 days; after 18 days; reaction mixture after 18 days accelerated aging and heating to 200 ^{o}C; ; reaction mixture after 18 days accelerated aging, washed with water; ; reaction mixture after 18 days accelerated aging, washed with water and evacuated; reaction mixture after 20 days accelerated aging; reaction mixture after 20 days accelerated aging, evacuated.

This journal is © The Royal Society of Chemistry 2013

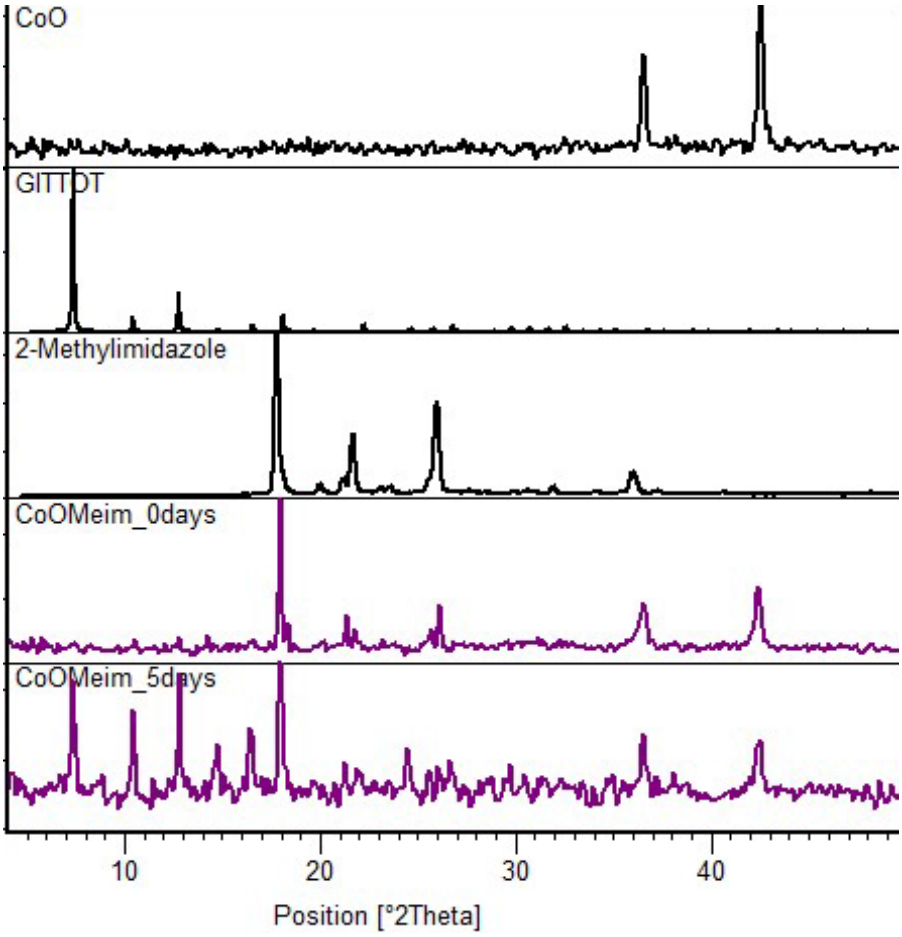

Figure S14. Powder X-ray diffraction patterns for the aging reaction of **HMeIm** and CoO without an ionic additive. The reaction mixture was prepared by 5 minute milling of reactants and the catalytic salt in a 10 mL stainless steel milling jar. Aging was conducted at 45 ^{o}C and 98% RH (from top to bottom): CoO reactant, **HMeIm** reactant; calculated pattern for ZIF-67 (CSD code GITTOT); reaction mixture immediately after mixing and after 5 days aging.

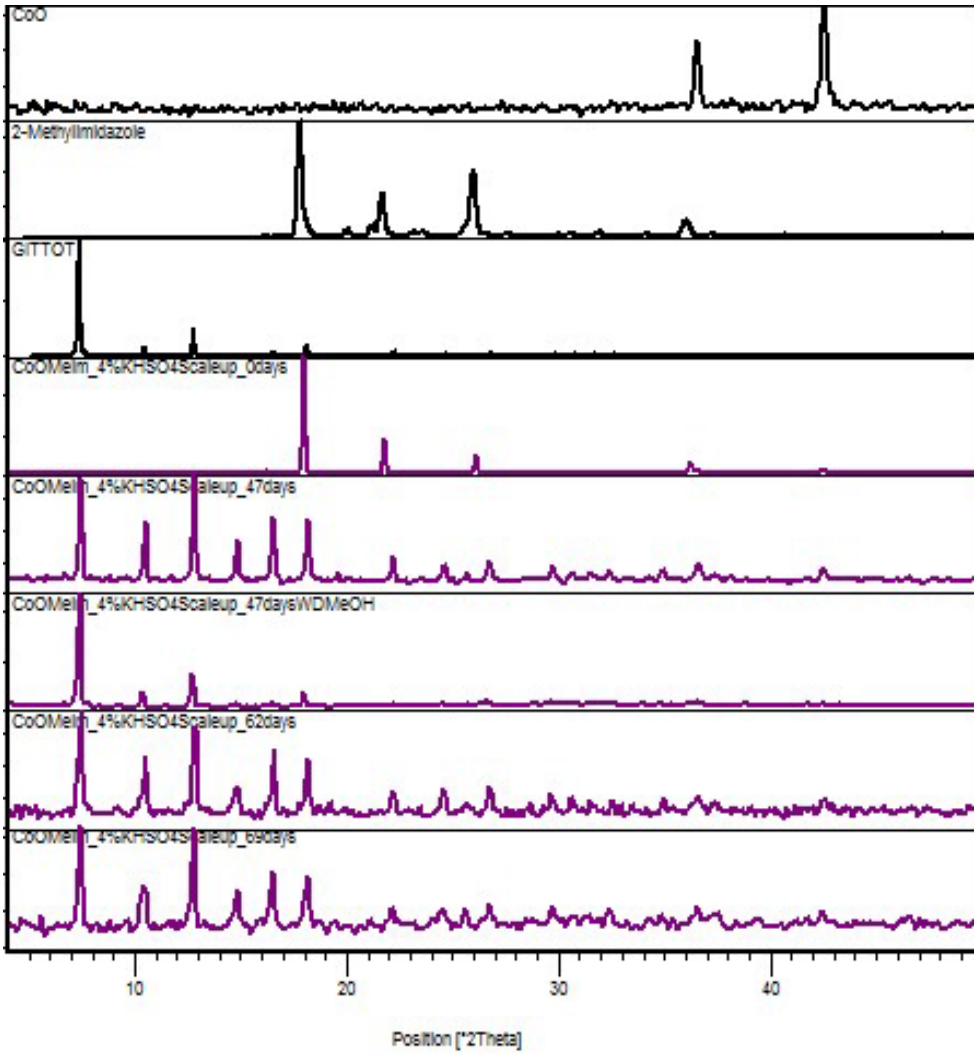

Figure S15. Powder X-ray diffraction patterns for the 5 gram scale accelerated aging reaction of **HMeIm** and CoO with $KHSO_4$ (4 mol% with respect to CoO) as the ionic additive. The reaction mixture was prepared by 5 minute milling of reactants and the catalytic salt in a 25 mL stainless steel milling jar. The accelerated aging was conducted at 45 ^{o}C and 98% RH (from top to bottom): CoO reactant, **HMeIm** reactant; calculated pattern for ZIF-67 (CSD code GITTOT); reaction mixture immediately after mixing; after 47 days; after 47 days and washing with methanol; after 62 days and after 69 days.

This journal is © The Royal Society of Chemistry 2013

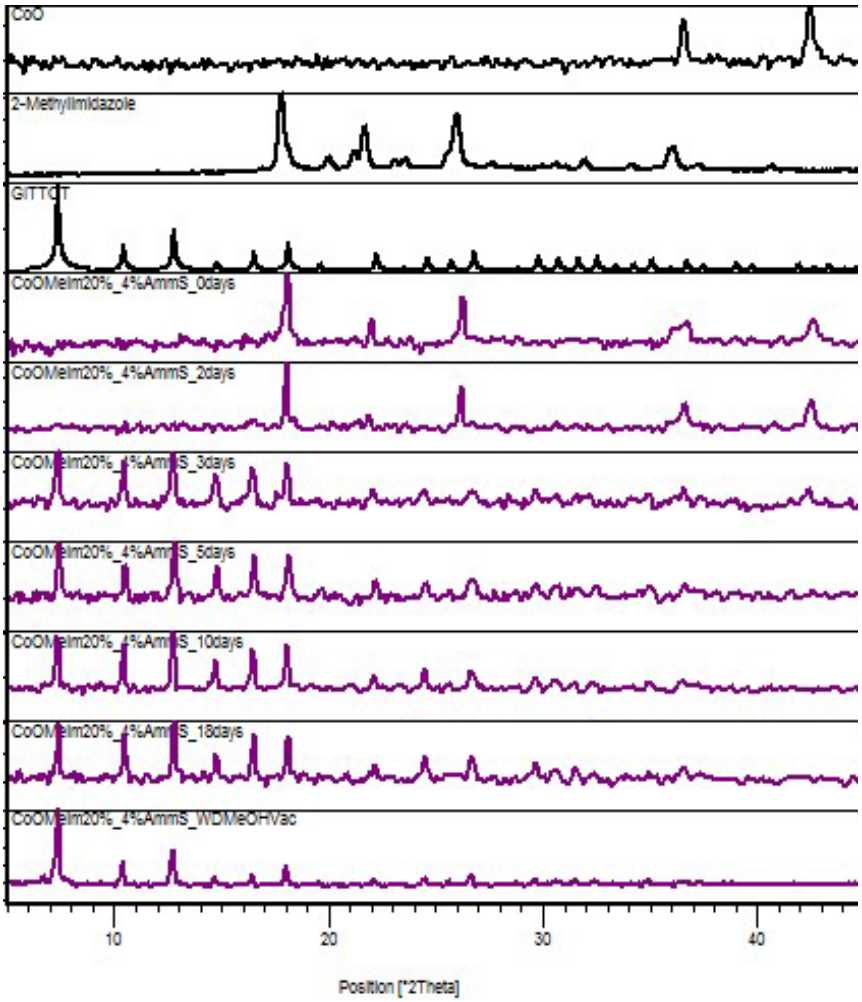

Figure S16. Powder X-ray diffraction patterns for the accelerated aging reaction of **HMeIm** and CoO with $(NH_4)_2SO_4$ (4 mol% with respect to CoO) as the ionic additive. The reaction mixture was prepared by 5 minute milling of reactants and the catalytic salt in a 10 mL stainless steel milling jar. The accelerated aging was conducted at 45 ^{o}C and 98% RH (from top to bottom): CoO reactant, **HMeIm** reactant; calculated pattern for ZIF-67 (CSD code GITTOT); reaction mixture immediately after mixing; after 2 days; after 3 days; after 5 days; after 10 days; after 18 days; reaction mixture after 18 days accelerated aging, washed with methanol and evacuated.

This journal is © The Royal Society of Chemistry 2013

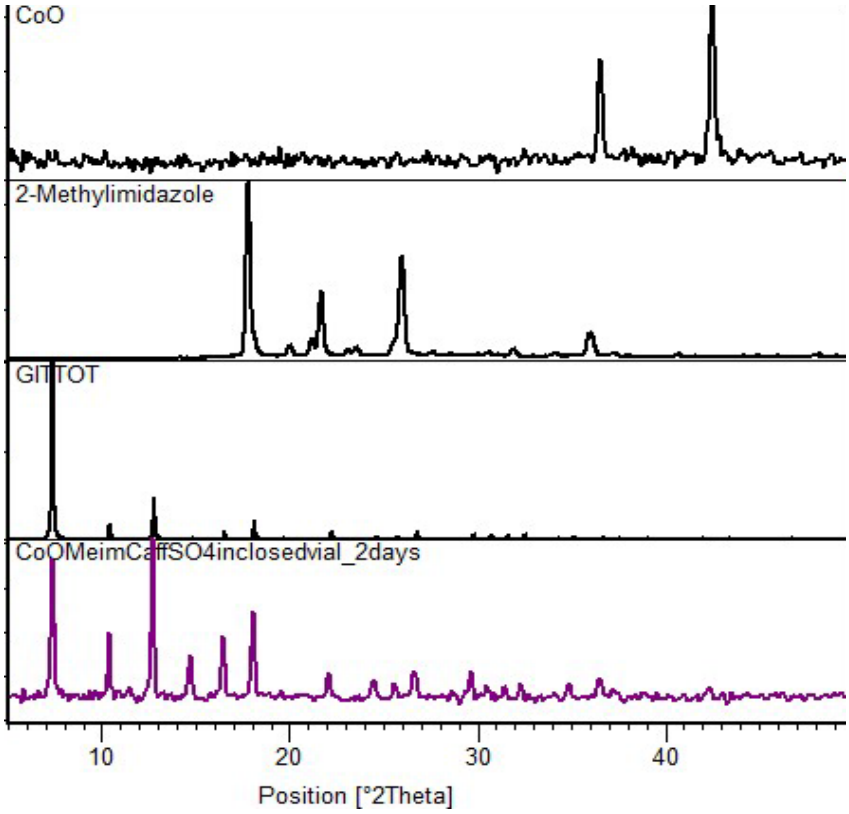

Figure S17. Powder X-ray diffraction patterns for the accelerated aging reaction of **HMeIm** and CoO with (**cafH**)(HSO_4) (4 mol% with respect to CoO) as the ionic additive. The reaction mixture was prepared by 5 minute milling of reactants and the catalytic salt in a 10 mL stainless steel milling jar. The accelerated aging was conducted at 45 ^{o}C and 100% RH (from top to bottom): CoO reactant, **HMeIm** reactant; calculated pattern for ZIF-67 (CSD code GITTOT); reaction mixture after 2 days.

This journal is © The Royal Society of Chemistry 2013

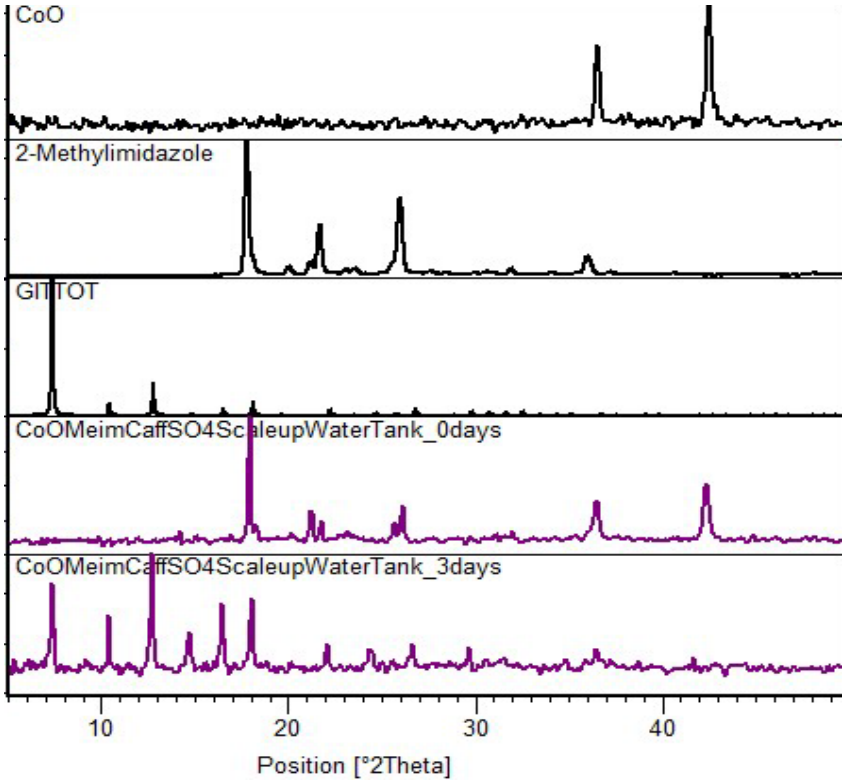

Figure S18. Powder X-ray diffraction patterns for the 5 gram accelerated aging reaction of **HMeIm** and CoO with (**cafH**)(HSO_4) (4 mol% with respect to CoO) as the ionic additive. The reaction mixture was prepared by 5 minute milling of reactants and the catalytic salt in a 10 mL stainless steel milling jar. The accelerated aging was conducted at 45 ^{o}C and 100% RH (from top to bottom): CoO reactant, **HMeIm** reactant; calculated pattern for ZIF-67 (CSD code GITTOT); reaction mixture immediately after mixing and after 3 days accelerated aging.

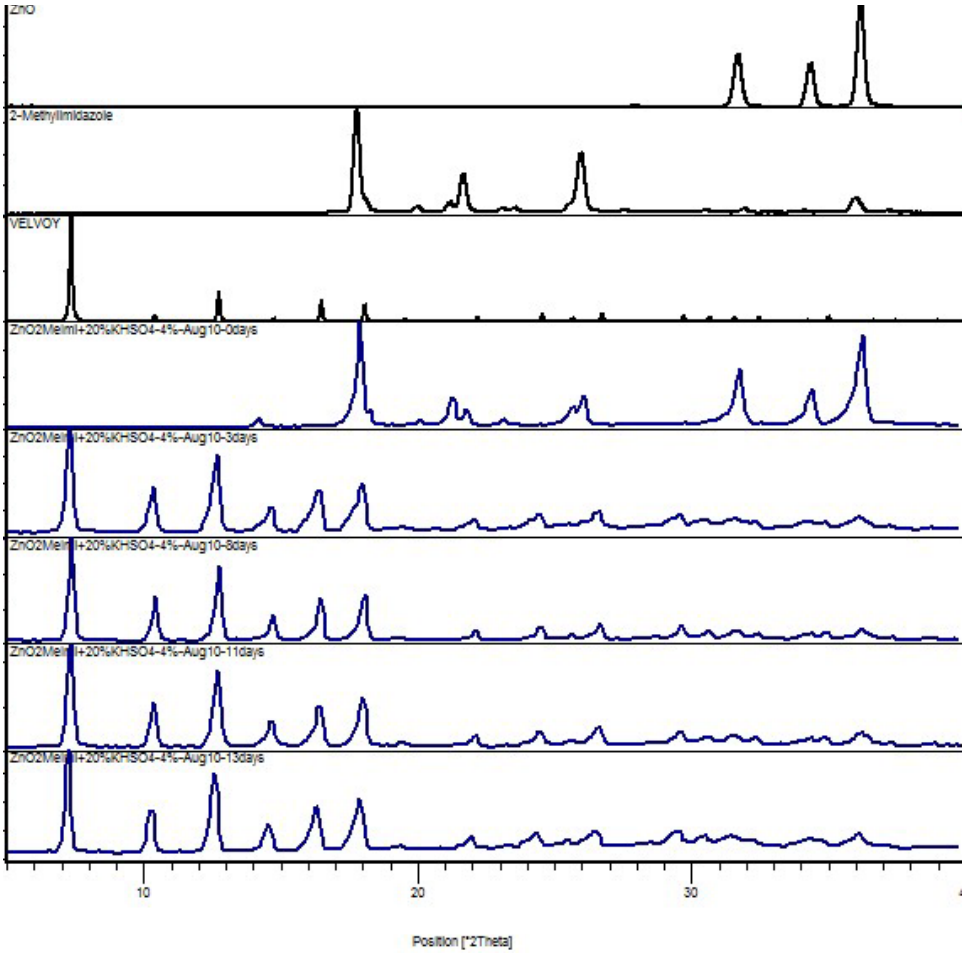

Figure S19. Powder X-ray diffraction patterns for the accelerated aging reaction of excess (20%) of **HMeIm** with ZnO in the presence of $KHSO_4$ (4 mol% with respect to ZnO) as the ionic additive. The reaction mixture was prepared by 5 minute milling of reactants and the catalytic salt in a 10 mL stainless steel milling jar. The accelerated aging was conducted at 45 ^{o}C and 98% RH (from top to bottom): ZnO reactant, **HMeIm** reactant; calculated pattern for ZIF-8 (CSD code VELVOY); reaction mixture immediately after mixing; after 3 days accelerated aging; after 8 days accelerated aging; after 11 days accelerated aging and after 13 days accelerated aging.

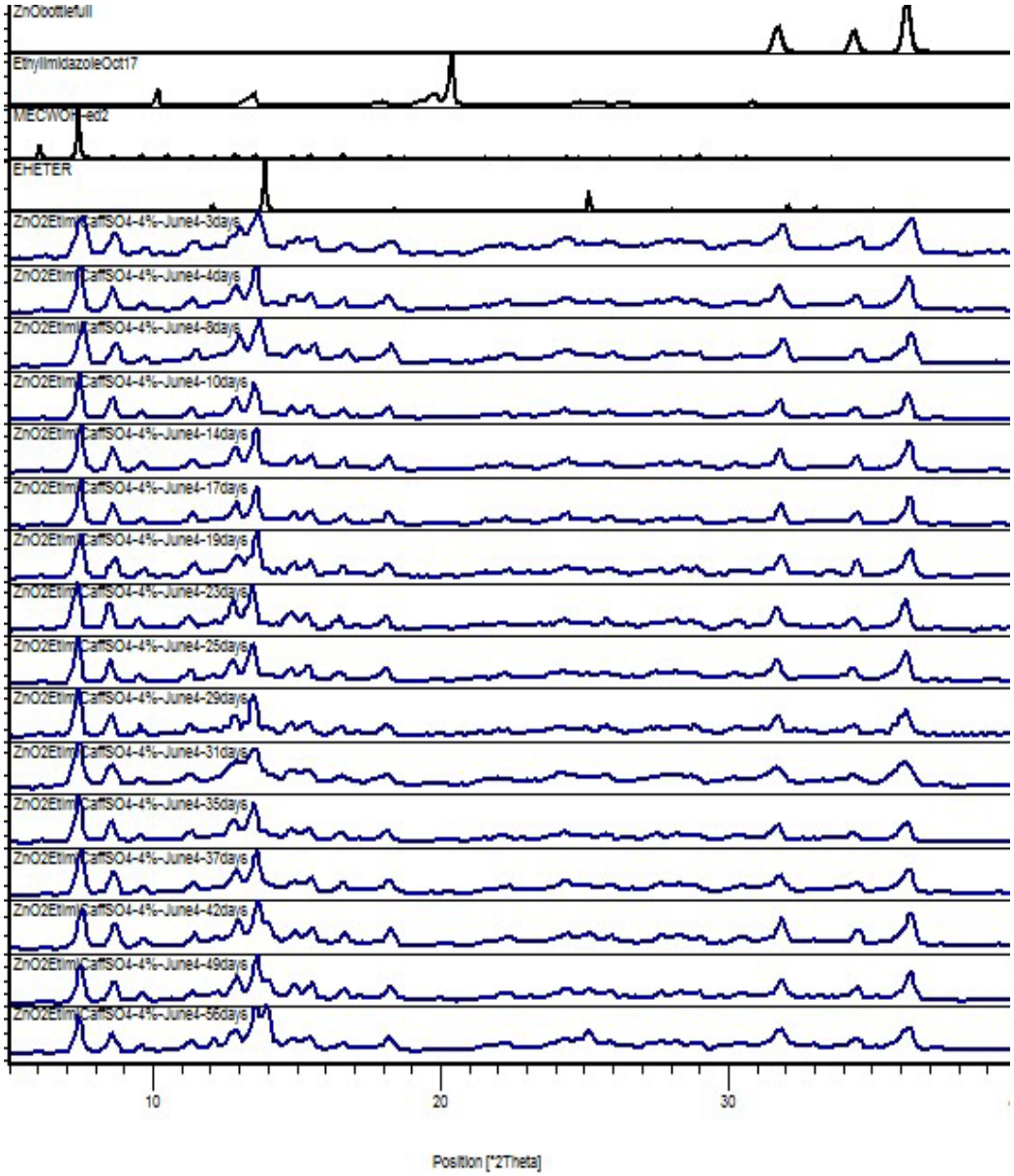

Figure S20. Powder X-ray diffraction patterns for the accelerated aging reaction of **HEtIm** with ZnO in the presence of (**cafH**)(HSO_4) (4 mol% with respect to ZnO) as the ionic additive. The reaction mixture was prepared by 5 minute milling of reactants and the catalytic salt in a 10 mL stainless steel milling jar. The accelerated aging was conducted at 45 ^{o}C and 98% RH (from top to bottom): ZnO reactant, **HEtIm** reactant; calculated pattern for zeolite rho topology Zn(**EtIm**)$_2$ porous framework (CSD code MECWOH); calculated pattern for quartz topology non-porous Zn(**EtIm**)$_2$ framework (CSD code EHETER); reaction mixture after 3 days accelerated aging; after 4 days accelerated aging; after 8 days accelerated aging; after 10 days accelerated aging; after 14 days accelerated aging; after 17 days accelerated aging; after 19 days accelerated aging; after 23 days accelerated aging; after 25 days accelerated aging; after 29 days accelerated aging; after 31 days accelerated aging; after 35 days accelerated aging; after 37 days accelerated aging; after 42 days accelerated aging; after 49 days accelerated aging and after 56 days accelerated aging.

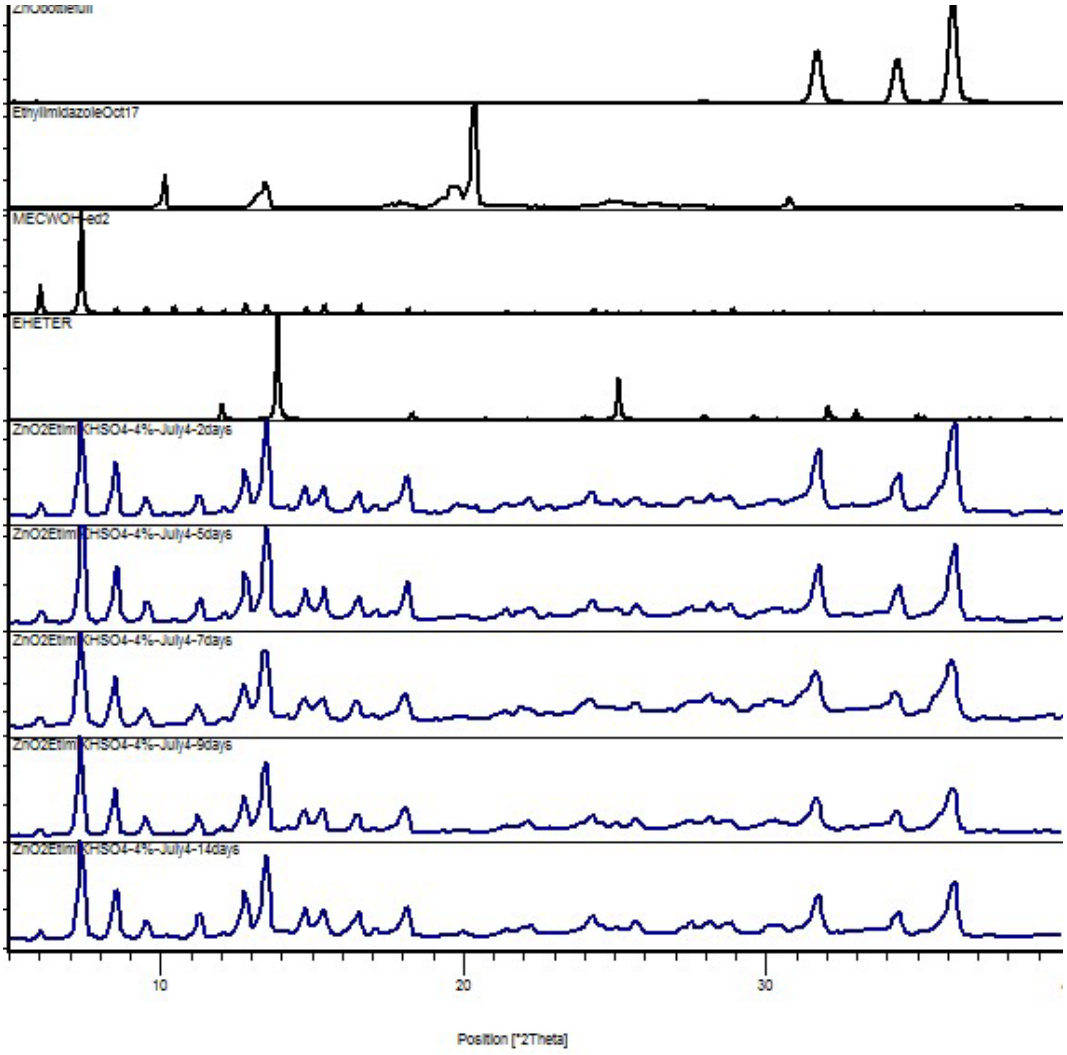

Figure S21. Powder X-ray diffraction patterns for the accelerated aging reaction of **HEtIm** with ZnO in the presence of $KHSO_4$ (4 mol% with respect to ZnO) as the ionic additive. The reaction mixture was prepared by 5 minute milling of reactants and the catalytic salt in a 10 mL stainless steel milling jar. The accelerated aging was conducted at 45 ^{o}C and 98% RH (from top to bottom): ZnO reactant, **HEtIm** reactant; calculated pattern for zeolite rho topology Zn(**EtIm**)$_2$ porous framework (CSD code MECWOH); calculated pattern for quartz topology non-porous Zn(**EtIm**)$_2$ framework (CSD code EHETER); reaction mixture after 2 days accelerated aging; after 5 days accelerated aging; after 7 days accelerated aging; after 9 days accelerated aging and after 14 days accelerated aging.

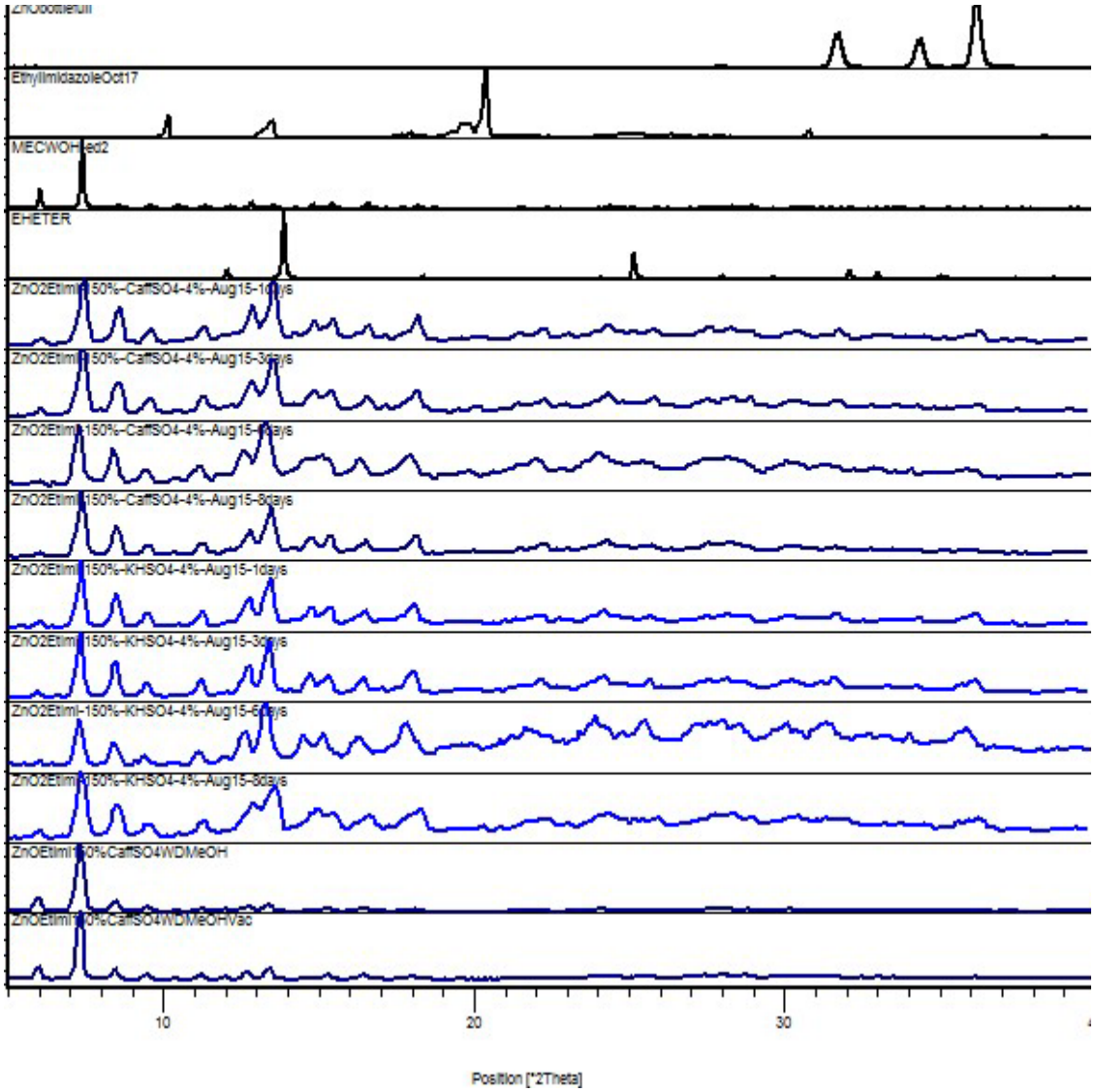

Figure S22. Powder X-ray diffraction patterns for the accelerated aging reaction of excess (150%) **HEtIm** with ZnO in the presence of either $KHSO_4$ or (**cafH**)(HSO_4) (each 4 mol% with respect to ZnO) as the ionic additive. The reaction mixtures were prepared by 5 minute milling of reactants and the salt additive in a 10 mL stainless steel milling jar. The accelerated aging was conducted at 45 ^oC and 98% RH (from top to bottom): ZnO reactant, **HEtIm** reactant; calculated pattern for zeolite rho topology Zn(**EtIm**)$_2$ porous framework (CSD code MECWOH); calculated pattern for quartz topology non-porous Zn(**EtIm**)$_2$ framework (CSD code EHETER); reaction mixture with (**cafH**)(HSO_4) after 1 day accelerated aging; reaction mixture with (**cafH**)(HSO_4) after 3 days accelerated aging; reaction mixture with (**cafH**)(HSO_4) after 6 days accelerated aging; reaction mixture with (**cafH**)(HSO_4) after 8 days accelerated aging; reaction mixture with $KHSO_4$ after 1 day accelerated aging; reaction mixture with $KHSO_4$ after 3 days accelerated aging; reaction mixture with $KHSO_4$ after 6 days accelerated aging; reaction mixture with $KHSO_4$ after 8 days accelerated aging; product of accelerating aging with (**cafH**)(HSO_4) additive after washing with methanol and after washing with methanol followed by evacuation.

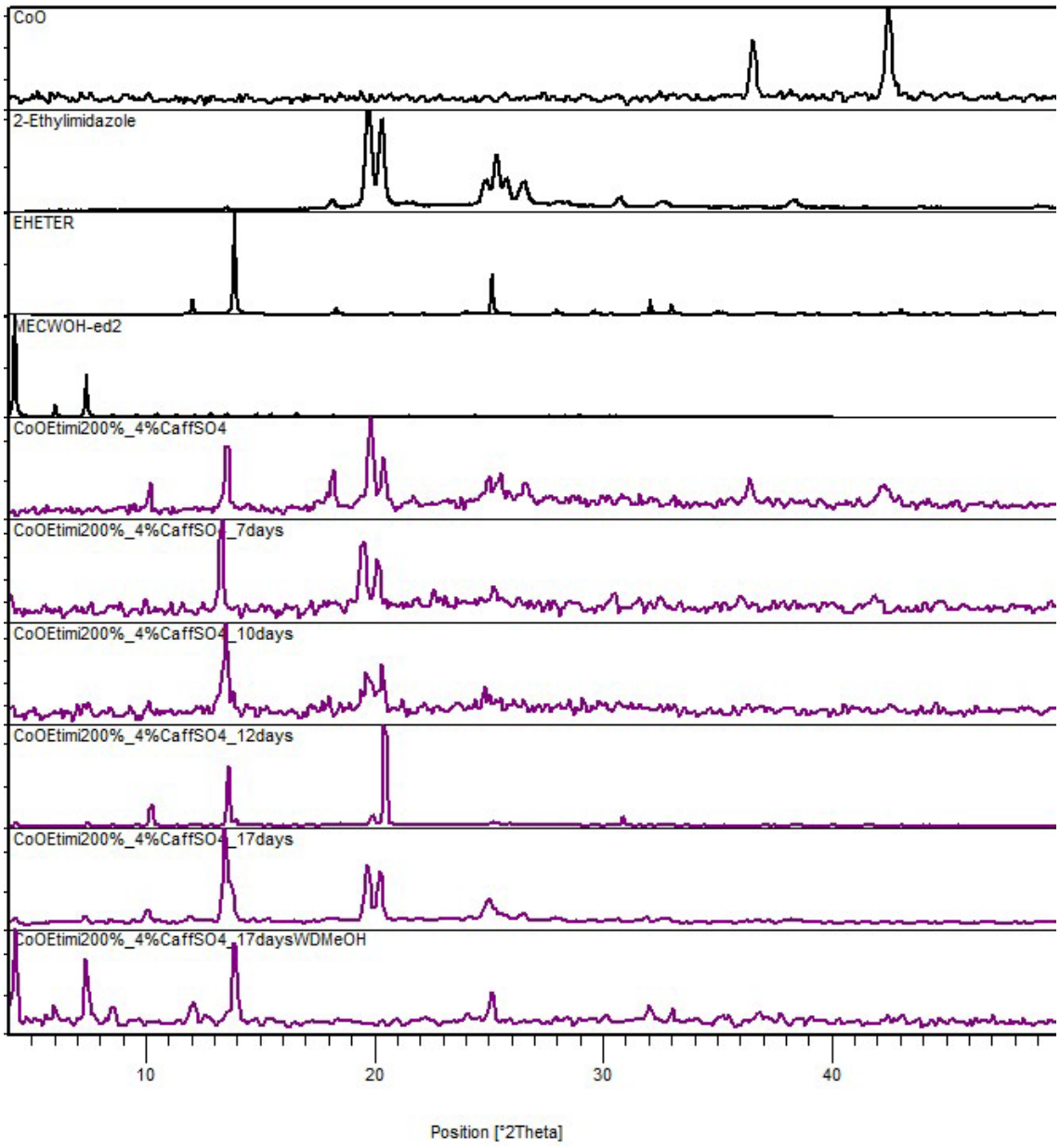

Figure S23. Powder X-ray diffraction patterns for the accelerated aging reaction of excess (200%) **HEtIm** with CoO in the presence of (**cafH**)(HSO_4) (4 mol% with respect to CoO) as the ionic additive. The reaction mixtures were prepared by 5 minute milling of reactants and the salt additive in a 10 mL stainless steel milling jar. The accelerated aging was conducted at 45 ^{o}C and 98% RH (from top to bottom): CoO reactant, **HEtIm** reactant; calculated pattern for quartz topology non-porous Zn(**EtIm**)$_2$ framework (CSD code EHETER); calculated pattern for zeolite rho topology Zn(**EtIm**)$_2$ porous framework (CSD code MECWOH); reaction mixture after 1 day accelerated aging; reaction mixture after 7 days accelerated aging; reaction mixture after 10 days accelerated aging; reaction mixture after 12 days accelerated aging; reaction mixture after 17 days accelerated aging and reaction mixture after 17 days accelerated aging, washed with methanol. Before washing with methanol, the PXRD patterns are dominated by the excess **HEtIm** ligand.

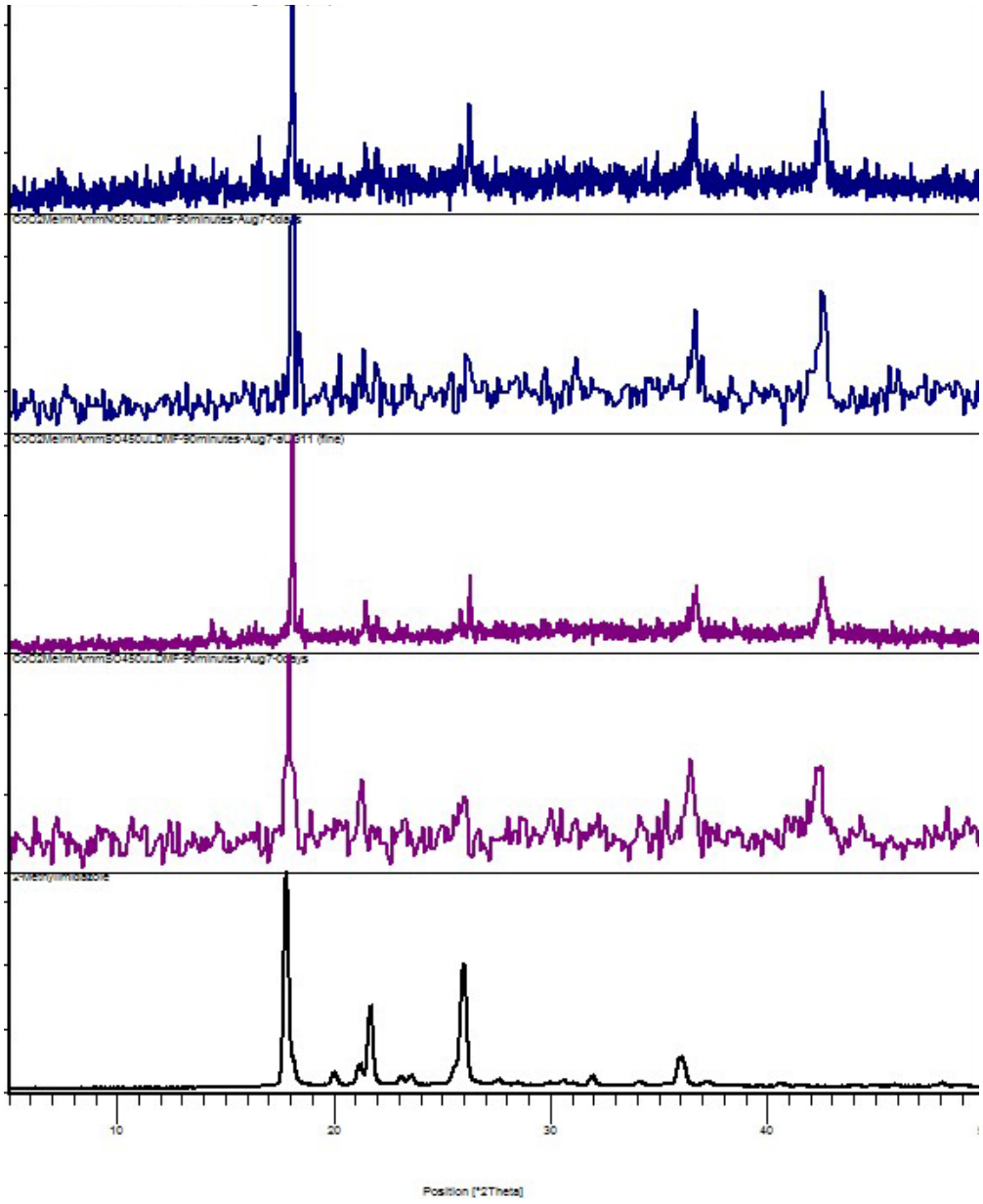

Figure S24. Powder X-ray diffraction patterns for attempted ion- and liquid-assisted (ILAG) mechanochemical syntheses of ZIF-67 (from top to bottom): mixture of CoO and **HMeIm** milled for 90 minutes in the presence of DMF and ammonium nitrate additive after 4 days sitting in a vial; mixture of CoO and **HMeIm** milled for 90 minutes in the presence of DMF and ammonium nitrate; mixture of CoO and **HMeIm** milled for 90 minutes in the presence of DMF and ammonium sulfate additive after 4 days sitting in a vial; mixture of CoO and **HMeIm** milled for 90 minutes in the presence of DMF and ammonium nitrate and commercial **HMeIm**. The reactions were designed to mimic the ones previously reported for the synthesis of ZIF-8 from ZnO, but the milling time was tripled (see: P. J. Beldon, L. Fábián, R. S. Stein, A. Thirumurugan, A. K. Cheetham, T. Friščić, *Angew. Chem. Int. Ed.*, **2010**, *49*, 9640)

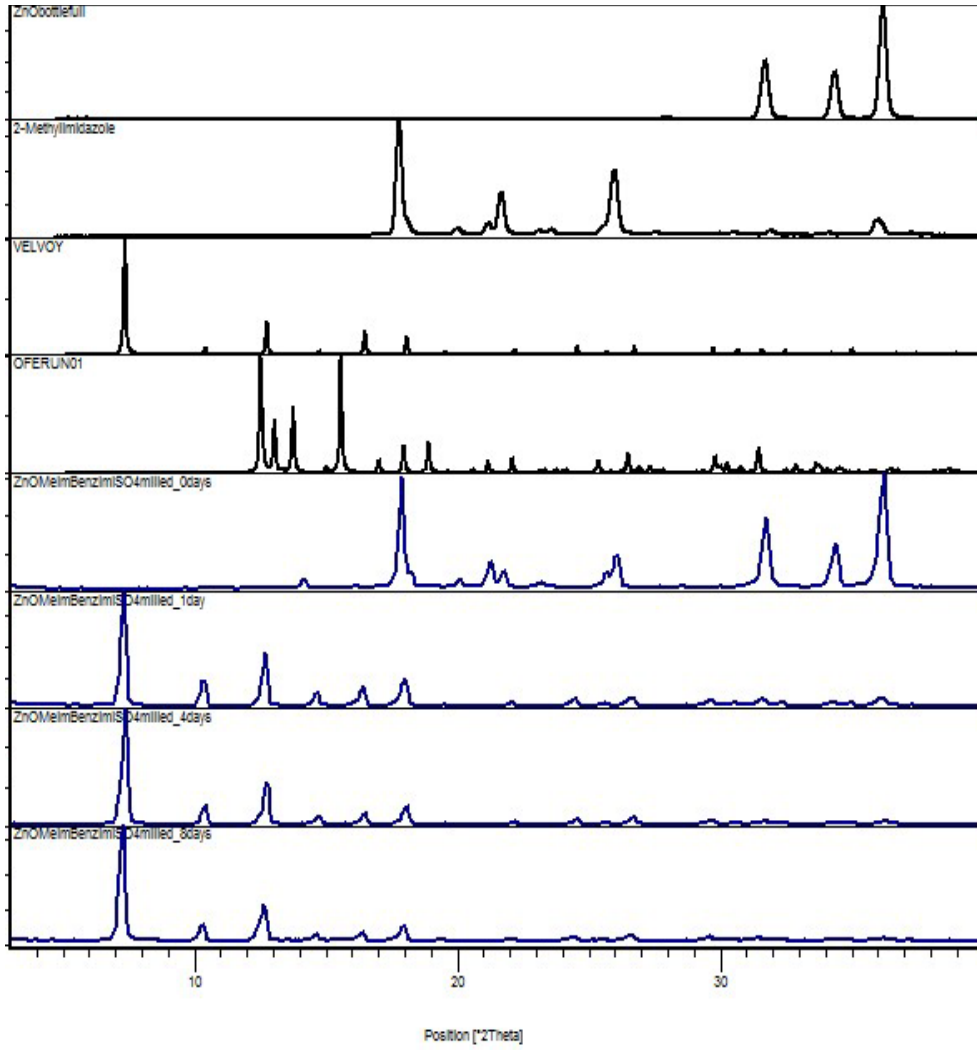

Figure S25. Powder X-ray diffraction patterns for the accelerated aging reaction of **HMeIm** with ZnO in the presence of (**HBIm**)$_2$(SO_4) (4 mol% with respect to ZnO) as the ionic additive. The reaction mixture was prepared by 5 minute milling of reactants and the salt additive in a 10 mL stainless steel milling jar. The accelerated aging was conducted at 45 ^oC and 100% RH (from top to bottom): ZnO reactant, **HMeIm** reactant; calculated pattern for the ZIF-8 sodalite-type framework (CSD code VELVOY); calculated pattern for the non-porous diamondoid Zn(**MeIm**)$_2$ framework (CSD code OFERUN01); reaction mixture immediately after mixing; after 1 day accelerated aging; after 4 days accelerated aging and after 8 days accelerated aging.

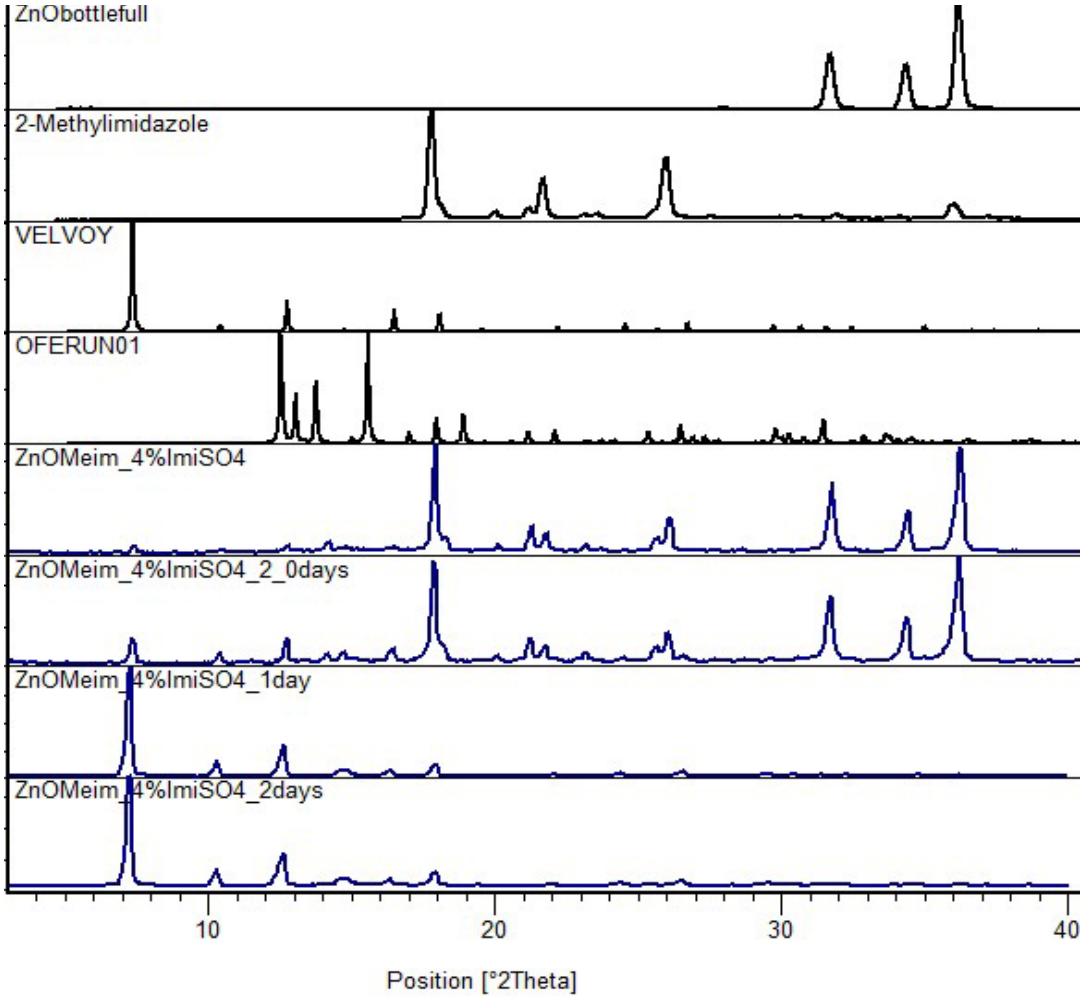

Figure S26. Powder X-ray diffraction patterns for the accelerated aging reaction of **HMeIm** with ZnO in the presence of (**H_2Im**)$_2$(SO_4)·2H_2O (4 mol% with respect to ZnO) as the ionic additive. The reaction mixture was prepared by 5 minute milling of reactants and the salt additive in a 10 mL stainless steel milling jar. The accelerated aging was conducted at 45 ^oC and 100% RH (from top to bottom): ZnO reactant, **HMeIm** reactant; calculated pattern for the ZIF-8 sodalite-type framework (CSD code VELVOY); calculated pattern for the non-porous diamondoid Zn(**MeIm**)$_2$ framework (CSD code OFERUN01); reaction mixture immediately after mixing; another identically prepared reaction mixture immediately after mixing; reaction mixture after 1 day accelerated aging and after 2 days accelerated aging.

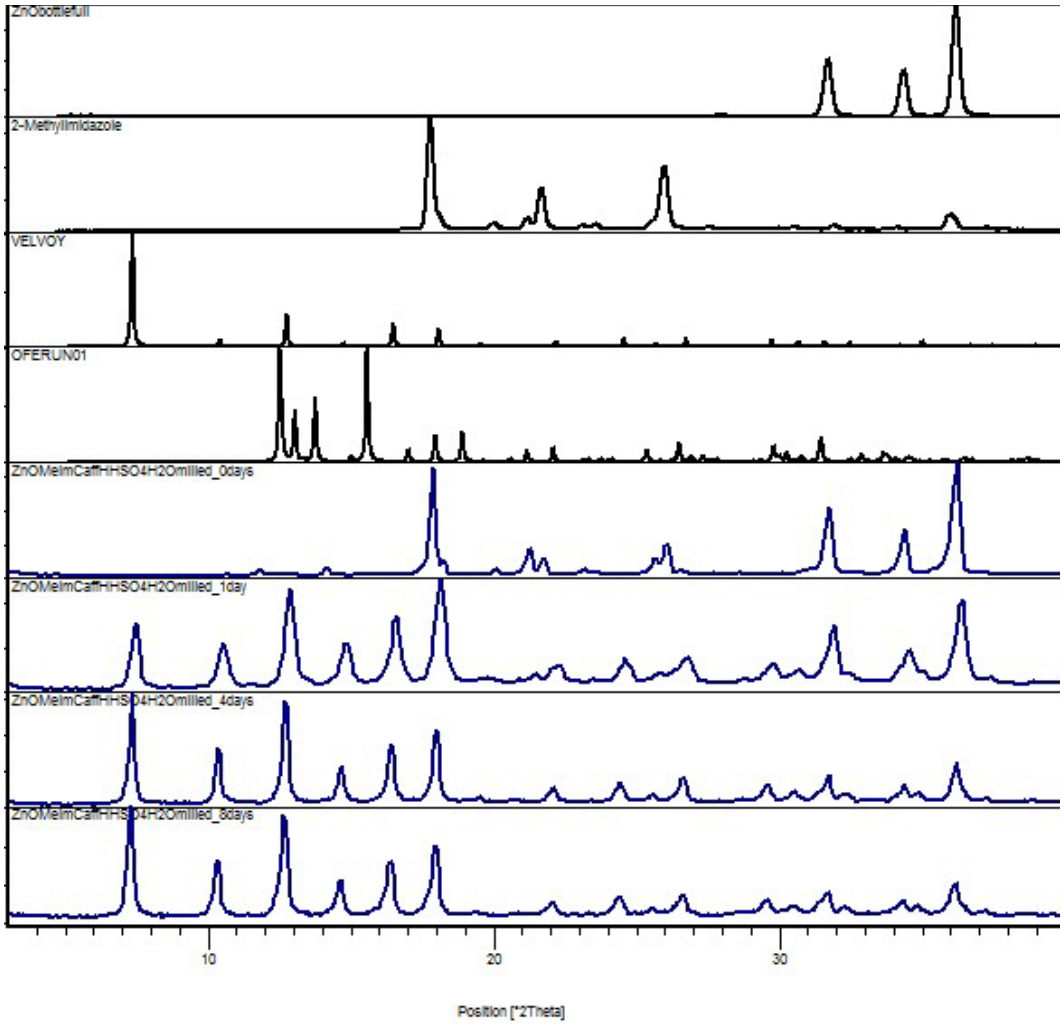

Figure S27. Powder X-ray diffraction patterns for the accelerated aging reaction of **HMeIm** with ZnO in the presence of (**Hcaf**)(HSO_4)·H_2O (4 mol% with respect to ZnO) as the ionic additive. The reaction mixture was prepared by 5 minute milling of reactants and the salt additive in a 10 mL stainless steel milling jar. The accelerated aging was conducted at 45 ^oC and 100% RH (from top to bottom): ZnO reactant, **HMeIm** reactant; calculated pattern for the ZIF-8 sodalite-type framework (CSD code VELVOY); calculated pattern for the non-porous diamondoid Zn(**MeIm**)$_2$ framework (CSD code OFERUN01); reaction mixture immediately after mixing; reaction mixture after 1 day accelerated aging; after 4 days accelerated aging and after 8 days accelerated aging.

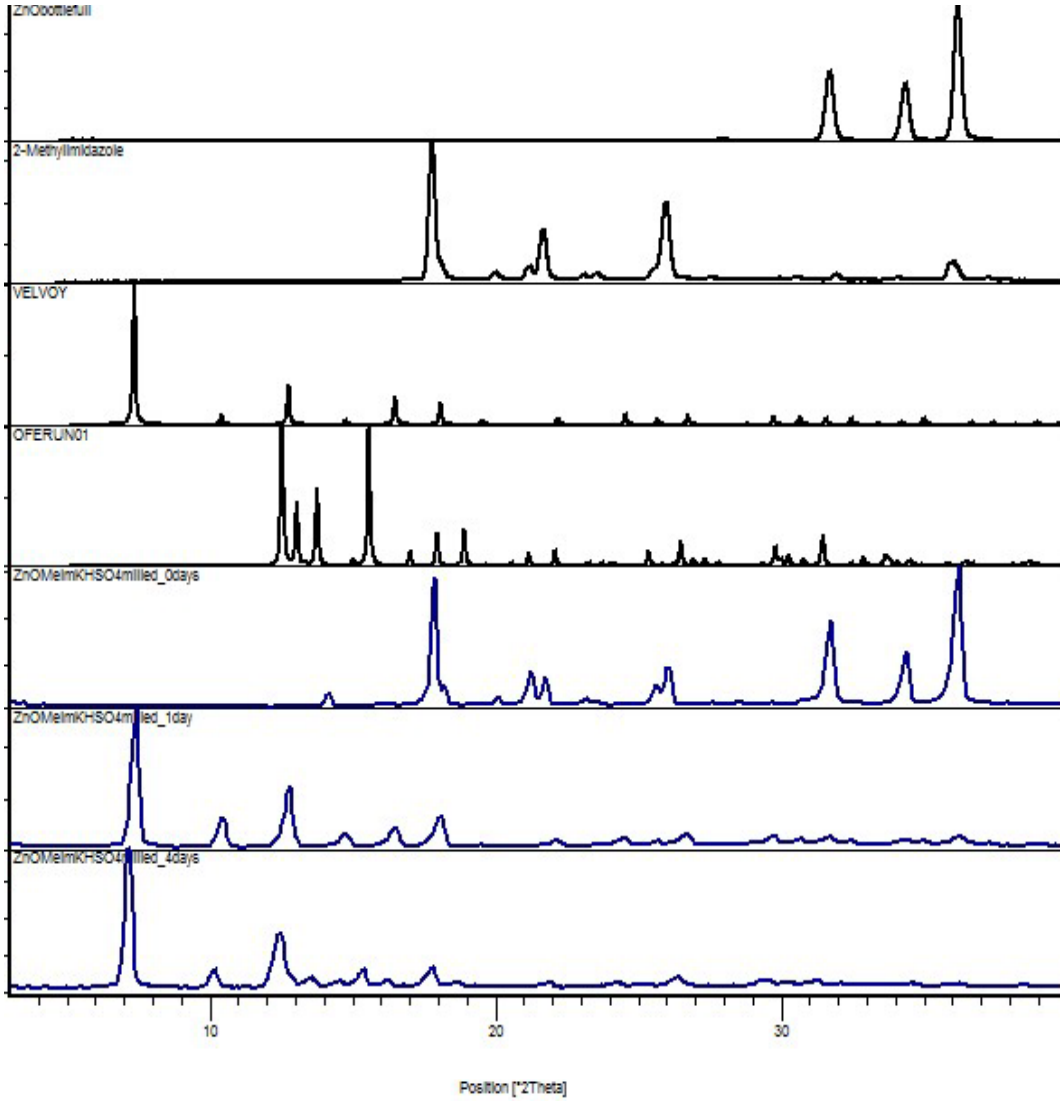

Figure S28. Powder X-ray diffraction patterns for the accelerated aging reaction of **HMeIm** with ZnO in the presence of $KHSO_4$ (4 mol% with respect to ZnO) as the ionic additive. The reaction mixture was prepared by 5 minute milling of reactants and the salt additive in a 10 mL stainless steel milling jar. The accelerated aging was conducted at 45 ^{o}C and 100% RH (from top to bottom): ZnO reactant, **HMeIm** reactant; calculated pattern for the ZIF-8 sodalite-type framework (CSD code VELVOY); calculated pattern for the non-porous diamondoid Zn(**MeIm**)$_2$ framework (CSD code OFERUN01); reaction mixture immediately after mixing; reaction mixture after 1 day accelerated aging and after 4 days accelerated aging.

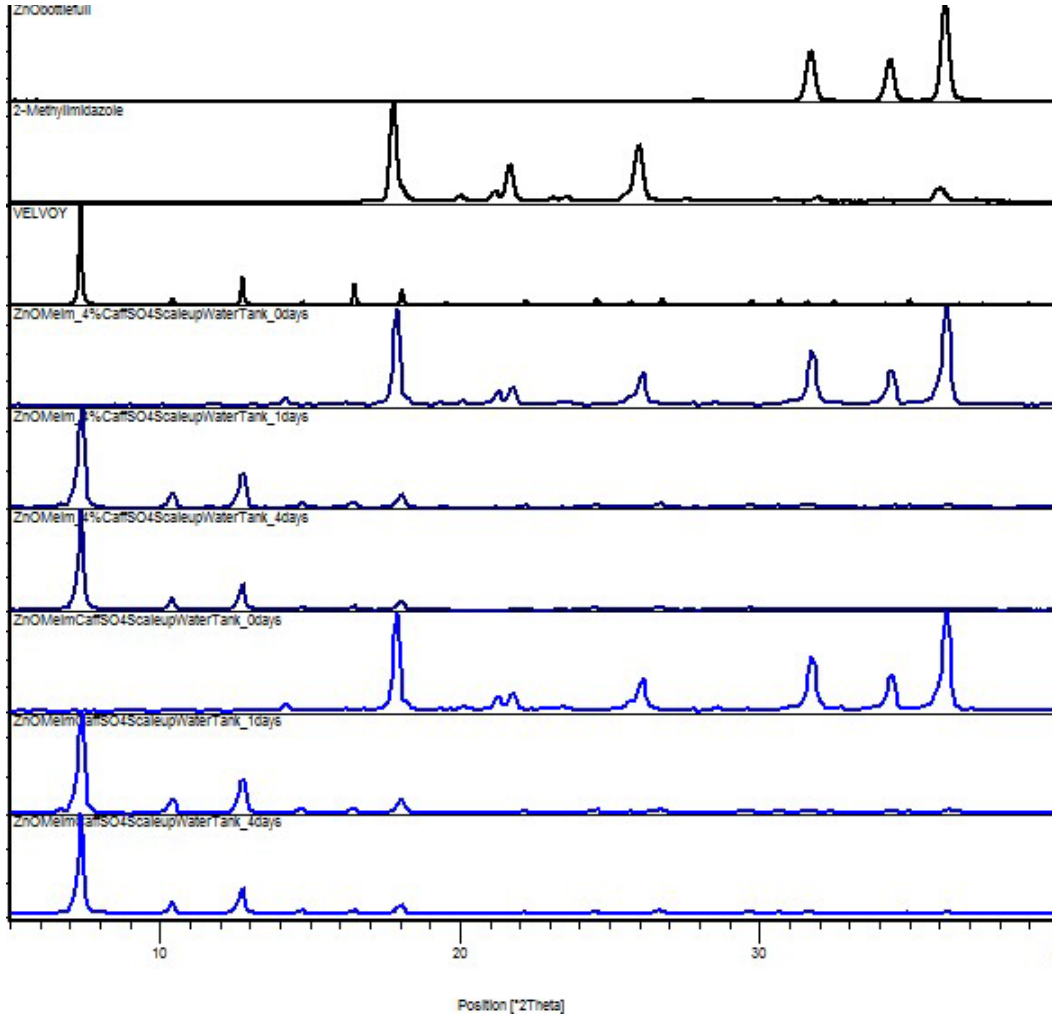

Figure S29. Powder X-ray diffraction patterns for two identically prepared 5 gram scale accelerated aging reaction of **HMeIm** with ZnO in the presence of (**Hcaf**)(HSO_4) (4 mol% with respect to ZnO) as the ionic additive. The reaction mixture was prepared by 5 minute milling of reactants and the salt additive in a 25 mL stainless steel milling jar. The accelerated aging was conducted at 45 ^{o}C and 100% RH (from top to bottom): ZnO reactant, **HMeIm** reactant; calculated pattern for the ZIF-8 sodalite-type framework (CSD code VELVOY); first reaction mixture immediately after mixing; first reaction mixture after 1 day accelerated aging; first reaction mixture after 4 days accelerated aging; second reaction mixture immediately after mixing; second reaction mixture after 1 day accelerated aging and second reaction mixture after 4 days accelerated aging.

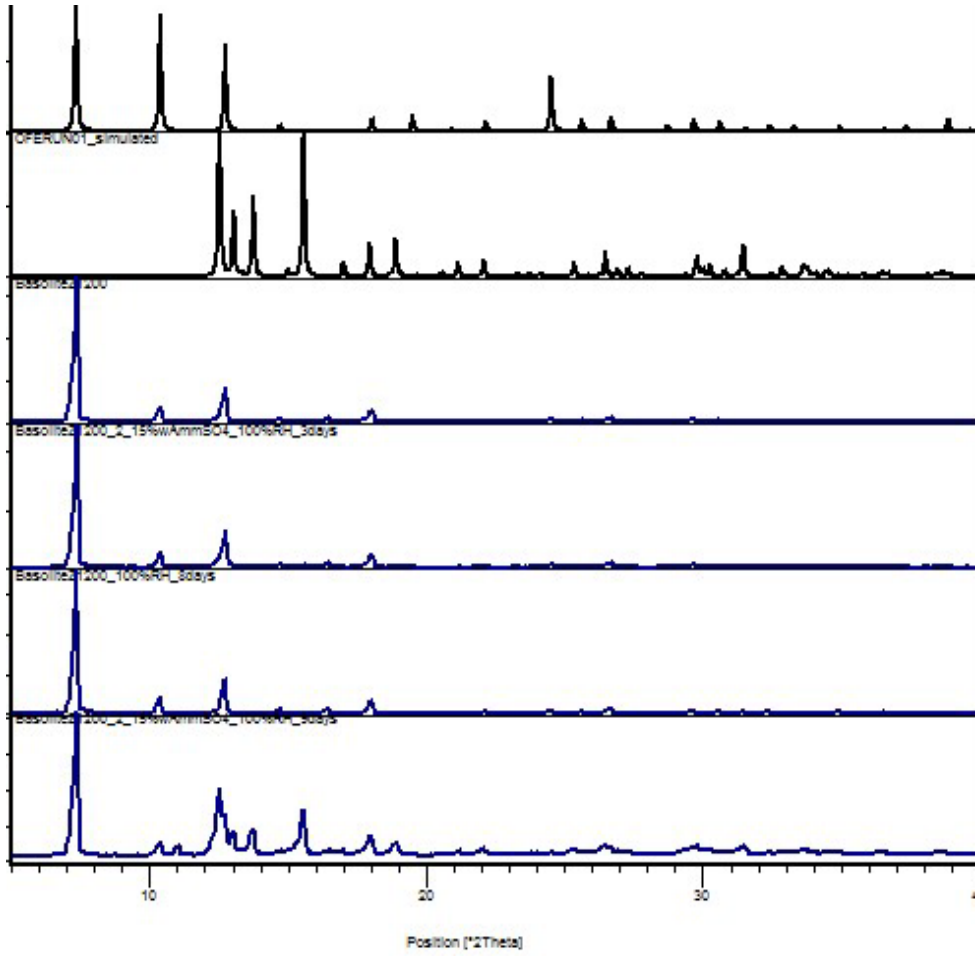

Figure S30. Powder X-ray diffraction patterns for the aging degradation of commercial ZIF-8 (Basolite Z1200) in the presence of 4 mol% ammonium sulfate (from top to bottom): simulated pattern for the ZIF-8 structure; simulated pattern for the close-packed *dia*-Zn(**MeIm**)$_2$; initial sample of Basolite Z1200; Basolite Z1200 after three days at 45 ^{o}C and 100% RH with 4 mol% $(NH_4)_2SO_4$; Basolite Z1200 after eight days in 100% RH with 4 mol% $(NH_4)_2SO_4$ and Basolite Z1200 after nine days in 100% RH with 4 mol% $(NH_4)_2SO_4$.

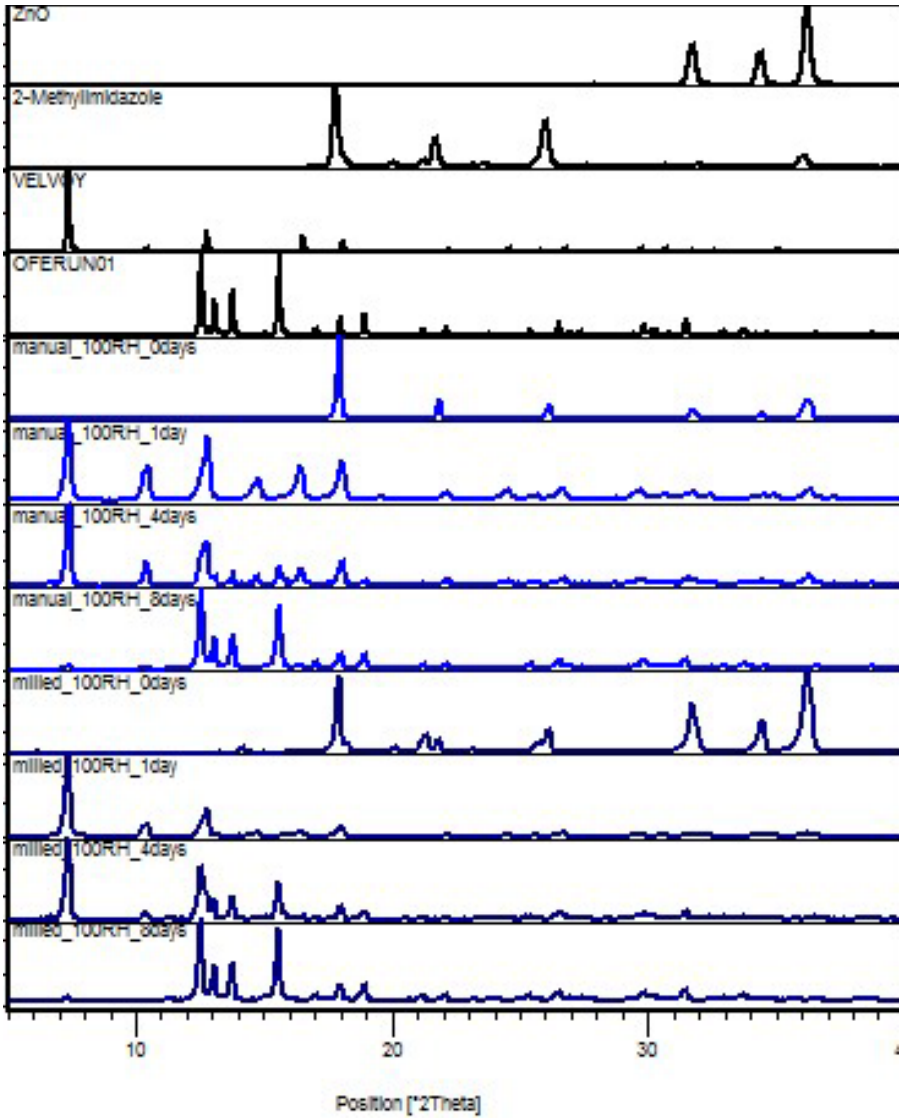

Figure S31. Powder X-ray diffraction patterns for the course of the accelerated aging reaction of ZnO and HMeIm using 4 mol% ammonium sulfate as the ionic additive, with reaction mixtures prepared either by manual mixing (blue) or mixed by ball milling for 5 minutes (dark blue) (from top to bottom): commercial ZnO, commercial **HMeIm**, simulated pattern for the ZIF-8 structure; simulated pattern for the close-packed *dia*-Zn(**MeIm**)$_2$; manually prepared mixture immediately after mixing, after 1 day, four days and 8 days aging at 45 ^{o}C and 100% RH; milled mixture immediately after mixing, after one day, four days and eight days of aging at 45^{o}C and 100% RH. The results strongly suggest very little difference between reaction mixtures mixed manually or by brief milling.

3. SOLID-STATE NMR SPECTROSCOPY DATA

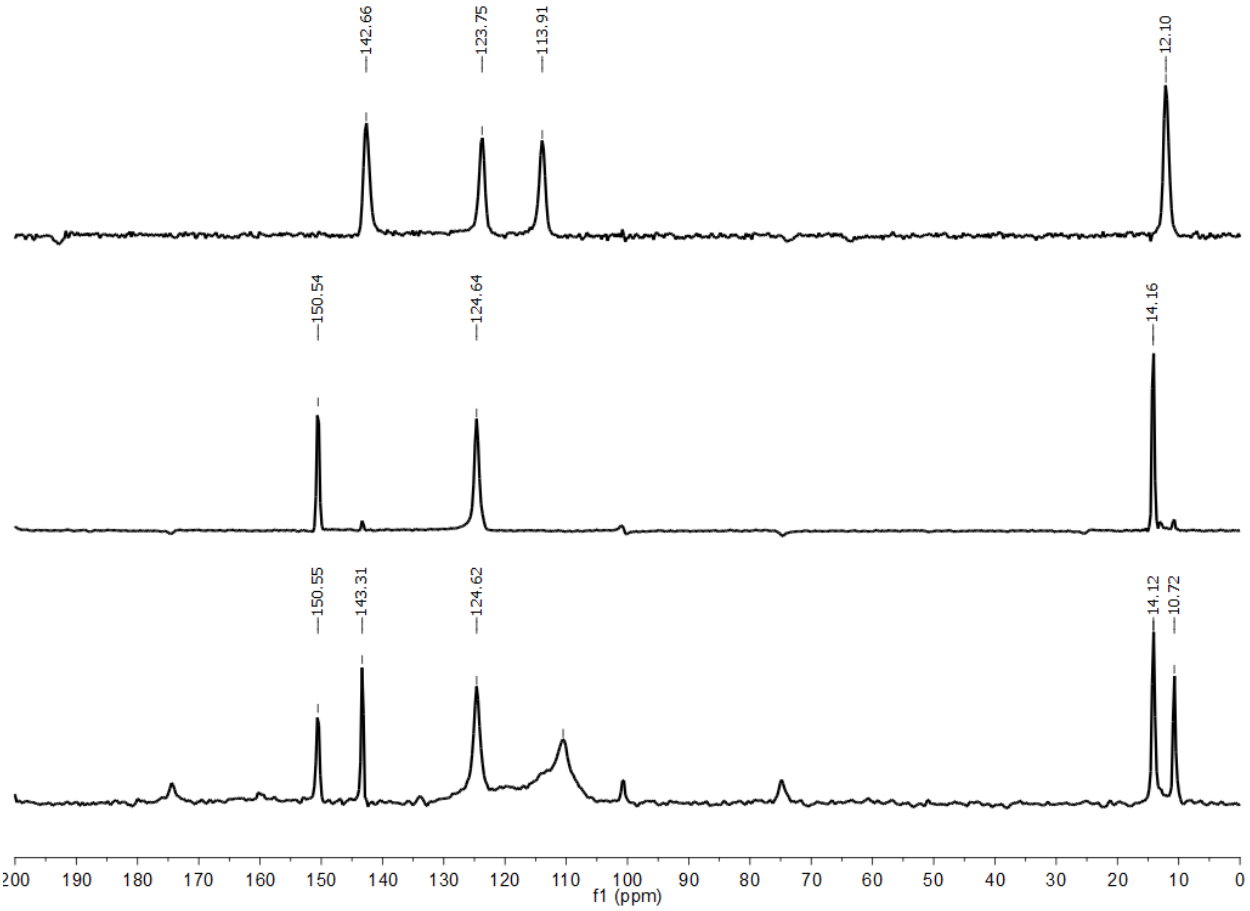

Figure S32. ^{13}C SSNMR spectra for reactions of ZnO and **HMeIm**, in the presence of 20% excess **HMeIm** and 4 mol% $KHSO_4$ ionic additive: (top) CP-MAS spectrum of crystalline **HMeIm**; (center) CP-MAS spectrum of the ZIF-8 structure Zn(**MeIm**)$_2$ obtained by accelerated aging and (bottom) DP-MAS spectrum of the ZIF-8 structure Zn(**MeIm**)$_2$ obtained by accelerated aging. Signal at 110 ppm corresponds to the teflon spacer of the sample holder.

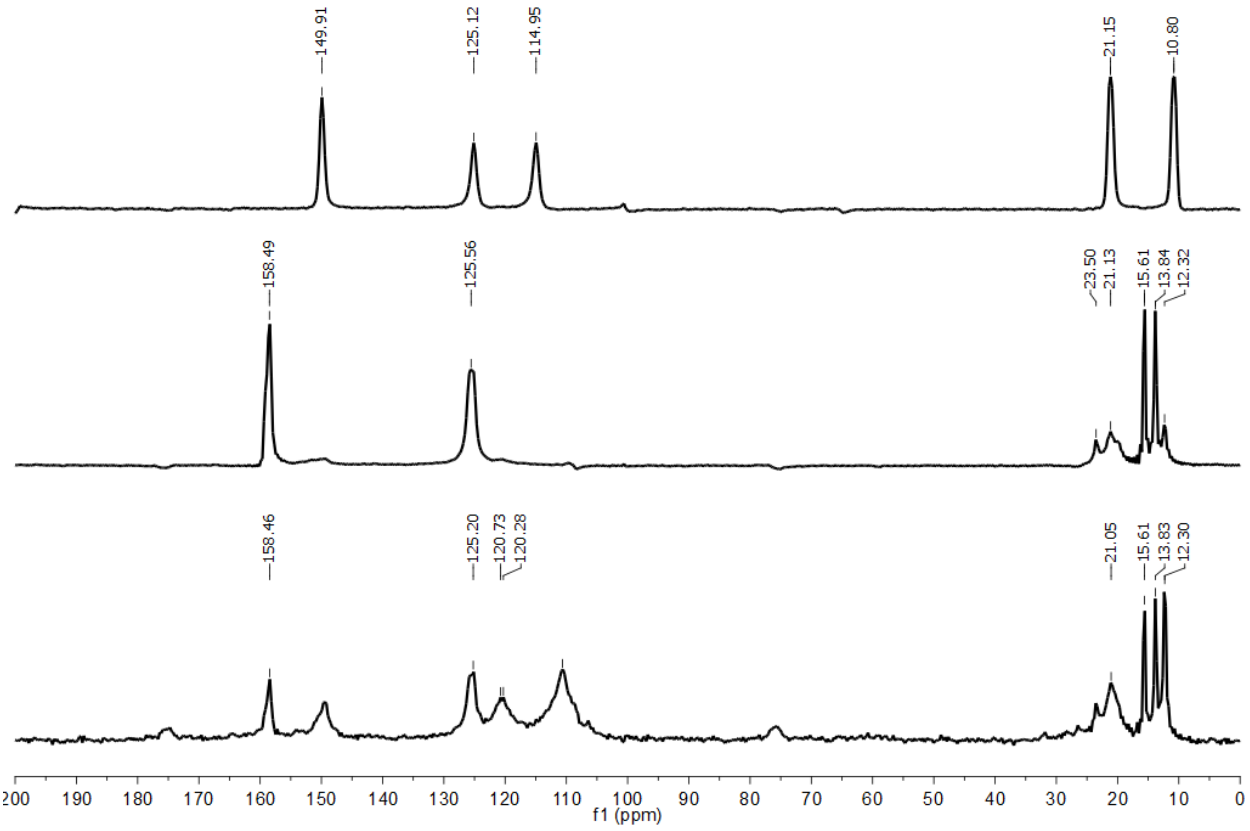

Figure S33. ^{13}C SSNMR spectra for reactions of ZnO and **HEtIm**, in the presence of 150% excess **HEtIm** and 4 mol% (**Hcaf**)(HSO_4) ionic additive: (top) CP-MAS spectrum of crystalline **HEtIm**; (center) CP-MAS spectrum of the RHO-Zn(**EtIm**)$_2$ obtained by accelerated aging and (bottom) DP-MAS spectrum of the RHO-Zn(**EtIm**)$_2$ made by accelerated aging. Signal at 110 ppm corresponds to the teflon spacer of the sample holder.

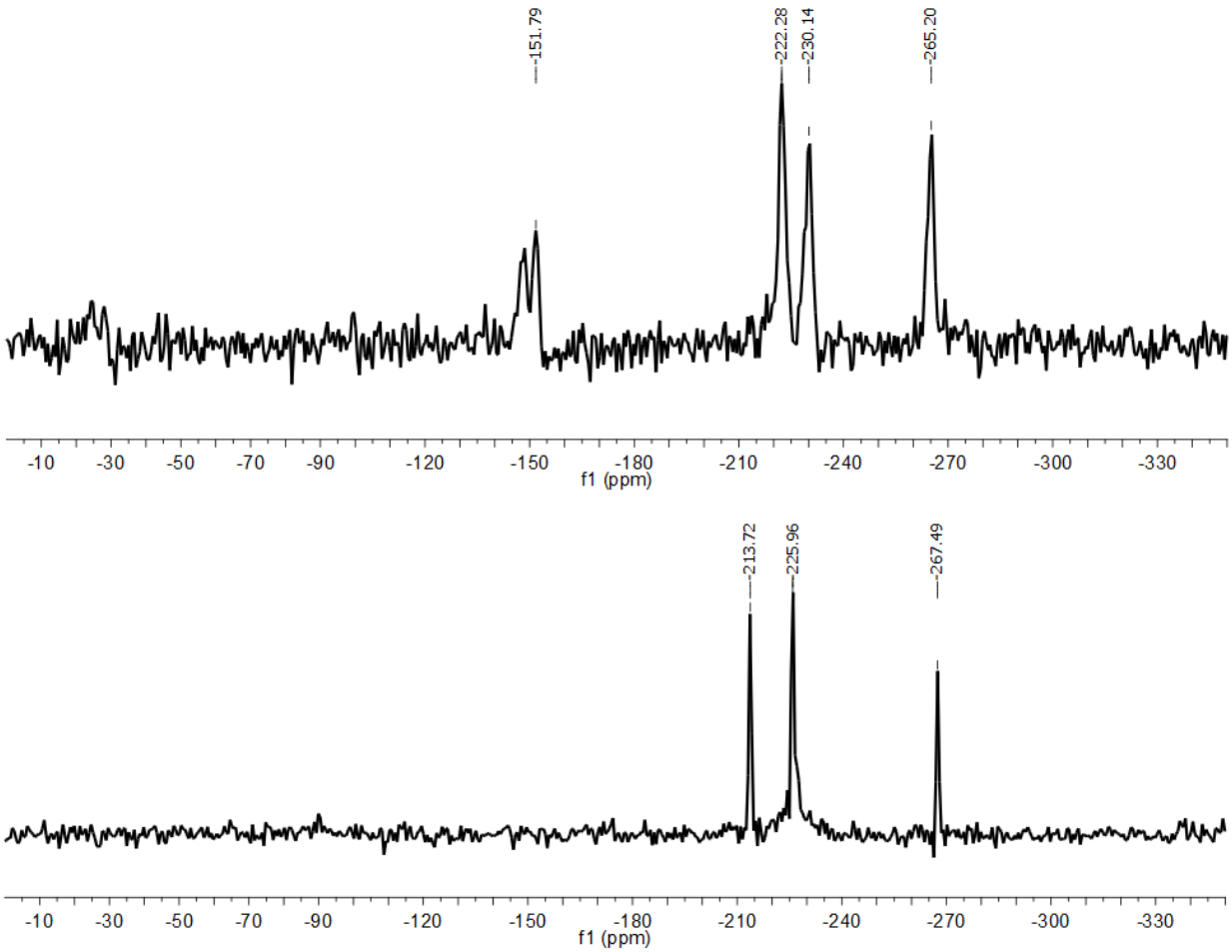

Figure S34. Natural abundance ^{15}N SSNMR spectra for commercial caffeine (top) and (**Hcaf**)(HSO_4) (bottom). The pattern of NMR signals for (**Hcaf**)(HSO_4) is consistent with the one previously reported for protonated caffeine in solid salts, see T. Friščić, D. G. Reid, G. M. Day, M. J. Duer, W. Jones, *Cryst. Growth Des.* **2011**, *11*, 972-981.

This journal is © The Royal Society of Chemistry 2013

4. SELECTED FOURIER-TRANSFORM ATTENUATED TOTAL REFLECTION (FTIR-ATR) DATA

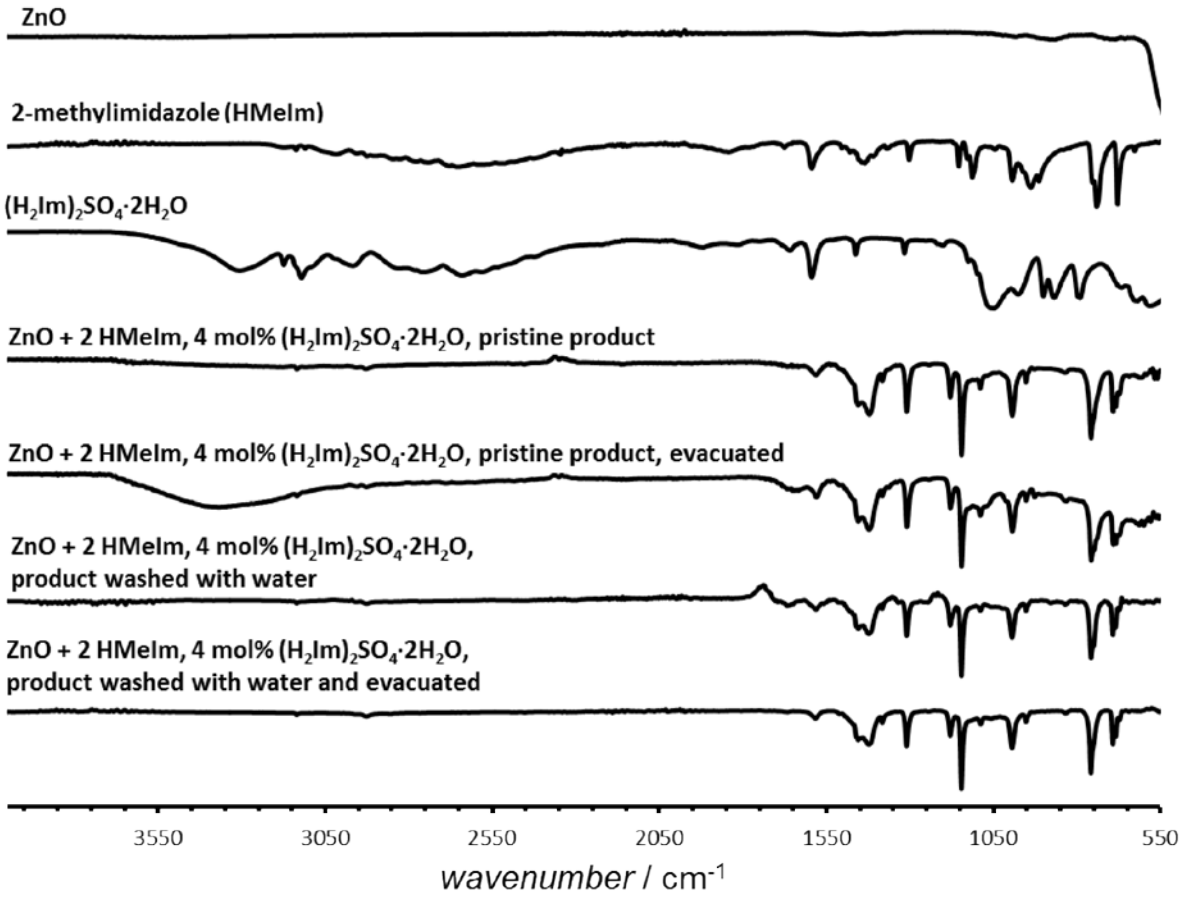

Figure S35. Selected FTIR-ATR spectra for reactants and products of accelerated aging reactions of ZnO and **HMeIm**, leading to the formation of the ZIF-8 structure, in the presence of 4 mol% (calculated based on ZnO) of (**H_2im**)$_2SO_4 \cdot 2H_2O$ as the ionic additive.

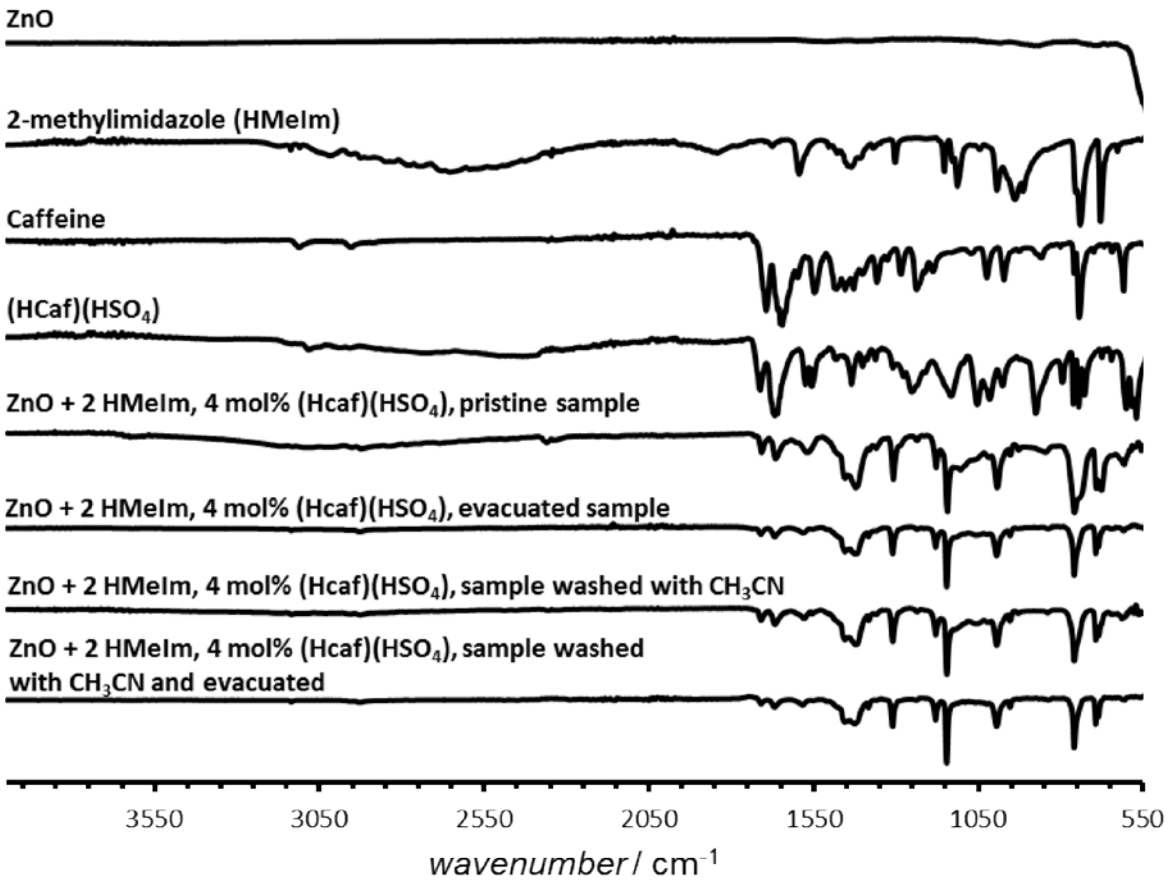

Figure S36. Selected FTIR-ATR spectra for reactants and products of accelerated aging reactions of ZnO and **HMeIm**, leading to the formation of the ZIF-8 structure, in the presence of 4 mol% (calculated based on ZnO) of (**Hcaf**)(HSO_4) as the ionic additive.

This journal is © The Royal Society of Chemistry 2013

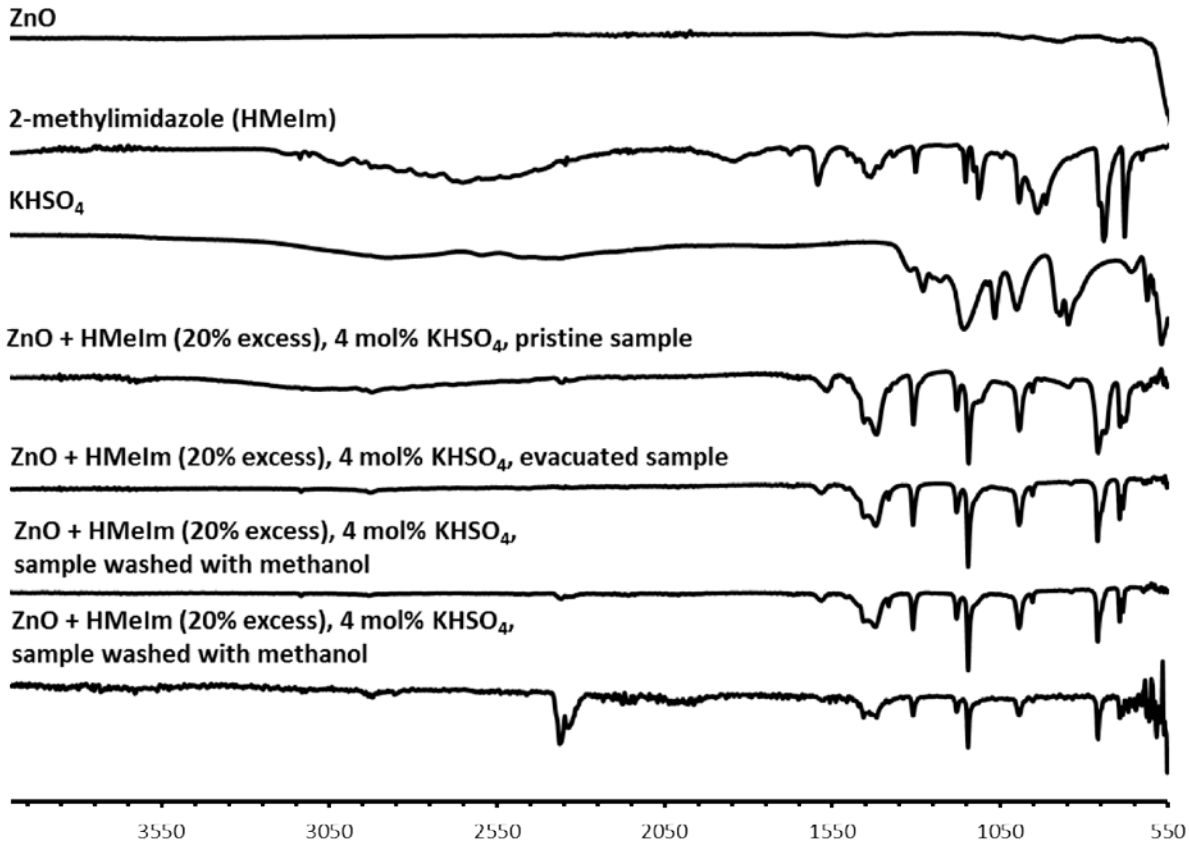

Figure S37. Selected FTIR-ATR spectra for reactants and products of accelerated aging reactions of ZnO and **HMeIm**, leading to the formation of the ZIF-8 structure, in the presence of 4 mol% (calculated based on ZnO) of $KHSO_4$ as the ionic additive and 20% excess of ligand **HMeIm**.

This journal is © The Royal Society of Chemistry 2013

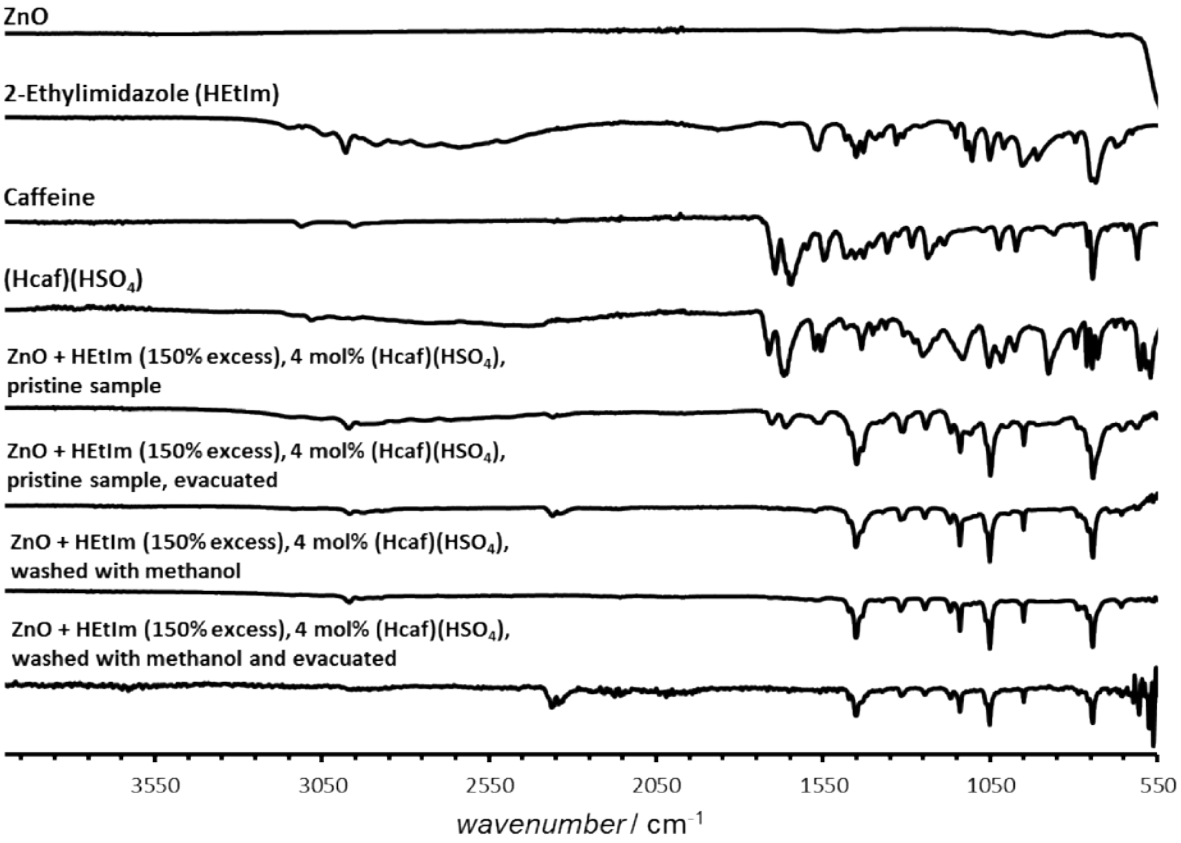

Figure S38. Selected FTIR-ATR spectra for reactants and products of accelerated aging reactions of ZnO and **HEtIm**, leading to the formation of the RHO topology Zn(**EtIm**)$_2$, in the presence of 4 mol% (calculated based on ZnO) of (**Hcaf**)(HSO_4) as the ionic additive and 150% excess of ligand **HEtIm**.

This journal is © The Royal Society of Chemistry 2013

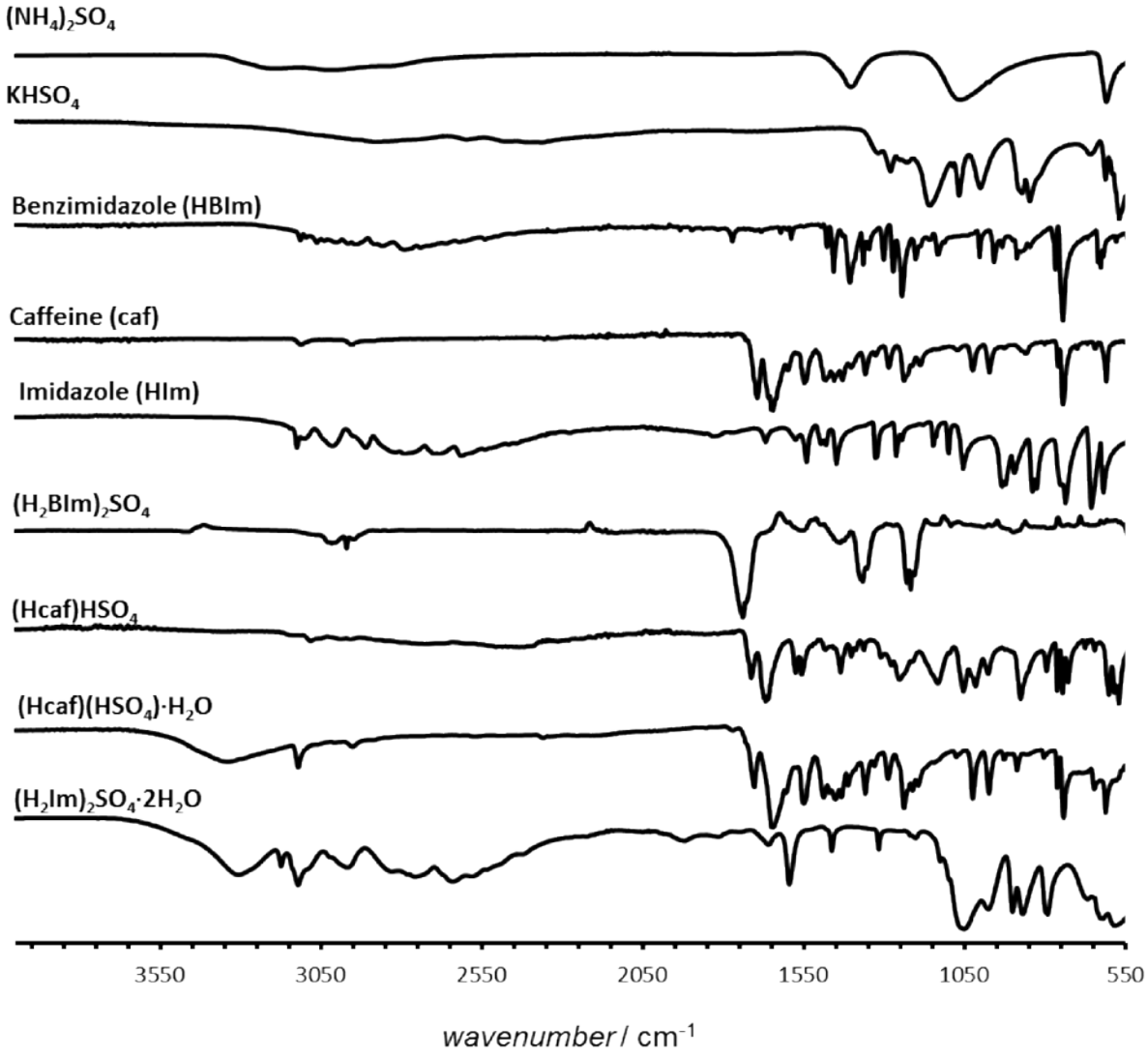

Figure S39. FTIR-ATR spectra for the salts used as additives in accelerated aging reactions, and for selected salt precursors.

This journal is © The Royal Society of Chemistry 2013

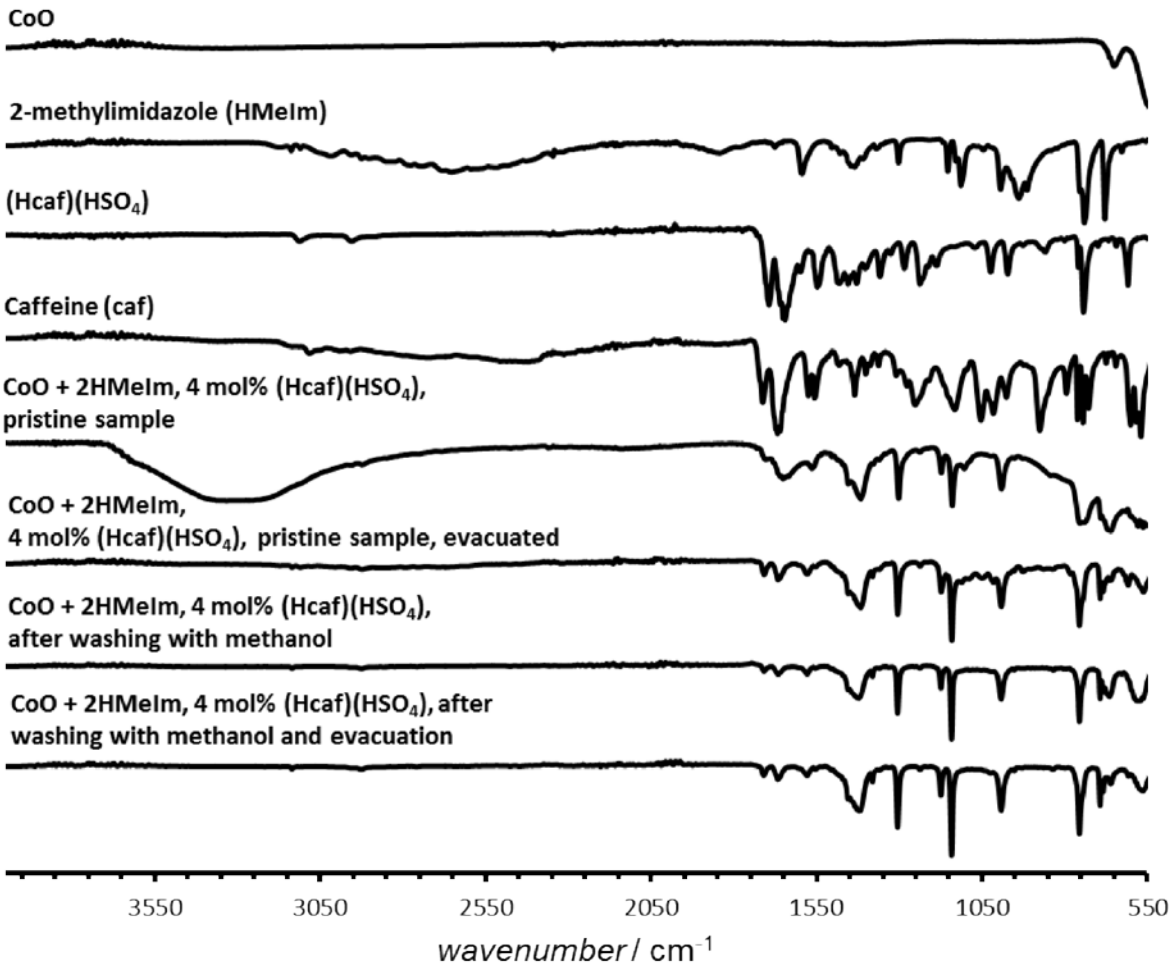

Figure S40. Selected FTIR-ATR spectra for reactants and products of accelerated aging reactions of CoO and **HMeIm**, leading to the formation of the ZIF-67 structure, in the presence of 4 mol% (calculated based on CoO) of (**Hcaf**)(HSO_4) as the ionic additive.

This journal is © The Royal Society of Chemistry 2013

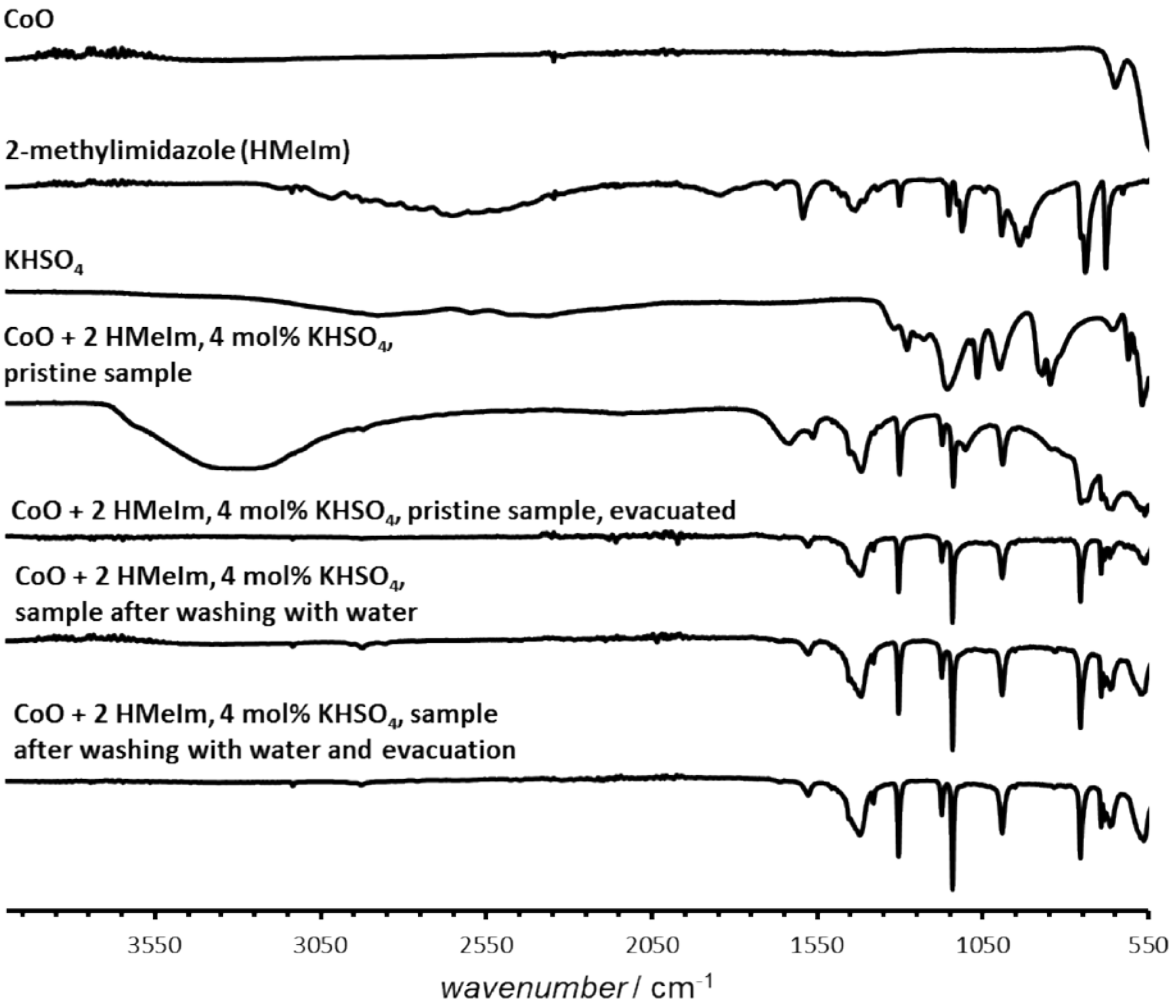

Figure S41. Selected FTIR-ATR spectra for reactants and products of accelerated aging reactions of CoO and **HMeIm**, leading to the formation of the ZIF-67 structure, in the presence of 4 mol% (calculated based on CoO) of $KHSO_4$ as the ionic additive.

This journal is © The Royal Society of Chemistry 2013

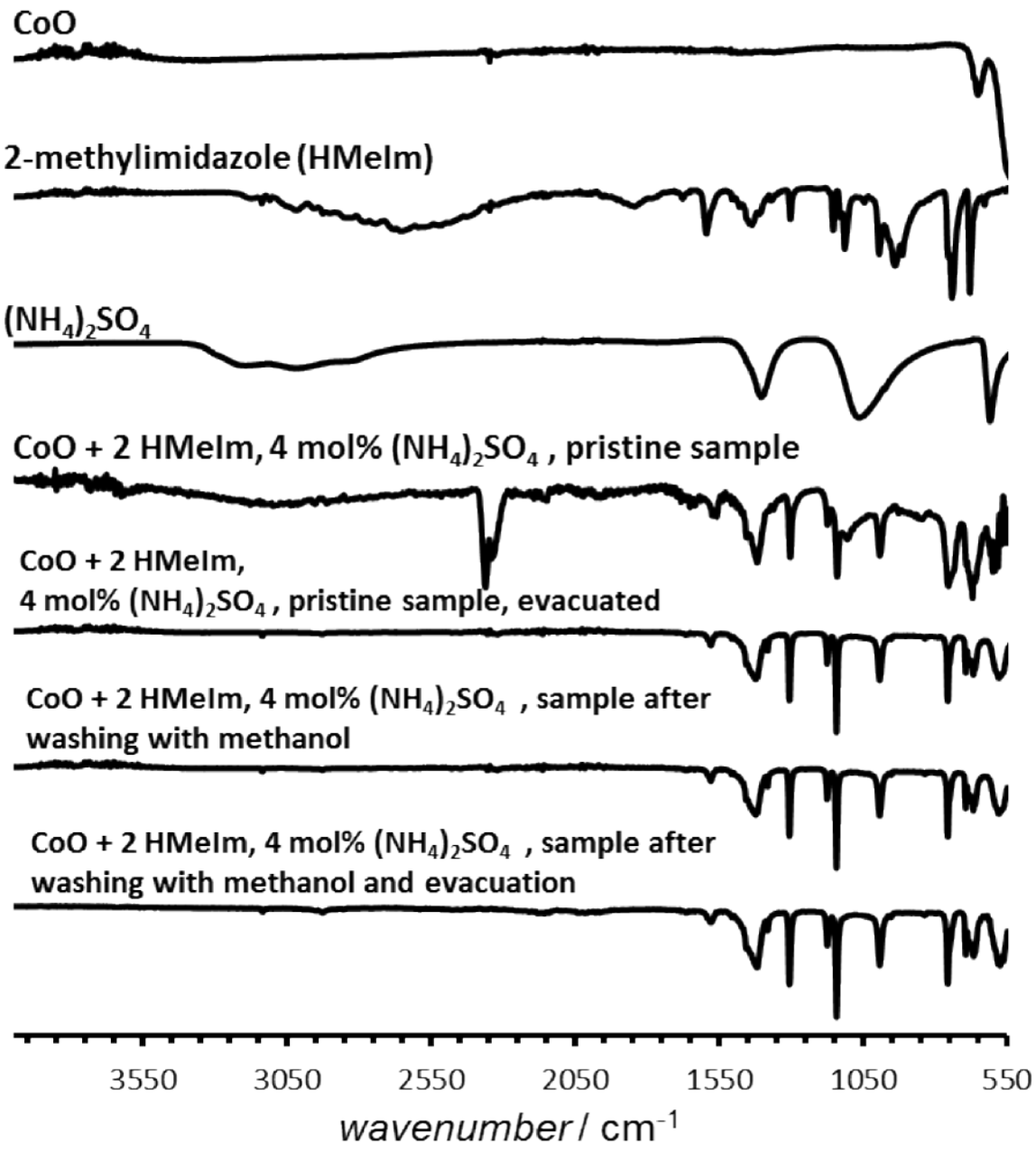

Figure S42. Selected FTIR-ATR spectra for reactants and products of accelerated aging reactions of CoO and **HMeIm**, leading to the formation of the ZIF-67 structure, in the presence of 4 mol% (calculated based on CoO) of $(NH_4)_2(SO_4)$ as the ionic additive.

This journal is © The Royal Society of Chemistry 2013

5. SELECTED THERMOGRAVIMETRIC ANALYSIS (TGA) DATA

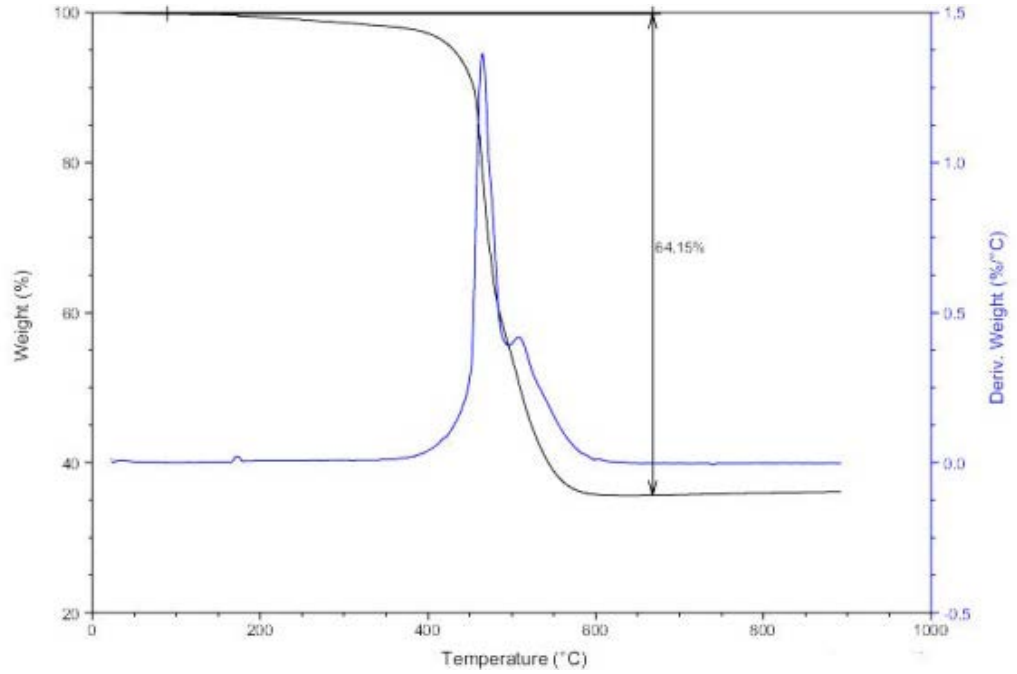

Figure S43. TGA thermogram for ZIF-8 sample obtained in the presence of 4 mol% (**Hcaf**)(HSO_4) as the ionic additive (98% RH, 45°C), after washing and evacuation, recorded in a dynamic atmosphere of air. Theoretically expected ZnO residue: 35.8%; observed: 35.8%; calculated yield: 100%.

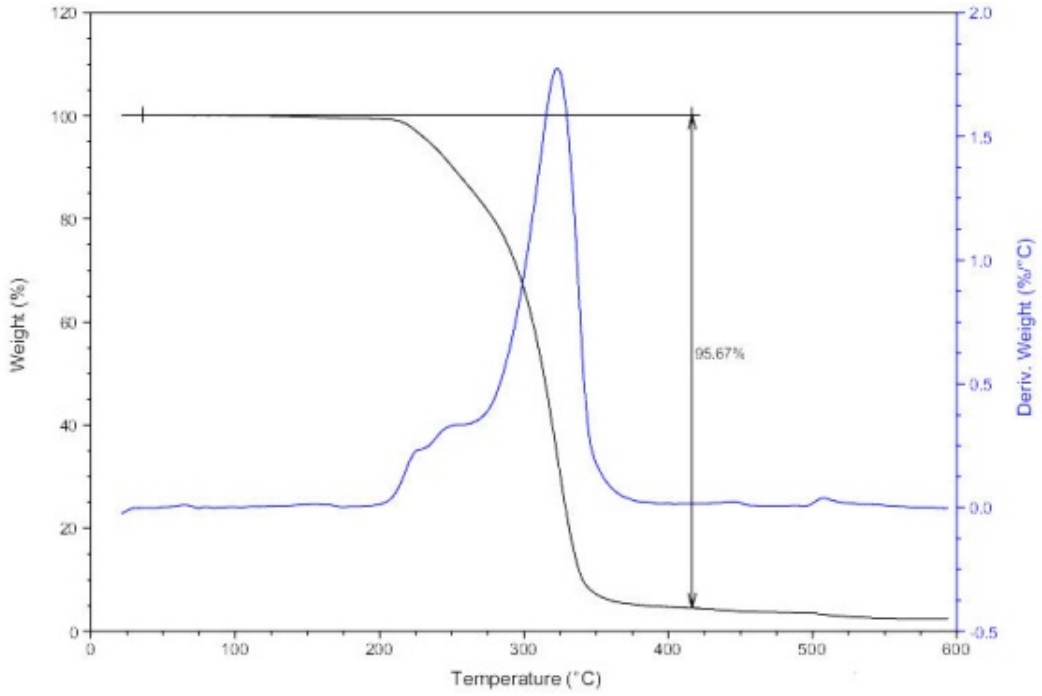

Figure S44. TGA thermogram for (**Hcaf**)(HSO_4), recorded in a dynamic atmosphere in air. The sample does not lose weight until above 200 °C, confirming it is not a solvate.

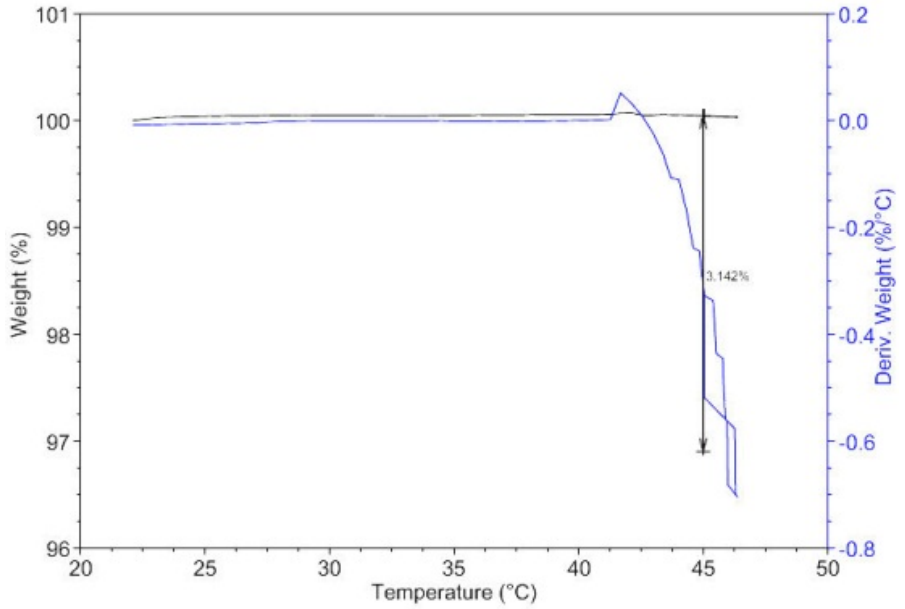

Figure S45. TGA thermogram of commercial **2-HMeIm**, heated at 45 °C for 14 hours in a dynamic atmosphere of nitrogen gas.

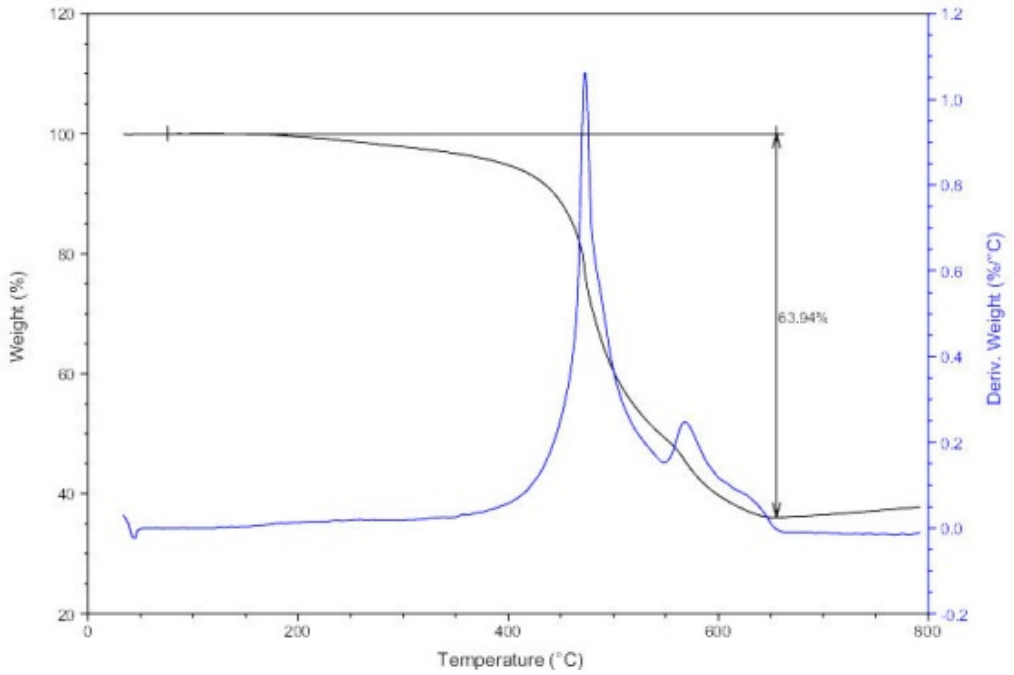

Figure S46. TGA thermogram for another ZIF-8 sample obtained in the presence of 4 mol% (**Hcaf**)(HSO_4) as the ionic additive (98%RH, 45 °C), after washing and evacuation, recorded in a dynamic atmosphere in air. Theoretically expected ZnO residue: 35.8%; observed: 36.0%; calculated conversion: 99%.

This journal is © The Royal Society of Chemistry 2013

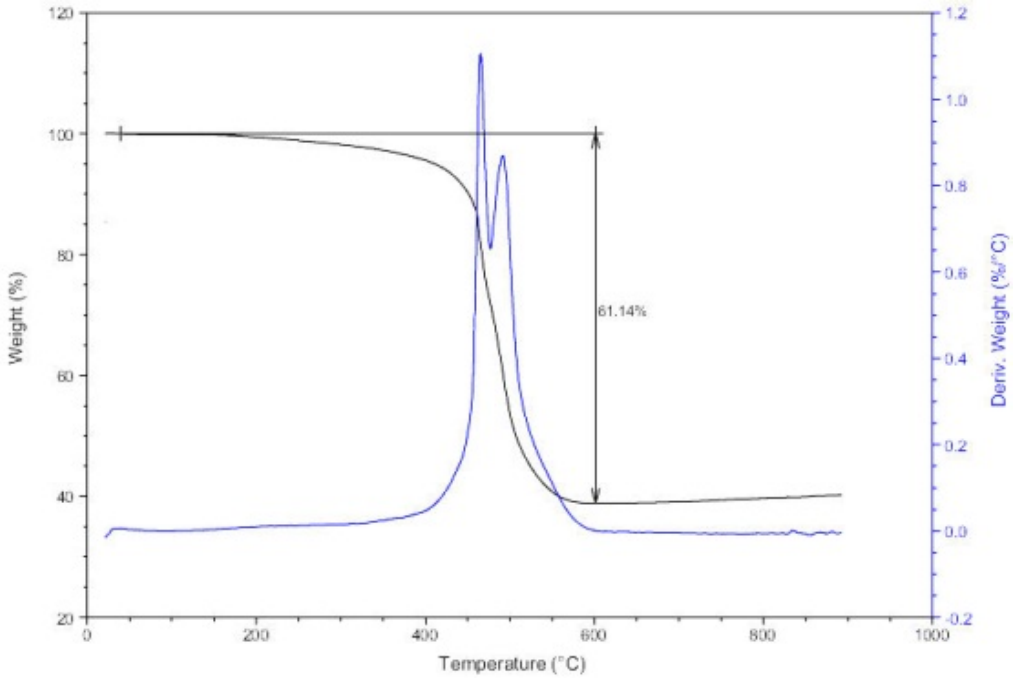

Figure S47. TGA thermogram for a ZIF-8 sample obtained in the presence of 4 mol% $(\mathbf{H_2Im})_2(SO_4)\cdot 2H_2O$ as the ionic additive (98% RH, 45 °C), after washing and evacuation, recorded in a dynamic atmosphere in air. Theoretically expected ZnO residue: 35.8%; observed: 39.0%; calculated conversion: 87%.

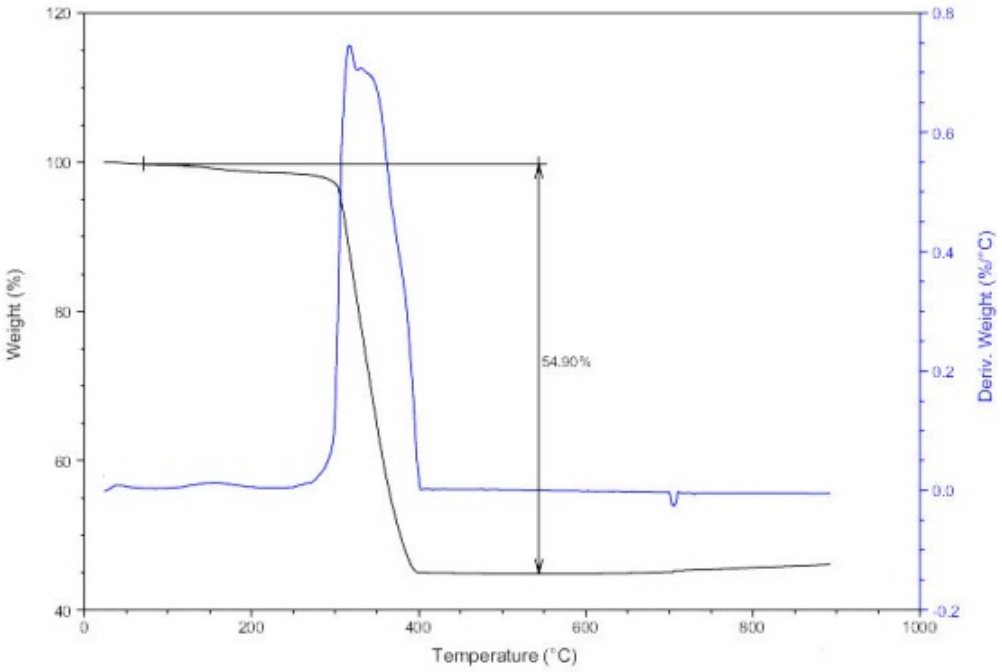

Figure S48. TGA thermogram for a ZIF-67 sample obtained in the presence of 4 mol% $(NH_4)_2(SO_4)$ as the ionic additive (98% RH, 45 °C), after washing and evacuation, recorded in a dynamic atmosphere in air. Theoretically expected Co_3O_4 residue: 36.3%; observed: 45.1%; calculated conversion: 71%. Reaction scale: 5 grams.

This journal is © The Royal Society of Chemistry 2013

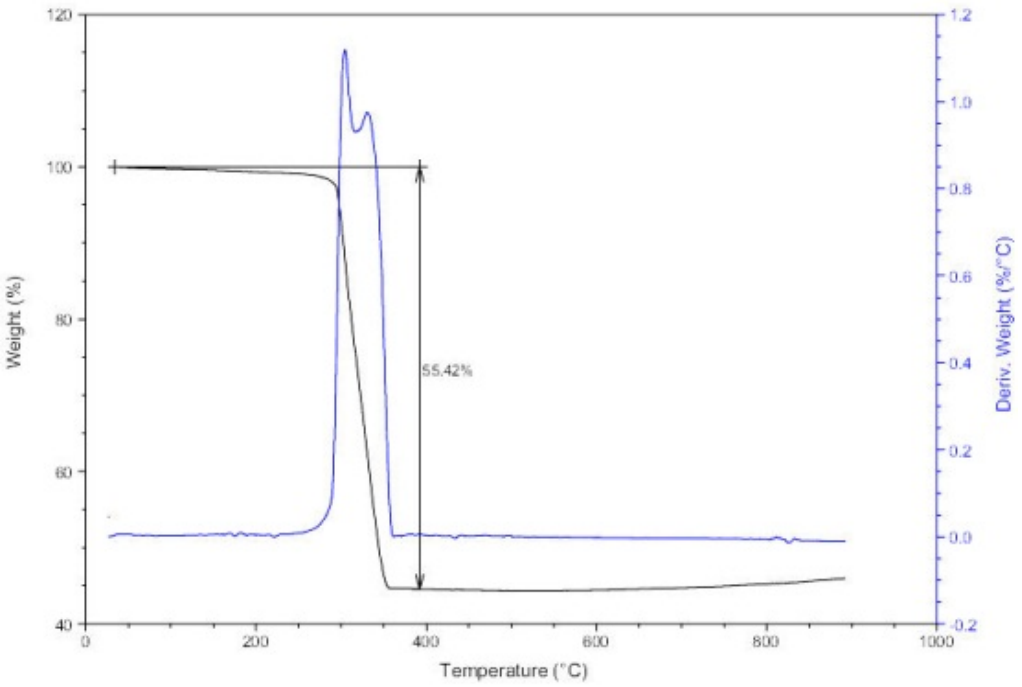

Figure S49. TGA thermogram for a ZIF-67 sample obtained in the presence of 4 mol% (**Hcaf**)(HSO_4) as the ionic additive (98% RH, 45 °C), after washing and evacuation, recorded in a dynamic atmosphere in air. Theoretically expected Co_3O_4 residue: 36.3%; observed: 44.6%; calculated conversion: 72%.

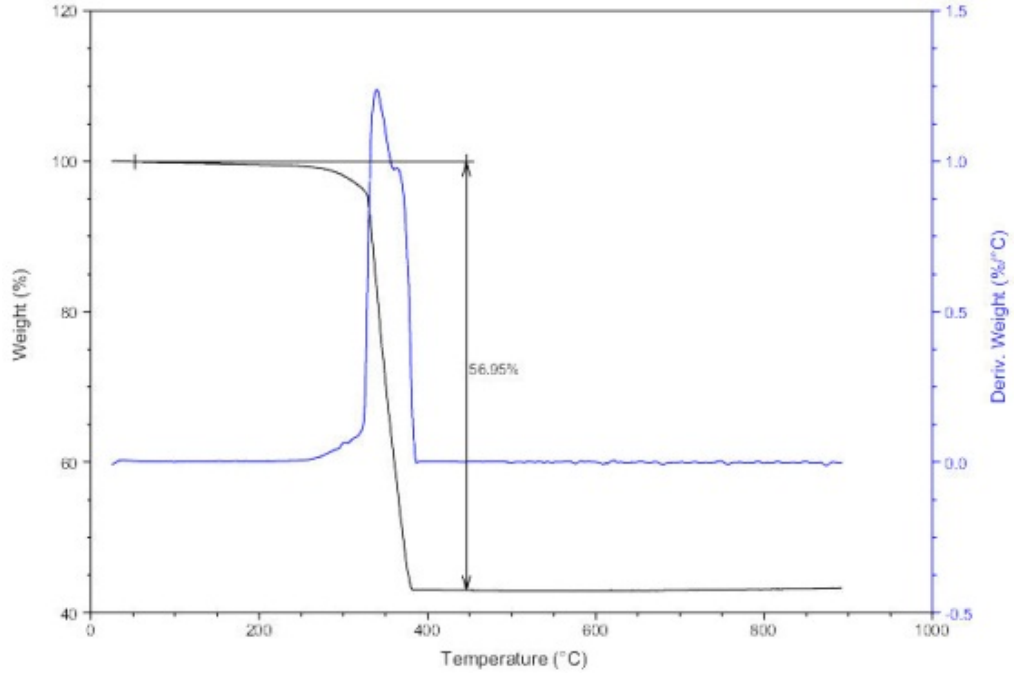

Figure S50. TGA thermogram for a ZIF-67 sample obtained in the presence of 4 mol% (**Hcaf**)(HSO_4) as the ionic additive and 100% RH, after washing and evacuation, recorded in a dynamic atmosphere in air. Theoretically expected Co_3O_4 residue: 36.3%; observed: 43.0%; calculated conversion: 77%.

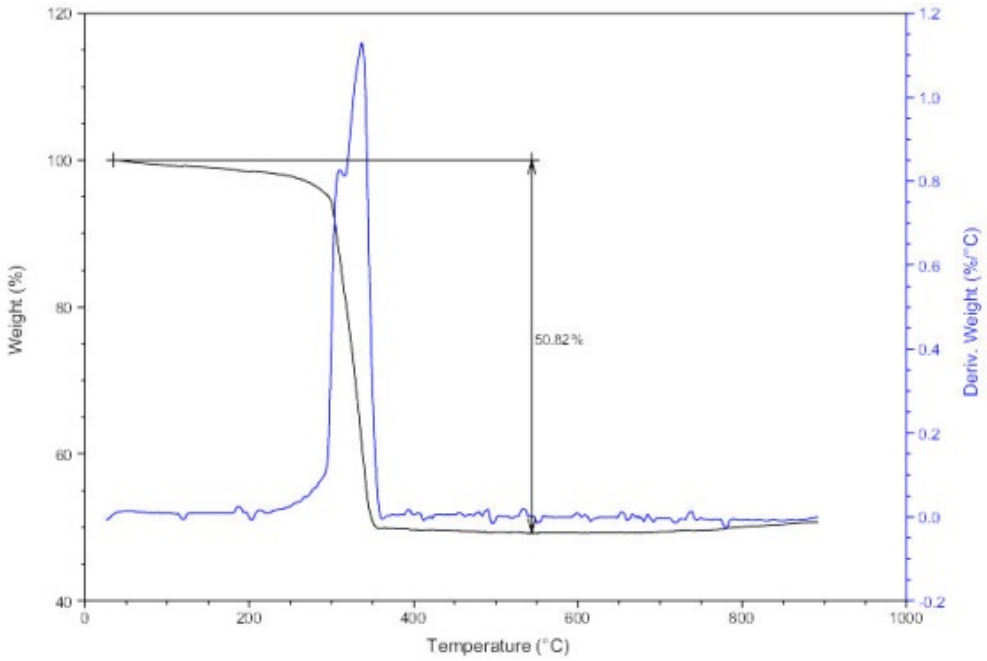

Figure S51. TGA thermogram for a ZIF-67 sample obtained in the presence of 4 mol% $KHSO_4$ as the ionic additive, after washing and evacuation, recorded in a dynamic atmosphere in air. Theoretically expected Co_3O_4 residue: 36.3%; observed: 49.1%; calculated conversion: 61%.

This journal is © The Royal Society of Chemistry 2013

6. SELECTED GAS SORPTION ANALYSIS DATA

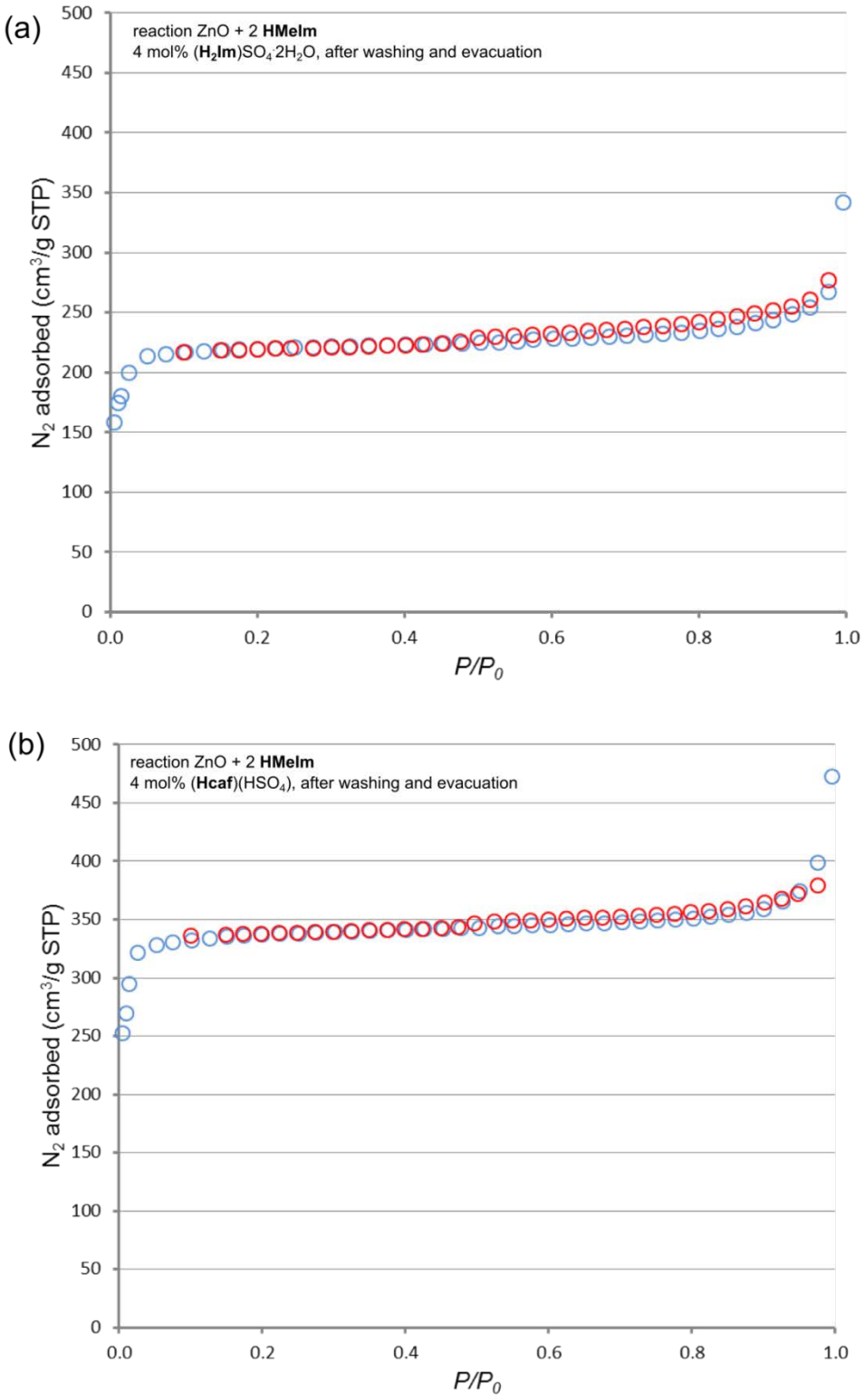

Figure S52. Nitrogen adsorption isotherms for ZIF-8 samples obtained by accelerated aging of ZnO and **HMeIm** using: (a) (**H_2Im**)$_2SO_4 \cdot 2H_2O$ or (b) (**Hcaf**)(HSO_4) ionic additives, after washing and evacuation.

This journal is © The Royal Society of Chemistry 2013

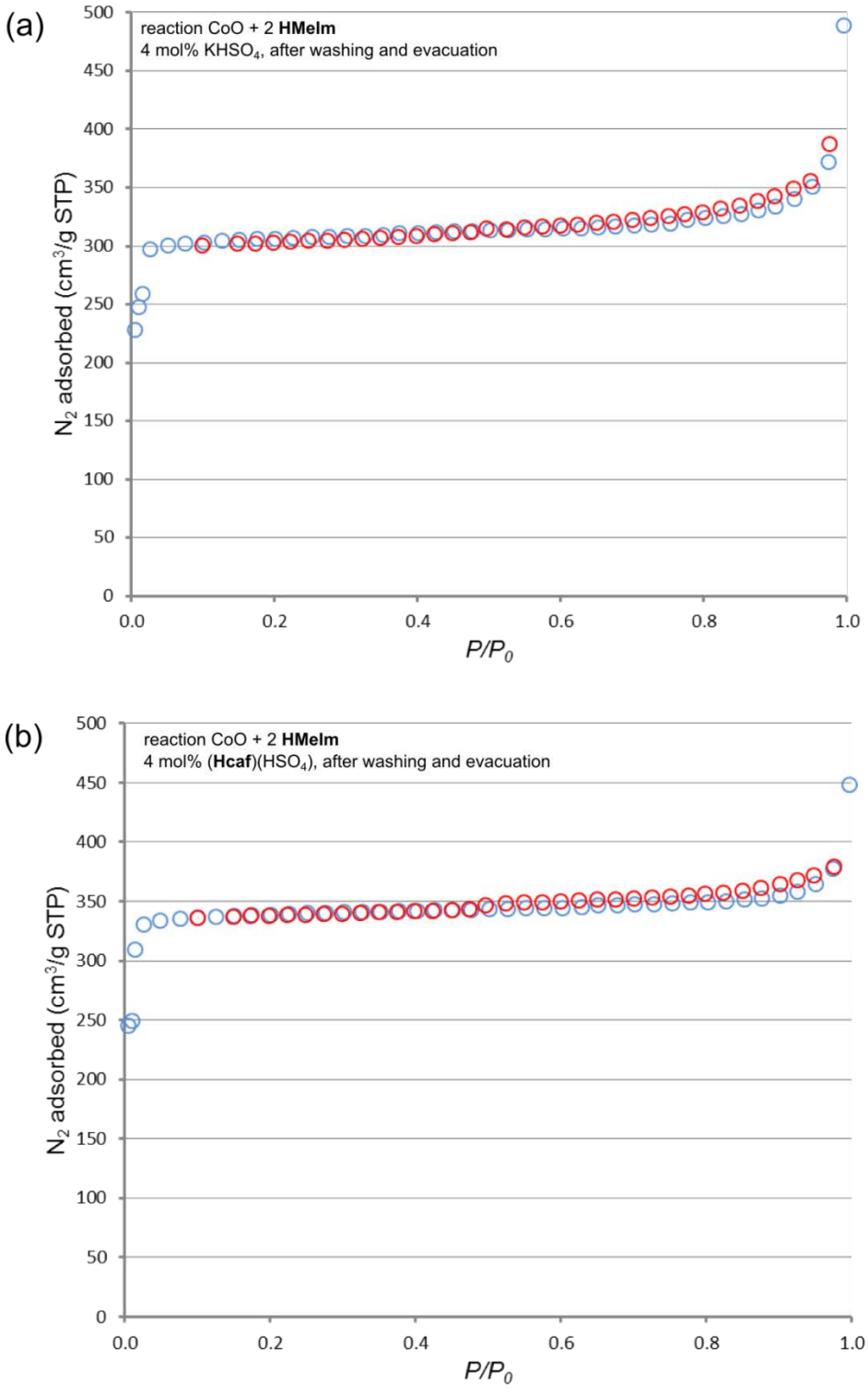

Figure S53. Nitrogen adsorption isotherms for ZIF-67 samples obtained by accelerated aging of CoO and **HMeIm** using: (a) $KHSO_4$ or (b) (**Hcaf**)(HSO_4) ionic additives, after washing and evacuation.

This journal is © The Royal Society of Chemistry 2013

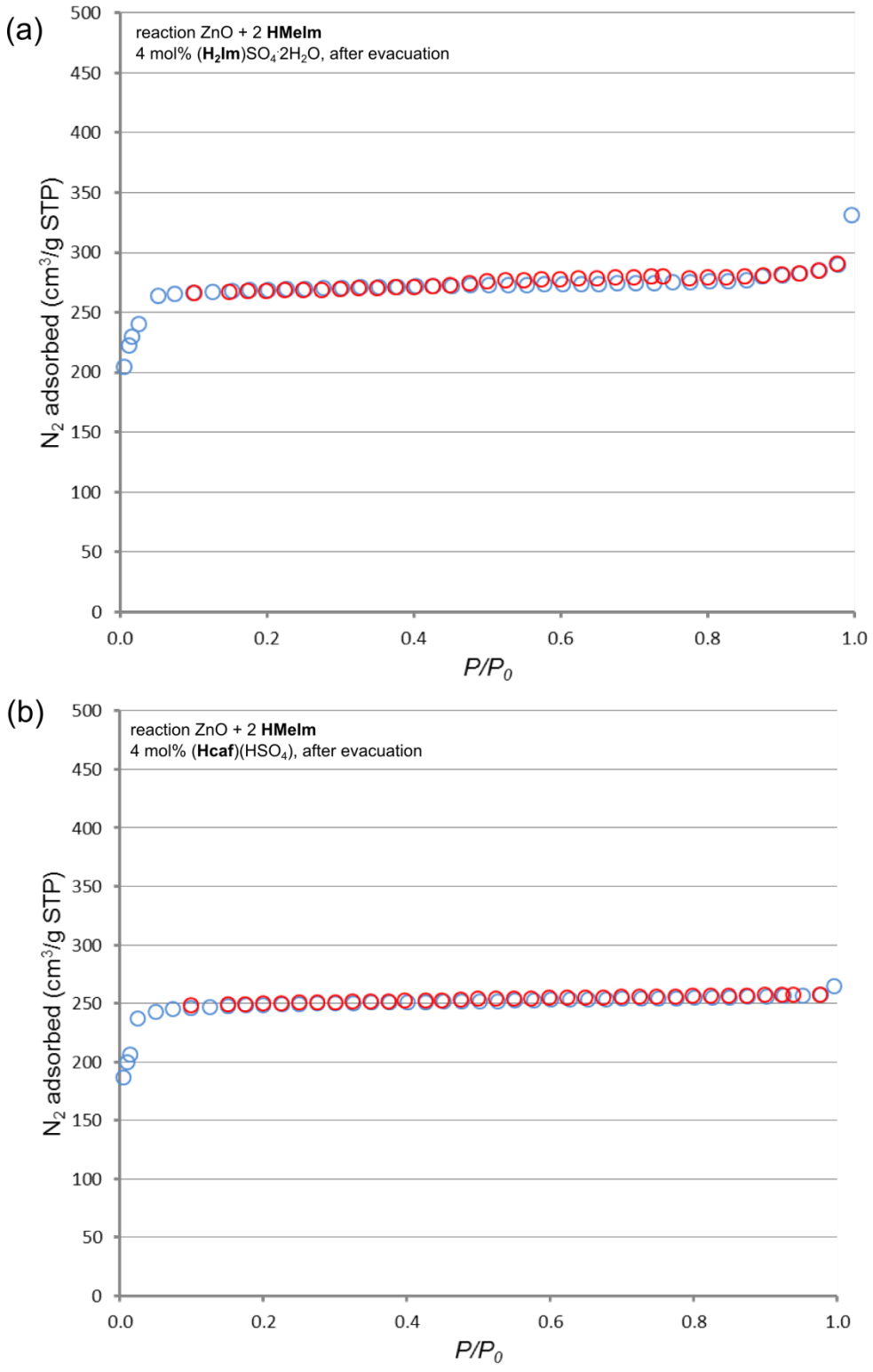

Figure S54. Nitrogen adsorption isotherms for ZIF-8 samples obtained by accelerated aging of ZnO and **HMeIm** using: (a) (**H$_2$Im**)$_2$SO$_4$·2H$_2$O or (b) (**Hcaf**)(HSO$_4$) ionic additives, after evacuation.

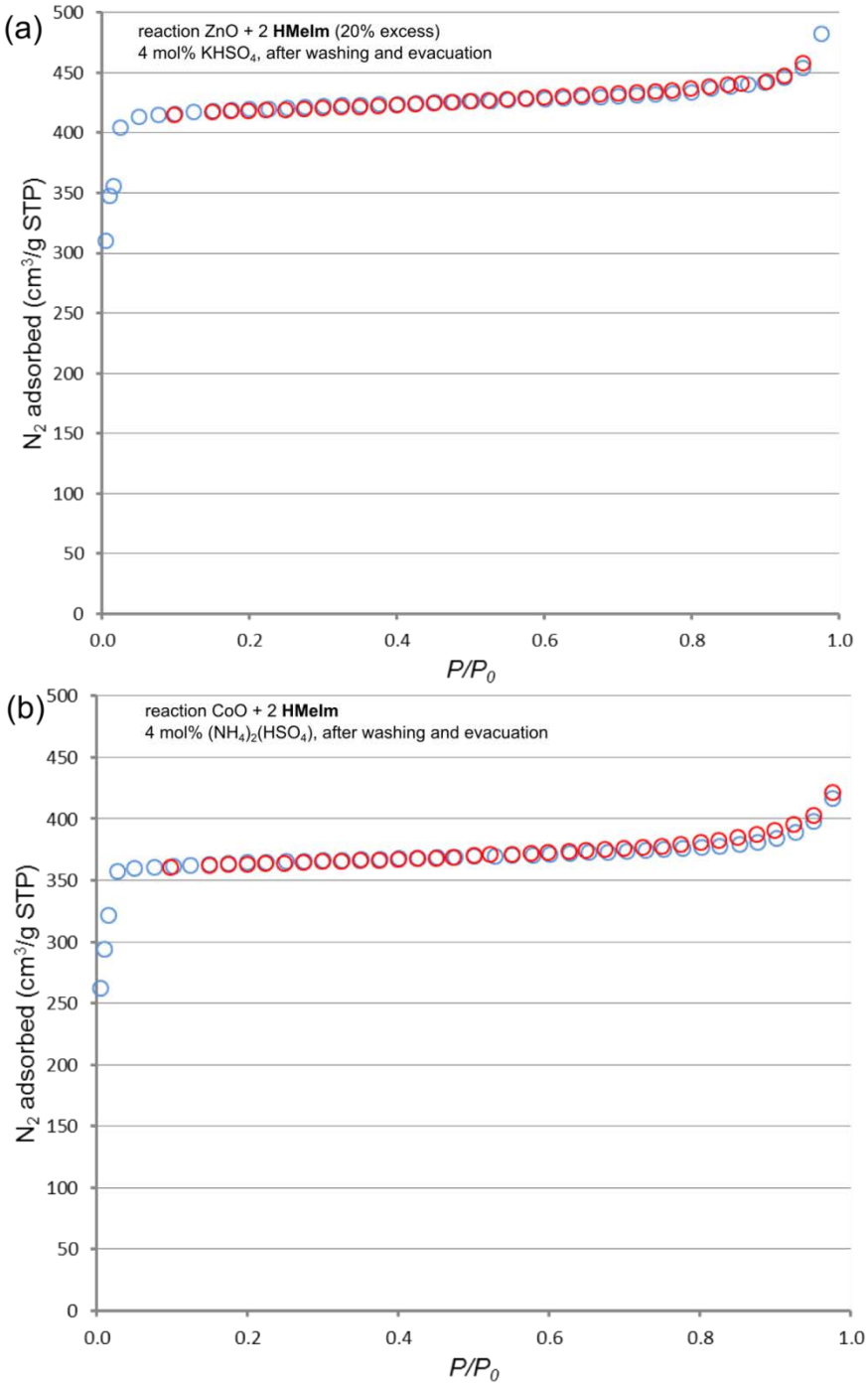

Figure S55. Nitrogen adsorption isotherms for: (a) ZIF-8 sample obtained by accelerated aging of ZnO and **HMeIm** using (**Hcaf**)(HSO_4) ionic additive in the presence of 20 mol% excess **HMeIm**, after washing and evacuation and (b) ZIF-67 sample obtained by accelerated aging of CoO and **HMeIm** using $(NH_4)_2SO_4$ ionic additive, after washing and evacuation.

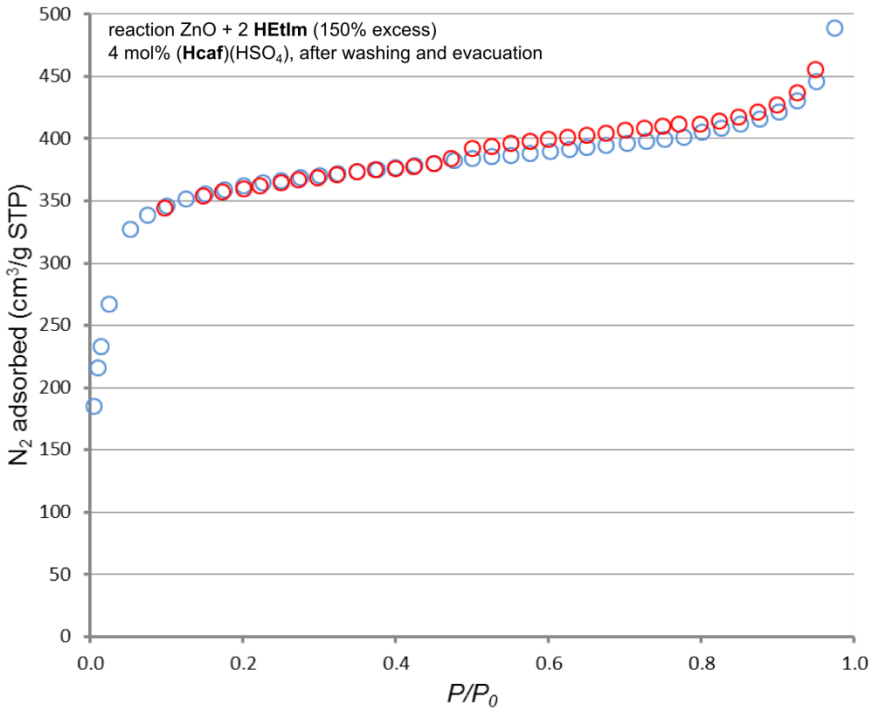

Figure S56. Nitrogen adsorption isotherm for the zeolite RHO topology Zn(**EtIm**)$_2$ obtained by accelerated aging of ZnO and **HEtIm** using (**Hcaf**)(HSO_4) ionic additive in the presence of 150 mol% excess **HEtIm**, after washing and evacuation.